a narrow temperature spike that is optically thin, hence incapable of producing an optical signature except in the Lyman continuum or in strong spectral lines.

The primary piston-driven shock finally emerges at $t \approx 1200$ s. Radiation losses have a profound effect on the propagation of this shock. First, the radiating shock's velocity remains nearly constant, in sharp contrast to an adiabatic shock that accelerates rapidly as it rises. Second, the temperature jump in the radiating shock is quite small, $T_{\text{shock}}/T_0 \lesssim 1.2$, in contrast to an adiabatic shock for which $T_{\text{shock}}/T_0 \lesssim 2$ to 10. The compression behind the nearly isothermal radiating shock is about a factor of 2 larger than in the adiabatic shock. When the shock finally reaches small optical depth, it cools rapidly. The emergence of the primary shock is essentially invisible in the emitted radiation field. The reason is that shock heating not only raises the source function S_ν locally, but also raises the opacity of the gas, hence shifts the effective radiating surface near $\tau_\nu \approx 1$ [recall the Eddington–Barbier relation (79.17)] outward into cooler gas. The two effects nearly cancel, and an external observer never actually sees the hot shock front until it is already too optically thin to affect the emergent radiation field significantly; precisely the same phenomenon occurs in fireballs from intense explosions, see (**R2**) and (**Z3,** 598–626).

A related study has been made by Kneer and Nakagawa (**K9**) who compute the time development of a nonequilibrium thermal transient in the solar chromosphere. They formulate the problem in terms of implicit Eulerian difference equations, ignoring all velocity-field effects on the radiation field, which is assumed to be quasi-static. They allow departures from LTE in a two-level hydrogen atom including the $Ly\,\alpha$ transition. They also calculate the response of the emergent $Ly\,\alpha$ radiation field to the thermal pulse.

106. Ionization Fronts

In §§104 and 105 we considered flows in which the radiation is essentially driven by the hydrodynamics, as when radiation is created in the high-temperature downstream gas behind a strong shock. In this and the following section we turn to the opposite case where instead the flow (perhaps including shocks) is driven by radiation. Specifically we examine the physics of *ionization fronts* (or *I-fronts*), which occur when intense radiation from a hot source (e.g., an O-star) eats its way into an ambient cold medium (e.g., the interstellar medium). An I-front is an *interface* only a few photon mean free paths thick, across which the material becomes essentially completely ionized while the temperature and pressure jump nearly discontinuously.

An I-front can produce a wide variety of hydrodynamic phenomena. For example, suppose the material is so rarefied and the incident radiation field is so strong that the photon number density is much larger than the particle number density and recombinations can be ignored. Then the I-front races into the medium at nearly the speed of light, ionizing every atom as it goes. Hydrodynamic motions will develop much more slowly because the speed of sound is much smaller than the speed of light. Thus at the front the upstream and downstream material will coexist at the same density, despite the fact that the temperature, hence pressure, in the downstream material is orders of magnitude larger than in the upstream material, simply because the I-front continually outruns the hydrodynamic motions that would otherwise be driven by the pressure difference. At the other extreme, suppose the medium is very dense. Then the radiation penetrates into the cold material only very slowly by diffusion, essentially in a Marshak wave (cf. §103). The effect of the I-front is to build a radiatively heated pressure reservoir, which drives a shock into the upstream material. Because the radiation front is choked in the dense material and therefore moves slowly, the shock will run ahead of the I-front.

I-FRONT JUMP CONDITIONS

Let us now derive the jump conditions that apply across a steady I-front. We will discuss only the simplest cases, with the goal of providing basic physical orientation, and refer the reader to more comprehensive treatments in the literature for details. Thus, consider an I-front driven by collimated radiation from a steady source incident normally on a planar slab of pure hydrogen. Assume that the material is completely neutral upstream and completely ionized downstream. Furthermore, for simplicity, assume that no recombinations occur in the ionized material so that radiation from the source always arrives unattenuated at the current position of the I-front. We can then have a steady flow, and it is convenient to transform to the frame moving with the front, using the geometric and sign conventions indicated in Figure 106.1. As usual, subscripts "1" and "2" refer to upstream and downstream quantities, respectively.

The density of the material is

$$\rho = (n_{\mathrm{H}} + n_{\mathrm{p}})m_{\mathrm{H}}, \tag{106.1}$$

the gas pressure is

$$p = (n_{\mathrm{H}} + n_{\mathrm{p}} + n_e)kT, \tag{106.2}$$

and the internal energy of the material is

$$\rho e = \tfrac{3}{2}kT(n_{\mathrm{H}} + n_{\mathrm{p}} + n_e) + \varepsilon_{\mathrm{H}} n_p. \tag{106.3}$$

Here n_{H} is the density of neutral hydrogen atoms, n_{p} is the proton density, n_e is the electron density, and ε_{H} is the ionization potential of hydrogen. From charge conservation we have $n_e \equiv n_{\mathrm{p}}$.

The radiation field has a specific intensity $I(\mu, \nu) = I_\nu\, \delta(\mu + 1)$, that is, it is nonzero only for $\mu = -1$. The number flux of ionizing photons (photons

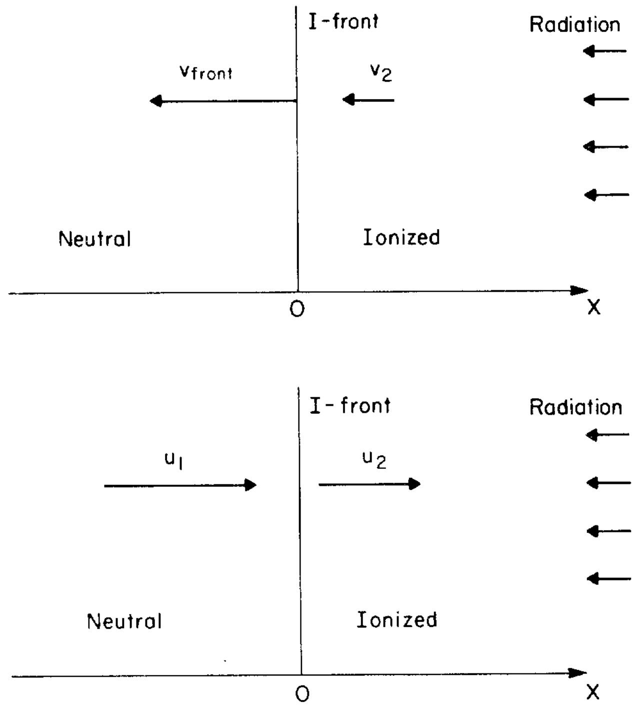

Fig. 106.1 Fluid velocities near ionization front, as measured in lab frame (top) and I-front's frame (bottom).

$\mathrm{cm}^{-2}\,\mathrm{s}^{-1}$) is

$$\phi = \int_{\nu_H}^{\infty} (I_\nu/h\nu)\, d\nu \tag{106.4}$$

where ν_H is the threshold frequency for hydrogen ionization. Because we neglect recombinations the transfer equation simplifies to

$$(dI_\nu/dx) = n_H \alpha_\nu I_\nu \tag{106.5}$$

(recall $\mu = -1$), which implies that

$$(d\phi/dx) = n_H \bar{\alpha}\phi, \tag{106.6}$$

where we have defined a mean cross section

$$\bar{\alpha} \equiv \left[\int_{\nu_H}^{\infty} (\alpha_\nu I_\nu/h\nu)\, d\nu\right] \Big/ \phi. \tag{106.7}$$

Similarly, we define a mean photon energy

$$\bar{\varepsilon} = h\bar{\nu} \equiv \left(\int_{\nu_H}^{\infty} \alpha_\nu I_\nu\, d\nu\right) \Big/ \bar{\alpha}\phi. \tag{106.8}$$

In the frame moving with the front, the statistical equilibrium equations become

$$d(n_{\rm H}u)/dx = -R_{1\kappa} + R_{\kappa 1} = -n_{\rm H}\bar{\alpha}\phi \tag{106.9}$$

and

$$d(n_{\rm p}u)/dx = R_{1\kappa} - R_{\kappa 1} = n_{\rm H}\bar{\alpha}\phi, \tag{106.10}$$

where we set the recombination rate $R_{\kappa 1} \equiv 0$. Adding (106.9) and (106.10) we get the equation of continuity

$$\frac{d}{dx}[(n_{\rm H}+n_{\rm p})u] = \frac{d}{dx}(Nu) = 0, \tag{106.11}$$

whence we have

$$Nu = (n_{\rm H}u)_1 = (n_{\rm p}u)_2 = \text{constant} \tag{106.12a}$$

or

$$\rho_1 u_1 = \rho_2 u_2 = \text{constant}, \tag{106.12b}$$

where we have used the assumption that $n_{\rm H,2} = n_{\rm p,1} \equiv 0$.

Combining (106.6) with (106.9) and (106.10) we find

$$(n_{\rm H}u)_1 = (n_{\rm p}u)_2 = \phi_2 \tag{106.13a}$$

or

$$\rho_1 u_1 = \rho_2 u_2 = m_{\rm H}\phi_2, \tag{106.13b}$$

which make the physically obvious statement that each ionizing photon incident at the front converts one hydrogen atom to a proton-electron pair. We have set $\phi_1 \equiv 0$ because all photons are absorbed in the front.

The fluid momentum equation in the frame of the I-front yields

$$\rho_1 u_1^2 + p_1 = \rho_2 u_2^2 + p_2 \tag{106.14}$$

where $p_1 = k(n_{\rm H}T)_1$ and $p_2 = k[(n_{\rm p}+n_e)T]_2 = 2k(n_{\rm p}T)_2$. The material energy equation in the frame of the front is

$$\frac{d}{dx}\{u[\rho(e+\tfrac{1}{2}u^2)+p]\} = n_{\rm H}\bar{\alpha}\bar{\varepsilon}\phi. \tag{106.15}$$

Integrating across the discontinuity with the aid of (106.6) we find

$$\tfrac{5}{2}(p_2/\rho_2) + \tfrac{1}{2}u_2^2 = \tfrac{5}{2}(p_1/\rho_1) + \tfrac{1}{2}u_1^2 + (\bar{\varepsilon} - \varepsilon_{\rm H})/m_{\rm H}. \tag{106.16}$$

Equations (106.12), (106.14), and (106.16) uniquely determine the downstream conditions in the flow for given upstream conditions and a specified photon flux (**K1**). However in astrophysical applications it is usually the case that radiative relaxation times are orders of magnitude smaller than typical flow times through the I-front. Hence, as was true for shocks (cf. §104), we can often make the simplifying assumption that both the upstream and downstream material remains isothermal at temperatures appropriate to the radiative heating and cooling mechanisms occurring in the neutral and ionized gases, respectively. We can thus replace (106.16) by the conditions

$$p_1/\rho_1 = kT_1/\mu_1 m_H = a_1^2 \tag{106.17a}$$

and

$$p_2/\rho_2 = kT_2/\mu_2 m_H = a_2^2, \tag{106.17b}$$

where a denotes the isothermal sound speed. In the interstellar medium, typical temperatures are $T_1 \approx 10^2$ K in the neutral gas, where $\mu_1 = 1$, and $T_2 \approx 10^4$ K in the ionized gas, where $\mu_2 = \frac{1}{2}$ (**S20**), (**S21**), (**S22**). Therefore typical sound speeds are $a_1 \approx 0.9$ km s^{-1} and $a_2 \approx 13$ km s^{-1}.

TYPES OF I-FRONTS

Solutions for the jump conditions written above are described in a fundamental paper by Kahn (**K1**), who developed a comprehensive classification scheme for I-fronts, discussed their basic physical properties, and delineated the conditions under which they can occur in nature. An exhaustive treatment of these questions was later given by Axford (**A8**), who also analyzed the structure of I-fronts in great detail.

Combining (106.13), (106.14), and (106.17) we find

$$\rho_2/\rho_1 = \{a_1^2 + u_1^2 \pm [(a_1^2 + u_1^2)^2 - 4a_2^2 u_1^2]^{1/2}\}/2a_2^2. \tag{106.18}$$

The restriction that ρ_2/ρ_1 be real implies that u_1 must satisfy the inequalities

$$u_1 \geq u_R \equiv a_2 + (a_2^2 - a_1^2)^{1/2} \approx 2a_2, \tag{106.19}$$

or

$$u_1 \leq u_D \equiv a_2 - (a_2^2 - a_1^2)^{1/2} \approx a_1^2/2a_2 \ll a_1, \tag{106.20}$$

where the approximations apply when $a_2 \gg a_1$.

When u_1 exceeds the critical velocity u_R we have an *R-type* ionization front; "R" stands for "rarefied" because such fronts occur when $\rho_1 < \rho_R \equiv m_H \phi/u_R$. For fixed ϕ, $u_1 \to \infty$ (more precisely $u_1 \to c$) as $\rho_1 \to 0$. Fronts for which $u_1 = u_R$ and $\rho_1 = \rho_R$ are called *R-critical.* Similarly, when $u_1 < u_D$ and $\rho_1 > \rho_D \equiv m_H\phi/u_D$ we have a *D-type* ionization front; "D" stands for "dense". Fronts for which $u_1 = u_D$ and $\rho_1 = \rho_D$ are called *D-critical.* Fronts for which $u_D < u_1 < u_R$ and $\rho_R < \rho_1 < \rho_D$ are called *M-type.*

In an R-front $u_1 \geq u_R > a_2 > a_1$. Hence R-fronts always advance supersonically into the neutral gas, and thus cannot be preceded by a hydrodynamic disturbance of the upstream material. D-fronts always advance subsonically into the neutral gas, and thus can be preceded by hydrodynamic disturbances (e.g., a shock or a rarefication). A steady I-front cannot advance into the neutral gas when conditions ahead of it are M-type.

R-FRONTS

We obtain simple expressions for the density jump and downstream velocity in R-fronts in the limiting case that $u_1 \gg u_R$. Expanding (106.18) and choosing the negative root we find

$$\rho_2/\rho_1 \approx 1+(a_2/u_1)^2 \approx 1. \tag{106.21}$$

Such fronts are called *weak R-fronts* because the material is only slightly compressed as it passes through the front. Choosing the positive root we find

$$\rho_2/\rho_1 \approx (u_1/a_2)^2[1-(a_2/u_1)^2] \gg 1. \tag{106.22}$$

Such fronts are called *strong R-fronts* because the material is greatly compressed.

The downstream velocity in a weak R-front is

$$u_2 \approx u_1[1-(a_2/u_1)^2] \gg a_2, \tag{106.23}$$

and in a strong R-front

$$u_2 \approx a_2^2/u_1 \ll a_2. \tag{106.24}$$

Thus a weak R-front moves supersonically with respect to both the neutral and the ionized gas. In the lab frame the neutral material is at rest, $v_1 = u_1 + v_f = 0$, hence the front moves to the left (cf. Figure 106.1) with a speed $v_f = -u_1$, and the ionized gas moves subsonically to the left with a speed

$$v_2 = u_2 + v_f = u_2 - u_1 \approx -a_2^2/u_1. \tag{106.25}$$

In contrast, a strong R-front moves supersonically with respect to the neutral gas but only subsonically with respect to the ionized gas. Therefore in the lab frame the ionized gas moves to the left supersonically, almost with the speed of the I-front:

$$v_2 \approx -u_1[1-(a_2/u_1)^2]. \tag{106.26}$$

For an R-critical front one finds

$$u_2 = a_2 \tag{106.27}$$

and

$$\rho_2/\rho_1 \approx 2 - \tfrac{1}{2}(a_1/a_2)^2 \approx 2. \tag{106.28}$$

Thus an R-critical front moves exactly sonically with respect to the ionized gas, and produces a moderate density jump across the front. In the lab frame the ionized gas moves to the left nearly sonically.

D-FRONTS

In contrast to an R-front, in which ρ_2 always exceeds ρ_1, the gas passing through a D-front undergoes *expansion.* We can obtain simple expressions for ρ_2/ρ_1 and u_2 by assuming that $u_1 \ll u_D \ll a_1$. Then by choosing the positive root in (106.18) we find that in a *weak D-front*

$$\rho_2/\rho_1 = (a_1^2/2a_2^2)(1+\delta) \approx (u_D/a_2)(1+\delta) \ll 1, \tag{106.29}$$

where

$$\delta \equiv [1-(2u_1a_2/a_1^2)^2]^{1/2} \tag{106.30}$$

increases from zero to one as u_1 decreases from u_D to zero. In a *strong D-front* we find

$$\rho_2/\rho_1 \approx (a_1^2/4a_2^2)(u_1/u_D)^2 \approx \tfrac{1}{2}(u_1/u_D)(u_D/a_2) \ll 1, \tag{106.31}$$

which is smaller than the density ratio in a weak D-front by an additional factor of (u_1/u_D).

The downstream velocities in weak and strong D-fronts are, respectively,

$$u_2/a_2 \approx (u_1/u_D)/(1+\delta) \ll 1 \tag{106.32}$$

and

$$u_2/a_2 \approx 2(u_D/u_1) \gg 1. \tag{106.33}$$

Thus weak D-fronts move subsonically with respect to both the neutral and ionized gas, whereas strong D-fronts move subsonically into the neutral gas but supersonically with respect to the ionized gas. For a D-critical front one finds

$$u_2 = a_2 \tag{106.34}$$

and

$$\rho_2/\rho_1 = a_1^2/2a_2^2 = (u_D/a_2) \ll 1. \tag{106.35}$$

Thus a D-critical front moves exactly sonically with respect to the ionized gas.

In the lab frame the ionized gas behind a D-front advancing into neutral material at rest always moves to the right, subsonically for weak fronts, nearly sonically for critical fronts, and supersonically for strong fronts.

A more detailed and complete discussion of the properties of steady I-fronts can be found in (**A8**).

RELATION TO COMBUSTION WAVES

Ionization fronts resemble *combustion waves* (**L2,** Chap. 14), (**C20,** Chap. 3, Sec. E) in many respects. In both cases the "chemical composition" of the gas changes across a sharp interface as a result of energy input into the gas: from exothermic chemical reactions (which *burn* the gas) in the case of combustion waves, and from an external radiation source in the case of I-fronts (which "dissociate" atoms into ions and electrons). In general terms D-fronts resemble *deflagrations* (or *flame fronts*) and R-fronts resemble *detonations*.

A significant difference between the two theories is that, according to the *Chapman–Jouguet hypothesis*, only weak deflagrations and strong detonations are possible. In the former case the front propagates subsonically with respect to both the unburnt (upstream) and burnt (downstream) gas; in the latter it is driven by a shock that propagates supersonically into the unburnt gas, but subsonically with respect to the combination products. Strong deflagrations and weak detonations are forbidden.

In contrast, for I-fronts, weak R-fronts (corresponding to weak detonations) are not only possible, but, as we will see below, play a central role in the dynamics of gaseous nebulae and ablation fronts. Similarly, whereas the D-fronts in gaseous nebulae are usually D-critical or weak-D, transient strong D-fronts can arise.

Indeed it is strong R-fronts (analogous to strong detonations) that are not expected to occur in nature because some additional (i.e., nonradiative) mechanism would be required to maintain the large velocity of the compressed, ionized gas behind the front. Moreover, sonic disturbances in the hot gas behind the front can catch up with the front and can continually weaken it. An essential reason for this difference is that the exothermic chemical reaction that powers a detonation wave is actually *driven* by the wave itself; that is, the high temperatures in the shock cause the upstream gas to ignite spontaneously as it passes through the front, while the energy thus released propels the shock forward. Thus the strong detonation (supersonic upstream, subsonic downstream) is the only natural solution. However an I-front will propagate naturally at the speed of light (a signal speed that is independent of the hydrodynamic state of the material) until the density, hence absorption coefficient, of the upstream material becomes large enough to slow the radiation front to a diffusion wave. Thus the weak R-front is a natural solution that reflects the properties of the externally imposed energy source.

A much more penetrating analysis of the differences between combustion waves and I-fronts was carried out by Axford (**A8**), who demonstrates that the Chapman–Jouguet hypothesis is invalid for I-fronts.

ABLATION FRONTS

When intense radiation from a hot source (e.g., an O-star) penetrates into optically thick cold material (e.g., an interstellar cloud) bounded by vacuum, an *ablation front* is driven into the medium, and hot ionized material expands rapidly away from the boundary surface in a *blowoff.* To gain insight we first assume planar geometry, and, following Kahn (**K1**), we consider what happens at the vacuum-cloud interface as the intensity of the incident radiation is progressively increased from a very low to a very high level.

When the incident photon flux is very small, conditions in the neutral gas are of extreme D-type, hence the radiation produces a very weak D-front which propagates only very slowly into the neutral material. The ionized gas expands gently into the vacuum, essentially as a mild *evaporation.* This loss of material induces a weak rarefaction (or *expansion wave*) to propagate at the speed of sound into the cold medium ahead of the I-front,

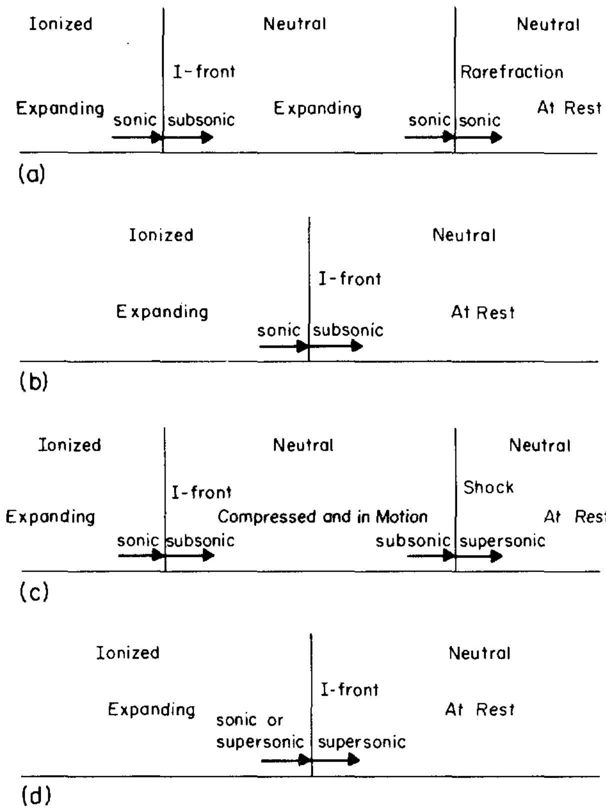

Fig. 106.2 State of flow in an I-front for (a) a very weak D-front; (b) a D-critical front; (c) a D-critical front preceded by a shock; and (d) an R-critical front.

which penetrates only subsonically. The resulting flow pattern is sketched in Figure 106.2a.

As the photon flux is increased, the rate of ablation increases, and the pressure in the ionized gas in the blowoff rises. Eventually the back pressure becomes large enough to prevent any expansion of the neutral gas, at which point conditions in the flow are D-critical, as sketched in Figure 106.2b.

A further increase in the photon flux would raise the I-front velocity above the D-critical limit u_D, hence the conditions in the neutral gas would become M-type, and the front could not propagate directly into the quiet material. But at the same time the pressure in the blowoff rises above the value necessary to just stop the backward expansion of the neutral gas, and thus drives a shock that moves supersonically into the quiet gas ahead of the I-front. This shock compresses the material passing through it enough that the postshock density rises to the value ρ_D required to permit continued D-critical propagation of the I-front at the specified value of ϕ.

The resulting flow, comprising an I-front and an *ablation-driven shock*, is sketched in Figure 106.2c.

As the photon flux is increased still further, the ionization rate becomes larger and larger, and the I-front travels through the gas at a speed closer and closer to that of its antecedent shock. Eventually the flux becomes large enough that the I-front and shock have the same speed and thus merge into a single front propagating into the quiet gas. Conditions are then R-critical, and the flow pattern is as sketched in Figure 106.2d.

If the photon flux is made even greater, the I-front moves into the cold material so fast that the shock can no longer keep up with it. The I-front then propagates directly into the neutral gas as a weak R-front.

Newton's third law of motion implies that the rapid loss of high-velocity material in the blowoff from an ablation front will accelerate the neutral medium in the opposite direction. Oort and Spitzer (**O2**) have suggested that this *rocket effect* can accelerate neutral interstellar clouds near O- and B-stars to very large velocities. Thus if radiation on a cloud of mass $\mathcal{M}$ forces it to lose mass at a rate $d\mathcal{M}/dt$ in material expanding into vacuum with a velocity V at the ablation front, then the velocity v of the cloud can be determined from

$$\mathcal{M}(dv/dt) = -V(d\mathcal{M}/dt), \tag{106.36}$$

which yields the standard rocket equation

$$v = V \ln (\mathcal{M}_0/\mathcal{M}). \tag{106.37}$$

Here $\mathcal{M}_0$ is the initial mass of the cloud, which is assumed to be initially at rest. The mass-loss rate is related to the photon number flux by

$$(d\mathcal{M}/dt) = -\pi R^2 \phi m_{\mathrm{H}}, \tag{106.38}$$

where R characterizes the projected cross section of the cloud to the stellar radiation. Here we have assumed that each photon ionizes an atom, and that the ionized material all leaves in the blowoff.

To trace the time history of a cloud in detail, one must make a variety of additional assumptions. But with reasonable, if simplified, models one can show that there is a critical initial mass $\mathcal{M}_{\mathrm{crit}}$ at which clouds engulfed in the region of ionized gas surrounding an O-star just evaporate as the cloud remnant reaches the edge of that region (**O2**), (**S20**), (**S21**). Clouds with $\mathcal{M}_0 < \mathcal{M}_{\mathrm{crit}}$ evaporate completely; clouds with $\mathcal{M}_0 > \mathcal{M}_{\mathrm{crit}}$ can survive and escape from the ionized region, sometimes with large velocities.

The efficiency of the rocket effect is somewhat reduced by recombination of ions and electrons in the blowoff. Neutral atoms formed by recombination attenuate the radiation from the external source before it reaches the ablation front; they thus produce an *insulating layer* that decreases the rate of energy deposition into the front. This decrease can be quite significant in planar geometry (**K1**), but is less serious for a uniformly irradiated spherical medium because the geometrical divergence of a radial blowoff leads to a rapid reduction of the density, hence recombination rate, in the expanding material. In this case we can get rather efficient energy deposition into a spherical ablation front that drives a *converging spherical shock* into the cold medium. The converging shock can collapse the core of the original sphere to very high densities. In fact it is just such *radiation-driven implosions* that are used in laser-fusion experiments to compress pellets containing appropriate isotopes of hydrogen to the high densities and temperatures needed to ignite thermonuclear reactions (**M2**).

Similar effects occur in interstellar cloud complexes near or around young clusters containing O- and B-stars. In particular the *bright rims* sometimes observed to surround dark clouds near very hot stars may be insulating layers formed by blowoff from the clouds. Furthermore, radiation-driven implosion of interstellar clouds may provide an effective mechanism of star formation (**E2**), (**S3**).

Thus suppose a single *seed* O-star "lights" deep inside a massive (10^5 to $10^6 \mathcal{M}_\odot$) interstellar molecular cloud complex that has a very inhomogeneous structure consisting of dense condensations surrounded by a more rarefied medium. Radiation from the seed star will preferentially burn through the less-dense interstices in the cloud complex, and can produce ablation fronts around several nearby condensations in the original cloud. Each of these fronts may implode a condensation to the point where it becomes *Jeans unstable*, collapses gravitationally, and forms a new star. Radiation from these new stars may then implode still more stars, and one can imagine the possibility of a multiplicative runaway leading to a violent burst of star formation in the cloud.

There is, of course, a competition between the loss of material into the blowoff and the effects of the converging shock. If the implosion proceeds too slowly, an initial condensation will evaporate before it can collapse gravitationally. Thus the radiation-driven implosion mechanisms may produce mainly high-mass stars, though recent work (**K6**) suggests that irradiation of a condensation by *multiple* driving stars may produce low-mass stars as well.

The multiplicative star-formation mechanism described above implies a rapid building of radiation inside the cloud complex. Ultraviolet stellar radiation will continually ionize the less-dense regions between condensations in the complex. In due course, each ionization is followed by a recombination, which results in the emission of one or more photons in subordinate continua and in spectral lines (including Lyman α). This recombination radiation scatters around within the transparent ionized interstices between condensations and steadily accumulates, as in a reservoir, because new ionizing photons are continually emitted by stars. The level of this reservoir, representing the time-integrated luminous output from all stars embedded in the cloud complex, can become quite high. Eventually the ionizing radiation burns through at some position on the outer boundary surface of the cloud complex. It is interesting to speculate whether one might observe an intense, nonequilibrium burst of radiation at this instant, as the radiation reservoir stored in the cloud pours out. At a somewhat later time one might also expect to observe an energetic hydrodynamic flow through the site of the radiative burn-out.

RADIATION-DRIVEN EXPLOSIONS

A radiation-driven explosion is produced when a large amount of radiant energy is released nearly instantaneously from a point source in a cold gas. The radiation both ionizes and strongly heats the gas and can thus drive violent hydrodynamic phenomena. Good examples are *H II regions*, which are regions of ionized hydrogen in the interstellar medium surrounding O- and B-stars, and *fireballs* produced by extremely strong explosions in the Earth's atmosphere.

The dynamics of fireballs is significantly influenced by gravity (stratification of the ambient atmosphere) and by reflected shocks (in explosions near the ground). As fireballs are discussed extensively in (**Z3,** Chap. 9) and the references cited therein, they will not be considered further here. Rather, we discuss qualitatively the dynamical behavior of an H II region as it expands into the surrounding H I region (i.e., the neutral interstellar medium) until it comes into equilibrium with its surroundings and forms a static *Strömgren sphere* (**S26**) around the exciting star. We assume that the H I region is initially homogeneous, and neglect gravitational forces.

Numerous studies have been made of the dynamics of H II regions. Simple analytical considerations are summarized in (**S20**), (**S21**). A similarity solution was constructed by Goldsworthy (**G6**), but unfortunately it is valid only for a particular initial density distribution ($\rho \propto r^{-3/2}$ in spherical geometry and $\rho \propto r^{-1}$ in cylindrical geometry). Moreover, for a steady photon flux the solution requires that the gas temperature must vanish at the origin in spherical geometry, which is unphysical, hence one is forced to cylindrical geometry, which is unrealistic. Thus these solutions have only limited value. Vandervoort (**V1**), (**V2**), (**V3**) discussed the early phases of evolution of H II regions using the method of characteristics. The effects of various physical processes on the structure of H II regions in the steady-flow approximation were analyzed by Hjellming (**H5**).

The most realistic models have been constructed by Mathews (**M6**) and Lasker (**L5**) using numerical methods. We will discuss these shortly, but first, following Mathews and O'Dell (**M7**), it is instructive to study the evolution of an H II region by an analysis of the behavior of the gas in the (p, V) diagram. As we saw in §56, conservation of mass and momentum across a front imply that

$$p_2 - p_1 = -\dot{m}^2(V_2 - V_1), \tag{106.39}$$

where $\dot{m}$ is the mass flux and $V \equiv 1/\rho$. This result, which applies for both shocks and I-fronts, shows that the initial and final states of the gas must be connected by a straight line of negative slope in the (p, V) diagram. For the

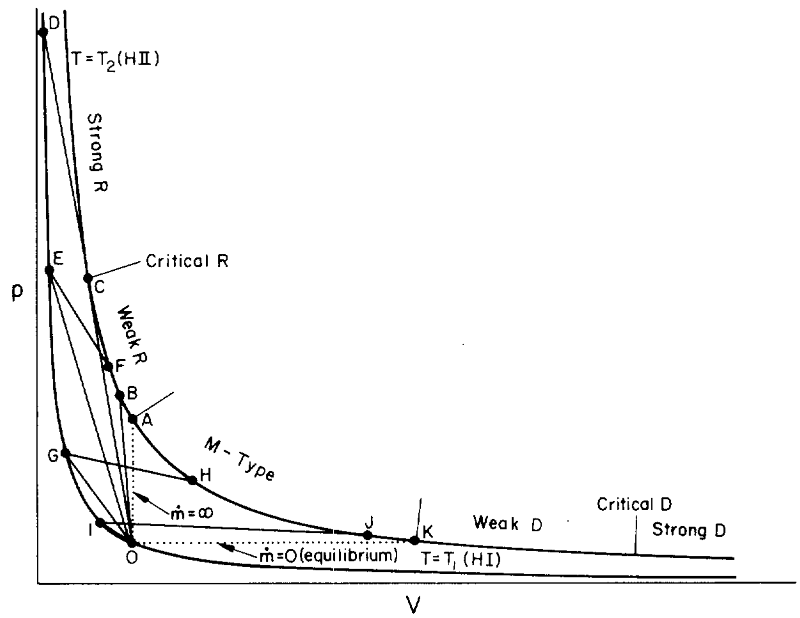

Fig. 106.3 Evolution of shocks and ionization fronts in an H II region, shown in (p, V) diagram. Adapted with permission, from (**M7**) in *Annual Review of Astronomy and Astrophysics*, Vol. **7**, © 1966 by Annual Reviews, Inc.

problem under consideration, the initial and final states must lie on the isotherms $T \equiv T_1$ and $T \equiv T_2$ which, as sketched in Figure 106.3, are hyperbolae in the (p, V) plane. Shocks are represented by straight lines joining two points on the same isotherm; I-fronts by straight lines with negative slope joining points on the two isotherms.

If the initial state of the gas is represented by point O at (p_1, V_1) on the H I isotherm, various types of I-fronts *with respect to this point* are shown on the H II isotherm. Thus the separation between M-type conditions and R-fronts occurs at infinite photon flux (which implies $\dot{m} = \infty$), and between M-type conditions and D-fronts at zero photon flux (which implies that $\dot{m} = 0$). A transition via an I-front from point O to any point in the M-type region is clearly impossible because the slope of the line joining the initial and final states would be positive. R-critical and D-critical fronts occur when the line from O is just tangent to the H II isotherm, for this is the condition that the front propagate sonically at $T = T_2$.

Suppose now that an O-star begins to radiate essentially instantaneously in a large, low-density H I cloud having $(p, V) = (p_1, V_1)$. Then initially $\dot{m}$ is very large and a weak R-front moves rapidly [$u_1 \sim 800 \text{ km s}^{-1}$ (**M6**)] outward, producing a transition such as OB in Figure 106.3. As the front moves outward, ϕ, hence $\dot{m}$, decreases owing to spatial dilution and to absorptions resulting from recombinations in the H II region. Eventually the front becomes R-critical, producing the transition OC in Figure 106.3, and moves at the sound speed relative to the ionized gas. The pressure in the H II region exceeds that in the H I region by two orders of magnitude, hence it must expand, and will drive a shock into the H I region. In fact, the transition OC can also be viewed as a strong shock (OD) in the neutral gas followed by a D-critical ionization front (DC) *relative to point D*.

As the I-front continues outward ϕ and $\dot{m}$ decrease further and the front moves subsonically relative to the ionized gas. The shock driven by the excess pressure of the H II region can thus outrun the I-front, and we now have transitions of the type OEF in which a shock in the isothermal neutral gas is followed by a weak D-front. The shock progressively slows and the I-front progressively weakens, passing from transitions like OGH to transitions like OIJ, in which the shock is very weak (OI is nearly tangent to the isotherm, hence the Mach number is near unity) and is followed by a very weak D-front ($\dot{m}$ is nearly zero). Ultimately, the system approaches equilibrium in the transition OK, with $\dot{m} = 0$, and a static Strömgren sphere is formed. Note, however, that all early type stars embedded in H II regions have strong winds (cf. §107) that are a major source of energy and momentum to the interstellar medium, hence the purely radiation-driven flow discussed above ceases to provide a realistic description at late times when the dynamical effects of the stellar wind dominate.

If the sequence just described is reversed, we recover the scenario discussed earlier for ablation fronts. An important difference is that in Kahn's analysis (**K1**) of an I-front backed by vacuum, rarefaction waves running ahead of a D-front tend to maintain it in a D-critical condition until ϕ becomes large enough to force the front to be R-critical. Much of the early analytical work on the propagation of I-fronts in H II regions was based on the simplifying assumption that the I-front following remained exactly D-critical. But numerical calculations show (**L5**) that in reality this approximation is not at all appropriate for H II regions (because the large pressure in the ionized gas drives a strong shock, which must be followed by a weak D-front) until the H II region expands nearly to its equilibrium position and $\phi \rightarrow 0$.

The numerical models (**M6**), (**L5**) of H II regions employ the one-dimensional Lagrangean hydrodynamics schemes discussed in §59. One uses the equation of continuity to relate radii to a Lagrangean mass or space variable as in (59.84); Euler's equation of motion with a pseudo-viscous pressure and zero gravity [cf. (59.82)]; and an energy equation of the general form

$$(De/Dt) + p[D(1/\rho)/Dt] = \mathcal{G} - \mathcal{L}, \qquad (106.40)$$

where $\mathcal{G}$ and $\mathcal{L}$ are radiative gains and losses per unit mass. The ionization state of the material is determined by the rate equation

$$(Dx/Dt) = (1-x)\bar{\alpha}\phi - (\rho/m_{\rm H})x^2\beta(T), \qquad (106.41)$$

where x is the ionization fraction and $\beta(T)$ is a recombination coefficient, while the photon flux follows from the (quasi-static) transfer equation

$$\frac{1}{r^2}\frac{\partial}{\partial r}(r^2\phi) = \frac{-\rho}{m_{\mathrm{H}}}(1-x)\bar{\alpha}\phi. \tag{106.42}$$

These equations are discretized and solved using basically the techniques described in §59. The I-front, however, requires special treatment. Mathews (**M6**) used a special integration scheme suggested by Henyey to handle the numerical stiffness of (106.41) as the ionization fraction approaches equilibrium. In addition he used extremely fine zones in the I-front along with a rezoning scheme that added new zones in the upstream gas as it entered the I-front and discarded unnecessary zones in the downstream flow. In contrast, Lasker (**L5**) used an algorithm that smears the discontinuous I-front over a few zones, a method analogous to using pseudoviscosity to smear shocks. In present-day computations it would be preferable to handle the I-front with an adaptive-mesh technique.

Lasker's calculations follow the evolution of an H II region well beyond the R-critical stage studied by Vandervoort and by Mathews. The exciting

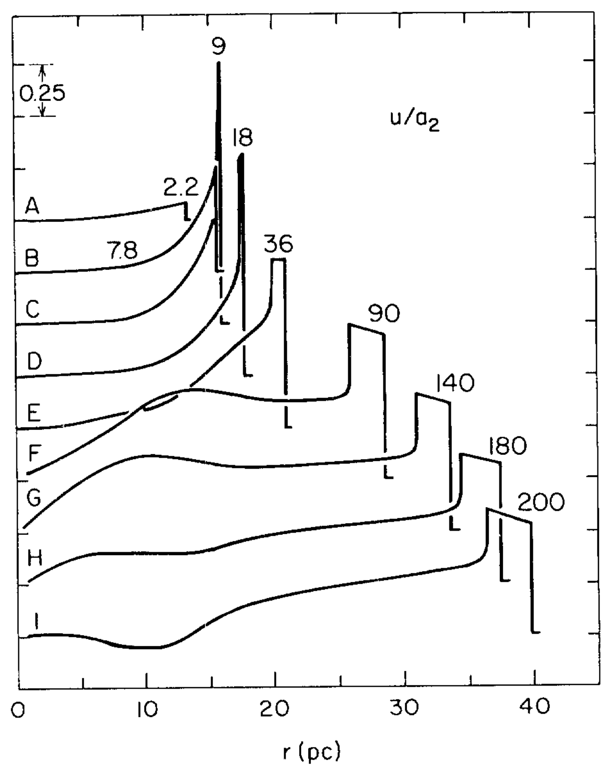

Fig. 106.4 Time evolution of velocity structure of an H II region. From (**L5**), by permission.

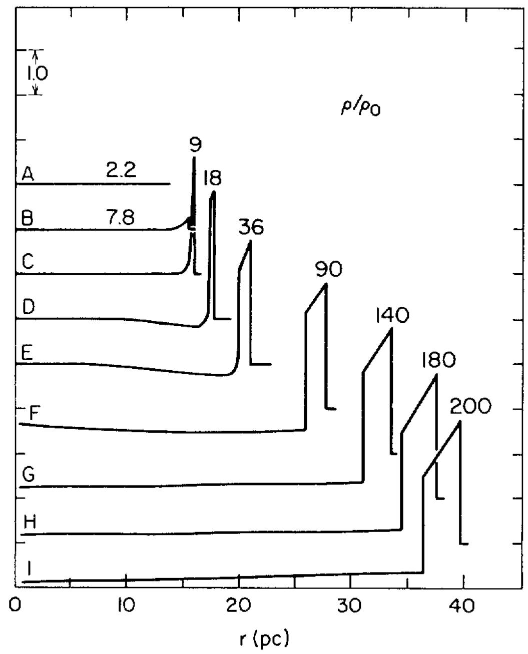

Fig. 106.5 Time evolution of density structure of an H II region. From (**L5**), by permission.

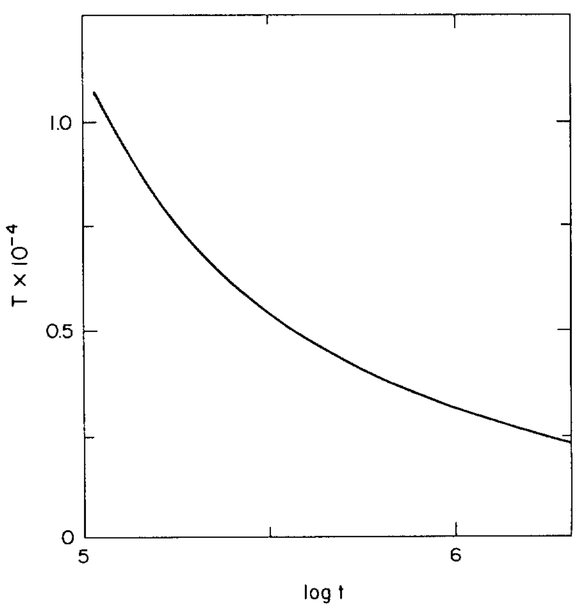

Fig. 106.6 Temperature immediately behind shock in an H II region. From (**L5**), by permission.

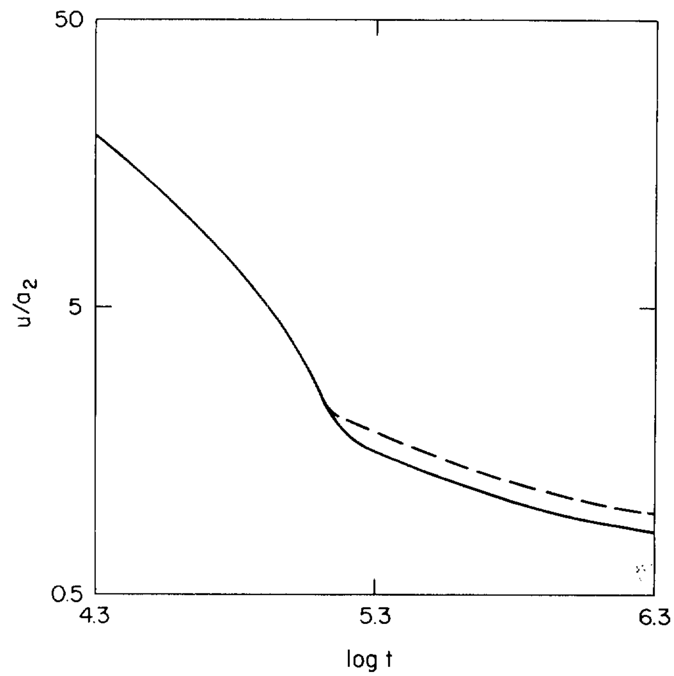

Fig. 106.7 Velocity of shock (upper curve) and I-front (lower curve) in an H II region. From (**L5**), by permission.

star is assumed to start radiating instantaneously in an infinite homogeneous cloud with an initial temperature $T_0 = 100$ K. The results shown in Figures 106.4 to 106.7 apply to a model with an initial number density $N_0 = 6.4 \text{ cm}^{-3}$. Models A to C cover the initial stages of R-front propagation; in model C the shock has just formed and is slightly separated from the I-front. The shock compresses the neutral material as it passes over it, and in model D a distinct shell of compressed neutral gas is evident. This shell, which is driven outward by excess pressure in the H II region, becomes thicker and thicker in subsequent models as the shock progressively moves away from the I-front. The strength of the shock decreases in time both because of geometrical divergence and because the pressure and density drop in the H II region as it expands. The temperature immediately behind the shock and the velocities of the I-front and shock as functions of time are shown in Figures 106.6 and 106.7.

107. Radiation-Driven Winds

The main effect of radiation in the radiation-driven flows we have considered so far is to provide an energy input to the gas, which heats it, hence raises its pressure, and thus drives a flow, perhaps explosively. We now consider an example of a flow driven by radiative *momentum* input to the gas, that is, a flow that results from the work done by the *radiation force* on the material, even in the absence of net energy exchange between the gas and the radiation field.

In recent years a variety of observations from spacecraft and ground-based observatories have shown that hot, luminous, early type stars have massive stellar winds. Analyses of line profiles and infrared emission (**A4**), (**A5**), (**G1**), (**L1**) imply mass-loss rates $\dot{\mathcal{M}}$ of order 10^{-6} to $10^{-5}\mathcal{M}_\odot$/year for O-stars, and perhaps up to $10^{-4}\mathcal{M}_\odot$/year for Wolf–Rayet stars; recall from §61 that the mass-loss rate in the solar wind is only $10^{-14}\mathcal{M}_\odot$/year. The observations indicate transonic winds, with flow velocities that rise from near zero in the stellar photosphere to highly supersonic values within one stellar radius from the surface. For O-stars the observed terminal velocities v_∞ are typically about three times the escape velocity v_{esc}, which is about 1000 to 1500 km s^{-1} for a main-sequence O-star and 600 to 900 km s^{-1} for an O-supergiant (**A1**), (**G1**). The sound velocity in the atmospheres of these stars is about 25 km s^{-1}.

Lucy and Solomon (**L10**) recognized that these flows cannot be explained by the thermal wind model described in §61 because if the specific enthalpy at the critical point is to provide the observed terminal kinetic energy flux, then the critical-point temperature would have to be $T_c \sim 3\times10^7$ K for $v_\infty \approx 3000$ km s^{-1}. This high value is excluded because lines from ions that would be destroyed by collisional ionization at temperatures greater than about 3×10^5 K are present throughout most of the flow. (However, soft X rays are also observed from O-stars, hence there must be at least some material at coronal temperatures embedded in the flow; nevertheless the bulk of the flow is too cool to be a thermal wind.)

The most natural way to explain the flow is that it is driven by momentum input to the gas from the intense radiation fields of these extremely luminous stars, in particular by the radiation force exerted on strong spectrum lines. We emphasize that, as in §61, our goal here is to elucidate some of the underlying physics of radiation-driven winds, not to develop realistic models of the winds of particular stars.

THE EDDINGTON-LIMIT LUMINOSITY

Radiative momentum input to the gas results when photons are absorbed from the anisotropic (indeed almost purely radially streaming at large distances from the star) stellar radiation field, and then scattered isotropically. The absorbed photons deposit all their outward-directed momentum into the material, but because the scattering process is isotropic, the reemitted photons produce no net change in the momentum of the material, which therefore experiences a net gain of outward momentum. The ions scattering the radiation are thus accelerated radially and they drag along the rest of the plasma through momentum exchange in Coulomb collisions.

Therefore the outward acceleration of the gas is

$$g_R = \int_0^\infty \chi_\nu F_\nu \, d\nu/\rho c, \tag{107.1}$$

where χ_ν is the total extinction from all sources (continua, electron scattering, and lines) and F_ν is the radiation flux. Note that a photon is not destroyed when it is scattered, but is merely redshifted by at most $\Delta\nu = \nu_0 v_\infty/c$; because $\Delta\nu/\nu_0 \ll 1$, each photon can in principle be scattered many times before it is extinguished.

The outward *radiative acceleration* g_R is to be compared with the inward acceleration of gravity, $g = G\mathcal{M}/r^2$; if g is everywhere greater than g_R then the atmosphere remains in hydrostatic equilibrium and does not expand. For convenience define the *force ratio*

$$\Gamma \equiv g_R/g. \tag{107.2}$$

In O-stars the continuous opacity is dominated by electron scattering in those spectral regions where most of the flux emerges. We therefore obtain a reasonable lower bound for Γ if we assume that the opacity is pure Thomson scattering, namely

$$\Gamma_e = s_e L/4\pi c G\mathcal{M}, \tag{107.3}$$

where $s_e \equiv n_e \sigma_e/\rho$ is the electron scattering coefficient per gram.

Consider now a spherically symmetric steady flow from a star. Parameterizing the radiation force as in (107.2), we write the momentum equation (96.2) as

$$\rho v(dv/dr) = -(dp/dr) - G\mathcal{M}(1-\Gamma)\rho/r. \tag{107.4}$$

The pressure can be expressed as $p = a^2\rho$, where a is the isothermal sound speed, assumed to be, in general, a function of r. [For brevity we drop the subscript "T" used in (51.26); no confusion should result because we will not be referring to the adiabatic sound speed in this section.] From the equation of state and the continuity equation we find

$$\rho^{-1}(dp/dr) = (da^2/dr) - (2a^2/r) - (a^2/v)(dv/dr), \tag{107.5}$$

whence we can rewrite (107.4) as

$$[1 - (a^2/v^2)]v(dv/dr) = (2a^2/r) - (da^2/dr) - G\mathcal{M}(1-\Gamma)/r^2. \tag{107.6}$$

We now ask under what conditions one can have a continuous transonic flow under the combined action of gravity and radiation (**M3**). For simplicity, assume the envelope is isothermal and drop (da^2/dr). It is then evident that to obtain a smooth transition from subsonic flow at small r to supersonic flow at large r, the right-hand side of (107.6) must (1) vanish at the sonic radius r_s where $v(r_s) \equiv v_s = a$; (2) be negative for $r < r_s$; and (3) be positive for $r > r_s$. The condition for $r < r_s$ can be met only if $\Gamma < 1$ in that region; that is, in the subsonic flow region the radiation force must be less than that of gravity if a steady flow is to accelerate outward. In contrast, in the supersonic flow region ($r > r_s$) Γ may become arbitrarily large; indeed the larger it is, the greater is the momentum input to the gas, and the larger (dv/dr), hence v_∞, will be.

If Γ is greater than unity everywhere in a stellar envelope, steady transonic flow is impossible; one must have either an initially subsonic flow that decelerates outward, an initially supersonic flow that accelerates outward, or (most likely) a time-dependent flow. As Eddington pointed out, if Γ_e (which always underestimates the radiation force because $\chi_\nu \geq n_e\sigma_e$) rises to unity at some point in the envelope, one can expect $\Gamma \gtrsim 1$ throughout the remainder of the stellar interior because both the radiation flux and the force of gravity scale as r^{-2}. In this event the material is unbound gravitationally, so the star becomes unstable, and can freely expand homologously on a short time scale. The critical luminosity

$$L_E \equiv 4\pi c G\mathcal{M}/s_e \qquad (107.7)$$

is called the *Eddington-limit luminosity*. Objects of radius R having $L \gg L_E$ can be expected to be blown apart by radiation pressure on a dynamical time scale of order

$$t_L \sim (4\pi c R^3/s_e L)^{1/2}. \qquad (107.8)$$

Numerically (107.3) gives $\Gamma_e \approx 2.5 \times 10^{-5}(L/L_\odot)(\mathcal{M}_\odot/\mathcal{M})$; for an O-star $L \approx 10^6 L_\odot$ and $\mathcal{M} \approx 60\mathcal{M}_\odot$, hence $\Gamma_e \approx 0.4$. Thus the radiation force from continuum opacity alone does not exceed gravity, which implies (1) that normal O-stars are stable against radiative disruption, and (2) that the continuum radiation force cannot drive a transonic wind by itself. We must therefore look to spectral lines to provide the required force.

THE RADIATION FORCE ON SPECTRAL LINES

In order to focus on the momentum (as opposed to energy) transfer from radiation to the material, we assume pure conservative scattering lines. At great optical depth where the diffusion approximation is valid, $F_\nu \propto \chi_\nu^{-1}$, hence in this regime the product $\chi_\nu F_\nu$ in (107.1) is independent of the value of χ_ν, and lines are no more effective than the continuum in delivering momentum to the gas. Therefore at depth Γ remains essentially equal to Γ_e. However in optically thin material the situation is quite different. Near the surface of a star F_ν can rise far above its diffusion-limit value because intense radiation emerges from the material below, and none is incident from above.

To estimate the maximum force that can result from a single line, assume that some optically thin material is irradiated from below with unattenuated continuum radiation, that is, $F_\nu = F_c = \pi B_\nu(T_{\text{eff}})$. Then an upper limit to the acceleration of the gas produced by a single line of an atom of chemical species k, in excitation state i of ionization state j, is

$$g_R^0 = (\pi^2 e^2/mc^2) f B_\nu(T_{\text{eff}})(n_{ijk}/N_{jk})(N_{jk}/N_k)(\alpha_k/X m_{\text{H}}), \qquad (107.9)$$

where n_{ijk} is the population of the particular level, N_{jk} is the total number of ions in all excitation states of ionization stage j, N_k is the total number density in all ionization stages of species k, α_k is the abundance of species k relative to hydrogen, and X is the mass fraction of the stellar material that is hydrogen. For example, Lucy and Solomon (**L10**) considered the C IV resonance line at $\lambda 1548$ Å; adopting an oscillator strength $f=0.2$, $T_{\text{eff}}=25{,}000$ K (to maximize B_ν), $\alpha_C = 3\times10^{-4}$, $X=1$, and $(n_{ijC}/N_{jC})=1$ they found

$$\log(g_R^0)_{\lambda 1548} = 5.47 + \log(N_{jC}/N_C) \tag{107.10}$$

For an O-supergiant $\log g \approx 3$; hence in the outer layers of such a star the upper limit for the radiation force from even this one line exceeds the force of gravity by a factor of 300!

The estimate just derived is (purposely) a gross upper limit because ions in the underlying stellar photosphere produce a dark absorption line in which $F_\nu \ll F_c$. To account for this effect, Lucy and Solomon solved the line transfer equation in detail and found that above a certain level in the atmosphere the radiation force given by (107.1) for the C IV line above still exceeded gravity. Similar results are also obtained from model atmosphere calculations for early type stars, where the radiation force from a realistic line spectrum is often found to exceed gravity at the surface of the model. Thus for O-stars the radiation force obtained when the atmosphere is assumed to be static is incompatible with that assumption; hence hydrostatic equilibrium in the outermost layers is not possible, and an outflow of material must inevitably occur.

To understand how the flow develops, consider the following scenario. Once the gas in the uppermost layer begins to move outward, its spectrum lines will be Doppler shifted away from their rest wavelengths and will therefore begin to intercept the intense photospheric flux in the adjacent continuum, which enhances the momentum input to the material, hence increases its outward acceleration. The underlying layers must expand to fill the rarefaction left by the outward motion of the upper layers. Furthermore, the absorption lines in these lower layers begin to desaturate because the lines in overlying layers have been Doppler shifted, hence the underlying layers also begin to experience a radiative force that exceeds gravity, and behave, in turn, in the manner just described. Clearly a flow can be initiated by this mechanism; we now must inquire whether (1) the rate of mass loss so produced is significant, and (2) the variation of the radiation force with depth will be consistent with the requirements for transonic flow.

In connection with the latter point, one should note that the radiation force on the continuum plus lines has precisely the right behavior to produce a transonic wind. That is, Γ is less than unity in the diffusion regime inside the star, approaches unity in the atmosphere as some lines begin to desaturate and the gas begins to flow, and reaches very large values in the supersonic flow region where the lines are sufficiently displaced from their rest frequencies to absorb continuum radiation from the underlying photosphere. Moreover, we will shortly see that to a good approximation the radiation force on lines varies as a power of the velocity gradient in the flow; this dependence allows the force and the flow it drives to accommodate to one another, so that a steady transonic flow can be attained.

The first attempt to obtain quantitative results was made by Lucy and Solomon, who evaluated (107.1) numerically for scattering lines formed in an expanding envelope above a hydrostatic photosphere. In solving the transfer equation, re-emissions can be ignored because they contribute nothing to the net force exerted by radiation on the material. Therefore, the incident photospheric intensity is simply attenuated exponentially as it scatters in a line, hence $I_\nu(\tau_\nu) = I_\nu(0) \exp(-\tau_\nu/\mu)$, where τ_ν is the optical depth, at lab-frame frequency ν, from the base of the envelope to the test point, allowing for Doppler shifting of the line profile along the path. Then

$$g_{R,l} = (2\pi/c\rho) \sum_l \int_0^1 d\mu \int_0^\infty d\nu \chi_l(\nu) I_\nu(0) \mu e^{-\tau_\nu/\mu} \qquad (107.11)$$

where the sum extends over all lines considered.

Lucy and Solomon coupled (107.11) to the equations of steady flow to construct radiatively driven wind models for O- and B-stars. They assumed planar geometry (adequate for the flow inside the sonic point), isothermal material, a simple nebular photoionization-recombination ionization equilibrium, and that the radiation force results from absorption in the resonance lines of a few abundant ions. The solution was obtained by an iteration procedure that yields the mass flux as an eigenvalue. A large number of models were constructed for a wide range of stellar parameters. These models successfully produced transonic flows having reasonable terminal velocities, $v_\infty \sim 3000 \text{ km s}^{-1}$, but the computed mass-loss rates were only $10^{-8} \mathcal{M}_\odot/\text{year}$ or less, which is two orders of magnitude smaller than the observed values.

The source of this discrepancy was identified by Castor, Abbott, and Klein (**C11**) who pointed out that *hundreds* of lines in the spectrum make important contributions to the total radiation force, so that Lucy and Solomon's estimate, based on only a few lines, is roughly a hundredfold too small (**C12**). As it would be hopeless to calculate the aggregate radiation force from hundreds of lines by a direct numerical solution of the transfer equation, recourse must be had to an approximate analytical method. The essential point is to account for saturation in the lines, so that the correct transition is made between the optically thick and thin limits. This problem was solved in detail by Castor (**C9**); here we make only a simple heuristic argument to recover the main result.

We assume that the incident photospheric radiation field on the lines is essentially radial, and approximate the momentum absorbed, per unit mass, by a line of opacity χ_l and width $\Delta\nu_D$ from the unattenuated continuum flux F_c as $g_{R,l}(0) = \chi_l\,\Delta\nu_D F_c/c\rho$. We ignore re-emissions, as before; then the incident flux is attenuated as $e^{-\tau_l}$ where, as in (107.11), τ_l is the line optical depth in a layer, allowing for Doppler shifts. The average rate of momentum input to a layer of optical depth τ_l is then

$$\langle g_{R,l}\rangle = g_{R,l}(0)\tau_l^{-1}\int_0^{\tau_l} e^{-\tau'}\,d\tau' \tag{107.12}$$

or

$$\langle g_{R,l}\rangle = (\chi_l\,\Delta\nu_D F_c/c\rho)(1-e^{-\tau_l})/\tau_l. \tag{107.13}$$

In their work Castor, Abbott, and Klein approximate $\tau_l^{-1}(1-e^{-\tau_l})$ by $\min(1, \tau_l^{-1})$. In the optically thin limit, (107.13) reduces to

$$\langle g_{R,l}\rangle_{\text{thin}} = \chi_l\,\Delta\nu_D F_c/c\rho, \tag{107.14}$$

so that, as in (107.9), the force on a line is proportional to its opacity, hence strong lines are more important than weak lines. In the optically thick limit (107.13) reduces to

$$\langle g_{R,l}\rangle_{\text{thick}} = \chi_l\,\Delta\nu_D F_c/c\rho\tau_l, \tag{107.15}$$

which shows that the force on a line is independent of its strength (because τ_l scales as χ_l), hence all lines are of equal importance, as expected in the diffusion limit.

We must now specify the effective optical thickness of the envelope. For a static medium

$$\tau_l = \int_R^\infty \chi_l\,dr, \tag{107.16}$$

hence τ_l is determined by the strength of the line and the amount of material in the line-forming layers.

For an expanding medium the situation is quite different. Here photons emitted at one position are always redshifted when they arrive at some other position in the flow by an amount proportional to the average velocity gradient times the distance between the two positions. Therefore photons emitted at line center at some point can interact with the material only within a localized *resonance region;* beyond this region they fall too far in the wing of the line profile of the material at the remote position to be absorbed effectively, hence they escape without further interactions. Line transport in such a flow regime is described by *Sobolev theory* (**S14**), (**S15**), (**C8**). We cannot discuss this theory in detail here, but from mere dimensional considerations one can see that for an idealized square-topped line profile of width $\Delta\nu = \nu_0 v_{\text{th}}/c$ (where v_{th} is the thermal speed of the absorbing atoms), the characteristic distance within which radiative interactions can occur must be of order $l \sim v_{\text{th}}/|\nabla v|$. Hence for radially streaming radiation in an expanding medium we can take

$$\tau_l \equiv \chi_l v_{\text{th}}/(dv/dr). \tag{107.17}$$

The important difference between (107.16) and (107.17) is that a large velocity gradient serves to reduce τ_l from its static value, hence to desaturate the line, and thus to increase the radiation force on that line, perhaps by orders of magnitude.

In estimating the total radiation force from an ensemble of lines, we will use (107.17) throughout the entire wind, even though it becomes invalid in the nearly hydrostatic photosphere (because the line radiation force is unimportant there anyway). It is convenient to use a depth variable that is independent of line strength, so we define $\beta_l \equiv n_e\sigma_e/\chi_l$ and introduce an equivalent electron optical depth scale

$$\ell \equiv \beta_l \tau_l = n_e \sigma_e v_{\text{th}}/(dv/dr). \tag{107.18}$$

The total radiation force is obtained by summing (107.13) over all lines, which gives

$$g_{R,l} = (s_e F/c) M(\ell) = (s_e L/4\pi c r^2) M(\ell) \tag{107.19}$$

where

$$M(\ell) \equiv \frac{1}{F} \sum_l \frac{F_c(\nu_l)\, \Delta\nu_{D,l} (1 - e^{-\ell/\beta_l})}{\ell} \approx \frac{1}{F} \sum_l F_c(\nu_l)\, \Delta\nu_{D,l} \min\left(\frac{1}{\beta_l}, \frac{1}{\ell}\right) \tag{107.20}$$

is the *line force multiplier.* The calculation of the radiation force is thus reduced to the evaluation of $M(\ell)$ which, for a specified temperature and density and a given set of lines, is a function of only the one parameter ℓ. The local excitation and ionization equilibrium enters through the parameter β_l.

It is important to note that (107.20) has only limited accuracy because two important approximations have been made in deriving it. (1) We assumed radially streaming radiation, and ignored the angular integration over the finite solid angle subtended by the stellar photosphere. The effect of this omission is to overestimate the radiation force close to the photosphere. (2) We assumed that each photon is scattered only once in one resonance region, and ignored the possibility of multiple scatterings in several (perhaps overlapping) lines. The effect of this omission is to underestimate the total amount of momentum that a photon can deposit in the gas in the high flow-velocity region. We return to these issues later.

LINE-DRIVEN WINDS

A comprehensive and internally consistent analytical theory for line-driven winds was first developed by Castor, Abbott, and Klein (**C11**), which, for brevity, we call the *CAK theory*. They assumed that the flow is steady and spherically symmetric, that the gas is a single fluid, and that conduction and viscosity can be neglected; these assumptions are justified in detail in (**C12**). The flow is calculated for a given temperature distribution $T(r)$, which ultimately is determined in an iteration procedure by imposing radiative equilibrium. The latter assumption is reasonable because the thermal relaxation time of the gas is much shorter than a characteristic flow time, but may lead to an unrealistic temperature distribution (e.g., if the flow is unstable and disintegrates into shocks) and to an unrealistic predicted spectrum. But we emphasize that the temperature distribution can have essentially no influence on the gross dynamics of the wind unless temperatures rise to order 10^7 K, and/or there are extreme temperature gradients. Gas pressure, hence temperature, is important only in the subsonic flow regime, which is also the part of the flow where radiative equilibrium is most likely to be a good approximation; it is inconsequential in the supersonic flow regime.

Castor, Abbott, and Klein evaluated the line force multiplier $M(t)$ for the spectrum of the representative ion C^{++}, and assuming that those results were typical they scaled them to account for the total abundance of C, N, and O. The occupation numbers were computed from LTE. Their results are well fitted by the formula

$$M(t) = k t^{-\alpha} \tag{107.21}$$

with $k \approx \frac{1}{30}$ and $\alpha = 0.7$. An exhaustive analysis (**A3**) based on a complete line list for all relevant ions of the elements H to Zn yields a more accurate expression valid for $10^4\,\mathrm{K} \leq T_{\mathrm{eff}} \leq 5\times 10^4\,\mathrm{K}$, namely,

$$M(t) = 0.28(N_{11})^{0.09} t^{-0.56}. \tag{107.22}$$

Here $N_{11} \equiv (n_e/W)\times 10^{-11}$ and W is the *dilution factor* of the radiation field [the fraction of 4π steradians subtended by photospheric radiation, cf. (**M10,** 120)]. Substituting (107.21) and (107.18) into (107.19) we have

$$g_{R,l} = \left(\frac{s_e L k}{4\pi c r^2}\right)\left(\frac{1}{n_e \sigma_e v_{\mathrm{th}}}\frac{dv}{dr}\right)^{\alpha} = \frac{C}{r^2}\left(r^2 v \frac{dv}{dr}\right)^{\alpha}. \tag{107.23}$$

The second equality follows from the equation of continuity, and the constant is

$$C = (s_e L k/4\pi c)(4\pi/s_e v_{\mathrm{th}} \dot{\mathcal{M}})^{\alpha}. \tag{107.24}$$

Using (107.23) for the line radiation force we can rewrite the equation of motion (107.6) as

$$\left(1-\frac{a^2}{v^2}\right)v\frac{dv}{dr} = \frac{2a^2}{r} - \frac{da^2}{dr} - \frac{G\mathcal{M}(1-\Gamma_e)}{r^2} + \frac{C}{r^2}\left(r^2 v\frac{dv}{dr}\right)^{\alpha}. \tag{107.25}$$

Unlike (61.13) for thermal winds, (107.25) is *nonlinear* in (dv/dr); as a result it has quite different mathematical properties. In particular, notice that the sonic point $(v = a)$ is not the critical point of (107.25) because when the left-hand side vanishes, the right-hand side can be made to vanish as well with a suitable choice of (dv/dr), which need not (1) vanish, or (2) become infinite, or (3) be discontinuous. This difference from thermal wind theory results from our use of a force law that has an *explicit* dependence on (dv/dr). Had we used some generic $g_{R,l}$ (perhaps obtained from a numerical line transfer computation) which depends explicitly on r but only *implicitly* on (dv/dr), we would again conclude that the sonic point r_s is the critical point. The solution would then proceed as in thermal wind theory, but at the cost, as we shortly see, of losing important physical insight (and possibly of poor numerical convergence as well).

Equation (107.25) is equivalent to

$$F(u, w, w') \equiv [1-\tfrac{1}{2}(a^2/w)]w' - h(u) - C(w')^\alpha = 0, \qquad (107.26)$$

where $w \equiv \tfrac{1}{2}v^2$, $u \equiv -1/r$, $w' \equiv (dw/du)$, and

$$h(u) \equiv -G\mathcal{M}(1-\Gamma_e) - 2(a^2/u) - (da^2/du). \qquad (107.27)$$

The differential equation (107.26) has a *singular point* at which solutions terminate, have cusps, or show other discontinuities; it is defined by the condition

$$\partial F(u, w, w')/\partial w' = 1 - \tfrac{1}{2}(a^2/w) - \alpha C(w')^{\alpha-1} = 0. \qquad (107.28)$$

One may eliminate w' between (107.26) and (107.28), and for a given value of C thus determine the *locus of singular points* $w(u, C)$. To guarantee that the solution passes smoothly through the singular point we demand that w' be continuous there; this requirement can be met only if the solution is *tangent* to the singular locus at its point of contact, which is guaranteed by imposing the *regularity condition*

$$(dF/du)_c = [(\partial F/\partial u) + w'(\partial F/\partial w)]_c = 0. \qquad (107.29)$$

Equations (107.26), (107.28), and (107.29) uniquely determine the *critical point* u_c (or r_c) for a given C, or, conversely, C for a specified r_c.

A detailed analysis (**C11**), (**A2**) of the behavior of (107.26) and (107.27) shows that the (u, w) plane is divided into five regions, in each of which there are zero (regions IV and V), one (regions I and III), or two (region II) mathematically valid solutions. An example is shown in Figure 107.1 for a case with $v_{\rm esc} = 4.9a$ and $\Gamma_{R,l} = g_{R,l}/g = 0.76(w')^{1/2}$; the photospheric radius is denoted as R. We see that there is a unique transonic solution in which the subcritical and supercritical branches join smoothly at tangency with the locus of singular points.

Figure 107.1 shows that a line-driven wind is already supersonic at the critical point. It thus appears that the critical point is located beyond the position in the flow where information can still be propagated upstream, and it is not obvious how conditions at r_c are able to determine conditions in the entire flow. We must therefore examine the physical significance of the critical point carefully. Abbott (**A2**) developed a physical interpretation of the critical point by examining the behavior of small-amplitude disturbances of the flow in its vicinity. Thus consider a time-dependent planar flow with velocity $v(z')$ and radiation force $f_l(z', v, dv/dz')$ directed along the z' axis. For simplicity ignore stratification effects. In the neighborhood

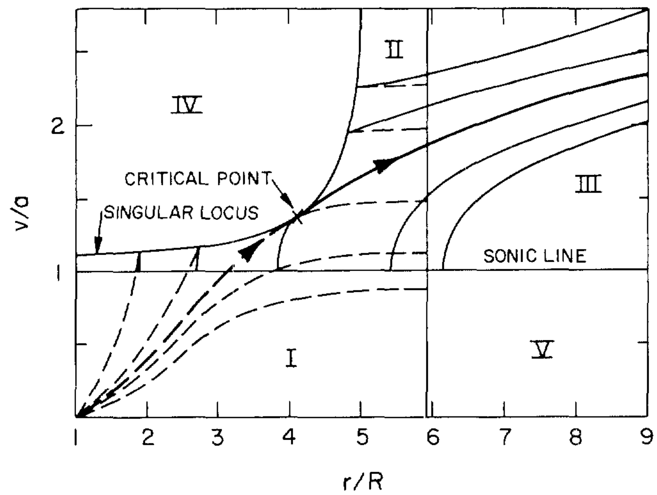

Fig. 107.1 Topology of radiatively driven wind solutions, showing singular locus, critical point, and regions with zero, one, or two mathematically valid solutions. From (**A2**), by permission.

of some point z_0' make a Galilean transformation to a frame moving with a uniform velocity $v_0 \equiv v(z_0')$, so that $z = z' - v_0 t$. Write the perturbed velocity as $v = v_0 + v_1$. Then the linearized continuity equation is

$$(\partial \rho_1/\partial t) + \rho_0(\partial v_1/\partial z) = 0, \qquad (107.30)$$

and the vertical component of the momentum equation is

$$\rho_0(\partial v_1/\partial t) = -(\partial p_1/\partial z) + \rho_0 f_l'(\partial v_1/\partial z), \qquad (107.31)$$

where we assumed $f_l = f_l(\ell) = f_l[\rho^{-1}(dv/dz)]$, and f_l' denotes the derivative of f_l with respect to (dv_1/dz). We restrict attention to vertically propagating disturbances; Abbott analyzes obliquely propagating disturbances as well.

Using the isothermal equation of state to eliminate the pressure perturbation $p_1 = a^2\rho_1$, we can combine (107.30) and (107.31) into

$$(\partial^2 v_1/\partial t^2) - a^2(\partial^2 v_1/\partial z^2) - f_l'(\partial^2 v_1/\partial t\, \partial z) = 0. \qquad (107.32)$$

Equation (107.32) is a wave equation that can be recast as

$$(\partial^2 v_1/\partial p\, \partial q) = 0 \qquad (107.33)$$

by transforming from (z, t) to new coordinates $p \equiv z + C_- t$ and $q \equiv z - C_+ t$, where

$$C_- = \tfrac{1}{2}f_l' + [(\tfrac{1}{2}f_l')^2 + a^2]^{1/2} \qquad (107.34a)$$

and

$$C_+ = -\tfrac{1}{2}f_l' + [(\tfrac{1}{2}f_l')^2 + a^2]^{1/2}. \qquad (107.34b)$$

The solution of (107.33) is composed of the two traveling waves

$$v_1(z, t) = V_1(z + C_- t) + V_2(z - C_+ t), \qquad (107.35)$$

where V_1 and V_2 are arbitrary functions of their arguments. In the CAK model it follows from (107.18), (107.21), and the planar version of (107.28) that near the critical point $f'_l/a \sim v/a \gg 1$, hence $C_- \approx f'_l \gg a$, and $C_+ \approx a(a/f'_l) \ll a$. Thus we have a slow radiation-modified acoustic wave traveling outward and a fast radiation-modified acoustic wave traveling inward. This result applies only to long wavelength disturbances, for which the CAK force law could be valid (**O6**).

Abbott showed (**A1**) that the full nonlinear continuity and momentum equations for a line-driven wind have characteristics in the (r, t) plane given by

$$(dr/dt) = (v - \tfrac{1}{2}f'_l) \pm [(\tfrac{1}{2}f'_l)^2 + a^2]^{1/2}. \qquad (107.36)$$

These characteristics define the speed at which a disturbance will propagate in the flow. Transforming (107.35) back to the rest frame we have

$$v_1(z', t) = V_1[z' - (v_0 - C_-)t] + V_2[z' - (v_0 + C_+)t], \qquad (107.37)$$

which represents disturbances propagating outward with speeds $v_0 + C_+$ and $v_0 - C_-$; from (107.34) we see that these speeds are in exact agreement with (107.36).

Now at the critical point, the CAK singularity condition (107.28) implies $[1 - (a^2/v_c^2)]v_c = f'_l$. When this relation is substituted into (107.36) we find that the velocity of the radiation-modified acoustic waves as seen by an observer in the rest frame is

$$v_\pm = \tfrac{1}{2}(v_c \pm v_c)[1 + (a^2/v_c^2)], \qquad (107.38)$$

or

$$v_+ = v_c[1 + (a^2/v_c^2)] \qquad (107.39a)$$

and

$$v_- = 0. \qquad (107.39b)$$

Thus *for the adopted force law* the flow speed at the critical point of a line-driven wind just equals the inward propagation speed of small disturbances, hence beyond this point information can no longer propagate upstream in the flow. Therefore, as is true for thermal winds, the critical point is, in fact, the point farthest downstream that can still communicate with all other points on a streamline. The main difference between the two theories is the characteristic signal speed: in the absence of radiation the signal and sound speeds are the same, hence the sonic and critical points coincide, whereas in a radiating fluid they differ, hence the sonic and critical points are distinct. These conclusions depend sensitively, however, on the force law adopted, and may not be valid in general (**O6**).

MOMENTUM TRANSPORT IN THE WIND

A line-driven wind deposits momentum (originally photon momentum) in the interstellar medium at a rate $\dot{\mathcal{M}}v_\infty$. If we assume that every photon emitted by the star scatters exactly once in the wind, then an upper bound on the mass-loss rate is

$$\dot{\mathcal{M}} \le L/v_\infty c = 7\times 10^{-12}(L/L_\odot)(3000/v_\infty) \tag{107.40}$$

where $\dot{\mathcal{M}}$ is measured in $\mathcal{M}_\odot$/year and v_∞ in km s^{-1}. For a typical O-star $L \approx 10^6 L_\odot$ and $v_\infty \approx 3000$ km s^{-1}, hence $\dot{\mathcal{M}} \approx 7\times 10^{-6}\mathcal{M}_\odot$/year, which is, in fact, a typical observed value. The parameter

$$\varepsilon \equiv c v_\infty \dot{\mathcal{M}}/L \tag{107.41}$$

provides a measure of the efficiency with which matter is radiatively ejected in a wind; for single scattering of all photons ε cannot exceed unity.

A more complete picture of the momentum distribution in a wind emerges from integrating the momentum equation (107.4) over all mass in the envelope (**A2**). For a general force law $f_l(r, v, dv/dr)$ we obtain

$$\int_0^{v_\infty} 4\pi r^2 \rho v\, dv + \int_R^\infty 4\pi r^2 \rho \left[\frac{G\mathcal{M}(1-\Gamma_e)}{r^2} + \frac{1}{\rho}\frac{dp}{dr}\right] dr = \int_R^\infty 4\pi r^2 \rho f_l\, dr. \tag{107.42}$$

The first integral in (107.42) is simply $\dot{\mathcal{M}}v_\infty$. To evaluate the second integral we argue that inside the sonic radius the gas is very nearly in hydrostatic equilibrium, in which case the integrand vanishes, whereas outside the sonic radius the gas pressure gradient is negligible compared to gravity because the line force dominates. Using (107.3) we can then approximate the second integral as

$$[L(1-\Gamma_e)/c\Gamma_e]\int_{r_s}^\infty n_e \sigma_e\, dr = L(1-\Gamma_e)\tau_e/c\Gamma_e, \tag{107.43}$$

where τ_e is the electron-scattering optical depth exterior to the sonic point. Finally, using (107.18) and (107.19), we can write the third integral in (107.42) as $\beta L/c$ where

$$\beta \equiv v_{\rm th}^{-1}\int_0^{v_\infty} M(t)t\, dv \tag{107.44}$$

is essentially the line optical depth of the envelope, and equals the equivalent number of strong lines a photon encounters as it traverses the wind. For a single-scattering model, $\beta \le 1$.

Thus momentum conservation in the wind implies that

$$\dot{\mathcal{M}}v_\infty + [\tau_e(1-\Gamma_e)/\Gamma_e](L/c) = \beta L/c, \tag{107.45}$$

which shows that the momentum transferred from photons to the gas goes partly into the momentum lost in the wind and partly into supporting the extended envelope against gravity. One sees that the parameter ε defined in (107.41) underestimates the total photon momentum consumed in driving a wind of a given $\dot{\mathcal{M}}v_\infty$ because it omits the momentum transfer rate required to support the envelope.

RESULTS FROM CAK THEORY

For the CAK radiation-force law, explicit analytical expressions can be obtained for the mass-loss rate, the velocity law, and the critical radius (**C11**). Assuming that $v_{\text{esc}} \gg a$ and taking the radius at which the velocity vanishes to be approximately the sonic radius r_s (which in turn is nearly the same as the photospheric radius R) one finds

$$\dot{\mathcal{M}} = \left(\frac{4\pi G\mathcal{M}}{s_e v_{\text{th}}}\right)\alpha\left(\frac{1-\alpha}{1-\Gamma_e}\right)^{(1-\alpha)/\alpha}(k\Gamma_e)^{1/\alpha}, \tag{107.46}$$

$$v^2 = \frac{2G\mathcal{M}(1-\Gamma_e)\alpha}{(1-\alpha)}\left(\frac{1}{r_s}-\frac{1}{r}\right), \tag{107.47}$$

and

$$r_c/r_s = 1+\{-\tfrac{1}{2}n+[\tfrac{1}{4}n^2+4-2n(n+1)]^{1/2}\}^{-1}. \tag{107.48}$$

Equation (107.48) is based on the assumption that $a^2 \propto T \propto r^{-n}$; likely values for n lie between 0 (isothermal) and $\frac{1}{2}$ (radiative equilibrium), hence $1.5 \lesssim (r_c/r_s) \lesssim 1.74$. From (107.47) we have

$$v_\infty/v_{\text{esc}} = [\alpha/(1-\alpha)]^{1/2}; \tag{107.49}$$

thus for $0.5 \lesssim \alpha \lesssim 0.7$, CAK theory predicts $1 \lesssim v_\infty/v_{\text{esc}} \lesssim 1.5$.

For the CAK model one can also evaluate τ_e in (107.45) analytically (**A1**), obtaining

$$\tau_e = [(1-\alpha)\Gamma_e/\alpha(1-\Gamma_e)](\dot{\mathcal{M}}v_\infty c/L). \tag{107.50}$$

Hence a momentum transfer rate $(1-\alpha)\dot{\mathcal{M}}v_\infty/\alpha$ is needed just to support the envelope in the CAK model. Combining (107.50) and (107.45) we find

$$(\dot{\mathcal{M}}v_\infty)_{\text{CAK}} = \alpha\beta(L/c), \tag{107.51}$$

or $\varepsilon_{\text{CAK}} = \alpha\beta$; inasmuch as $0.5 \lesssim \alpha \lesssim 0.7$ and $\beta \leq 1$ for single scattering, ε_{CAK} can never exceed unity, and is more likely of order 0.5.

To construct a complete stellar wind model with CAK theory one chooses L, $\mathcal{M}$, R, and an assumed temperature distribution $T(r)$; for a given choice of k and α in (107.21) the mass-loss rate is determined almost entirely by $\mathcal{M}$ and L via Γ_e. One next makes an initial guess for r_c from (107.48) with $r_s = R$; equation (107.25) is then integrated numerically, and the run of optical depth with radius is computed. The value of r_c is adjusted until an optical depth of about $\frac{2}{3}$ is reached at the photospheric radius R. Having constructed a dynamical model, one may use the resulting density structure in a spherical model atmosphere code and calculate the temperature structure by enforcing radiative equilibrium. This new temperature distribution can then be used to reconstruct the dynamical model, and the procedure iterated. Because the dynamics is insensitive to the temperature structure, the iteration process converges rapidly.

Castor, Abbott, and Klein published a solution for parameters appropriate to an O5 star: $\mathcal{M} = 60\mathcal{M}_\odot$, $L = 9.7 \times 10^5 L_\odot$, $R = 9.6 \times 10^{11}$ cm $= 13.8 R_\odot$, $T_{\rm eff} = 49{,}300$ K, $\log g = 3.94$, and $\Gamma_e = 0.4$. The resulting mass-loss rate is $\dot{\mathcal{M}} = 6.6 \times 10^{-6} \mathcal{M}_\odot$/year, a reasonable value for a star like ζ Puppis. The terminal velocity is $v_\infty = 1515$ km s^{-1}, so $\dot{\mathcal{M}} \approx \frac{1}{2} L/v_\infty c$, which shows that about one half of the momentum originally carried by radiation is transferred to the flow. Stellar evolution theory gives main-sequence lifetimes of about 3×10^6 years at this mass, which implies a total mass-loss in the wind of about one-third the original mass of the star. Thus the stellar winds from O-stars may have very significant effects on their evolution.

Some results for this model are shown in Figure 107.2. The letters P, S, and C designate the photosphere, sonic point, and critical point respectively. The velocity variation (Figure 107.2a) is quite abrupt, with highly

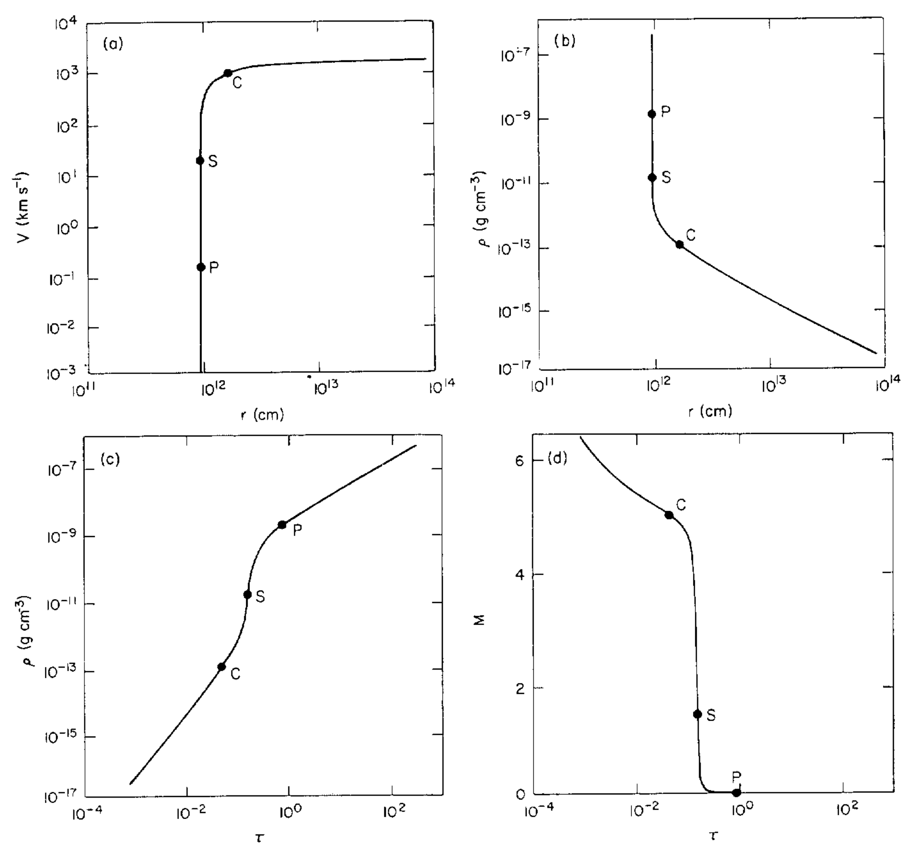

Fig. 107.2 Velocity, density, and force multiplier in CAK model. From (**C11**), by permission.

supersonic flow being achieved within a fraction of a stellar radius above the photosphere. The density distribution (Figure 107.2b) has a decided "core-halo" nature: inside the sonic point the density gradient is nearly hydrostatic, while outside the critical point the velocity is essentially constant at v_∞, hence $\rho \propto r^{-2}$. As seen in Figure 107.2c the halo is transparent in the continuum, and radiates mainly in strong spectral lines. The run of the radiation-force multiplier is shown in Figure 107.2d. In the outer envelope $M \approx 5$, which implies that the radiation force on the lines is about twice the force of gravity (recall that $\Gamma_e = 0.4$); adding the radiation force on the electrons and subtracting the force of gravity we find that the gas outside the critical point experiences a net outward acceleration of about 1.5 times gravity.

COMPARISON WITH OBSERVATIONS

On the whole, CAK gives a coherent and satisfying account of the basic dynamics of line-driven winds. Nevertheless it also shows significant discrepancies with observations, an analysis of which leads to a deeper understanding of the physics of the flow. (1) A critical comparison of observed mass-loss rates with those computed from CAK theory shows (**A3**) that for a comprehensive line list the radiation force is sufficient to drive the observed mass flux; if anything the computed values of $\dot{\mathcal{M}}$ are about a factor of 2 too large. Furthermore, the predicted scaling of $\dot{\mathcal{M}}$ with L agrees with observation over about four orders of magnitude. (2) In contrast, the computed values of $v_\infty/v_{\rm esc}$ are systematically too low. Whereas the observations show that $v_\infty/v_{\rm esc}$ is about 1 to 1.5 for early-A and late-B stars, and rises to about 3.0 for early-B and O-stars, CAK theory always predicts $1 \lesssim v_\infty/v_{\rm esc} \lesssim 1.5$ [cf. (107.49)]. Thus (107.20) fails to provide sufficient radiative acceleration in the high-velocity part of the flow. (3) the CAK velocity distribution (107.47) likewise rises much too sharply inside the critical point. A variety of observations (**B2**), (**C7**), (**L1**) indicate a "softer" velocity law, rising like

$$v = v_\infty[1-(R/r)]. \tag{107.52}$$

Evidently (107.20) gives too large a radiation force in the low-velocity regime near the stellar photosphere. (4) The CAK model cannot provide the total momentum flux observed in the winds of some stars. Using empirical values of v_∞, τ_e, and Γ_e, Abbott (**A2**) shows that for two well-observed stars, β in (107.45) exceeds unity even though ε in (107.41) is less than unity. This result is in conflict with CAK theory and demonstrates the need to account for multiple scattering of the stellar photons.

TRANSFER AND MULTIPLE-SCATTERING EFFECTS

To improve upon the CAK models one must use a more accurate radiation-force law, which implies that the transfer problem in the lines must be solved more accurately. A step in this direction was made by

Weber (**W3**) who calculated self-consistent, line-driven, steady-flow models by solving the comoving-frame line transfer equations numerically [cf. (**M10,** Chap. 14), (**M11**)] for a prechosen distribution of line strengths. This approach is expected to yield better results because: (1) it removes the Sobolev approximation inherent in (107.17) and (107.20) (which surely breaks down near the photosphere because the velocity gradient becomes small and continuum sources and sinks become increasingly important), and (2) it accounts accurately for the angular distribution of the radiation field instead of assuming radial streaming (again, an effect that is important near the stellar surface).

Weber's results are encouraging. First, the velocity rise is softer, mimicking (107.52) fairly closely near the surface of the star, and shifting towards a relation like (107.47) at large distances. Second, the terminal velocities are larger, by about a factor of 4, than the CAK results for the same line strengths. Weber finds that these improvements result mainly from accounting for the radiation field's angular distribution, in particular for the finite solid angle subtended by the stellar photosphere. This result is in harmony with the analysis by Castor (**C10**) who showed that neglect of the angular distribution causes CAK theory to overestimate the line force by about a factor of 2 near the stellar photosphere. In fact, the radiation force calculated from the CAK formula (with an optimized choice of k and α) using the wind structure obtained from the transfer solution agrees closely with the force given by the transfer calculation. Therefore the velocity distribution in the flow is quite sensitive to even small departures from the CAK force law; Abbott shows (**A2**) that this sensitivity to small changes is a peculiarity of the CAK model and is not a general property of line-driven winds.

In Weber's approach each line is modeled in detail. It is hopeless to use such a method to obtain the force law for a realistic line spectrum having hundreds to perhaps thousands of important lines, each of which may have a distinctive response to variations of temperature and density. It is therefore necessary to develop a simpler theory that still accounts for the important physics. The problem has been addressed by Castor and Friend (**C10**), (**F3**) who calculate the line radiation force allowing for multiple scattering in an ensemble of lines described by a statistical model for the distribution of lines over frequency and line strength, and also accounting for the angular distribution of the radiation field. They perform a consistent solution of the dynamical equations and random-line transfer equations to evaluate a correction factor to the force computed for radially streaming radiation.

As predicted by Castor (**C10**) the resulting force is substantially smaller near the star and much larger at large distances. Most of the discrepancies between theory and observation are removed by Friend and Castor's work (FC). For example, for a model that closely resembles the one published by CAK, $v_\infty(\text{FC}) = 3900 \text{ km s}^{-1}$ instead of $v_\infty(\text{CAK}) = 1515 \text{ km s}^{-1}$, while near the star the velocity behaves like (107.52) instead of (107.47), as desired. The mass-loss rate is nearly unchanged: $\dot{\mathcal{M}}(\text{FC}) = 8.6 \times 10^{-6} \mathcal{M}_\odot$/year, $\dot{\mathcal{M}}(\text{CAK}) = 6.6 \times 10^{-6} \mathcal{M}_\odot$/year. The velocity at the critical point drops from $v_c(\text{CAK}) = 950$ km s^{-1} to $v_c(\text{FC}) = 275$ km s^{-1}, and the critical point moves inward from $r_c(\text{CAK}) = 1.5R$ to $r_c(\text{FC}) = 1.06R$. The radiation force at r_c in the FC model is only two thirds as large as the force in the CAK model, but the total momentum flux in the wind is much larger, $\varepsilon(\text{FC}) = 1.71$ compared to $\varepsilon(\text{CAK}) = 0.51$. Likewise, the effective number of scatterings is $= 1.93$; both of these results vividly illustrate the effect of multiple scattering.

Recent models of line-driven winds include the effects of rotation and magnetic fields; see (**C10**), (**F4**), (**N2**).

ALTERNATIVE WIND THEORIES

The cool (i.e., radiative equilibrium), line-driven wind model appears to provide a good basic picture of the dynamics of the flow, but yields little, if any, information about the temperature structure and excitation-ionization equilibrium of the material. The latter are quantities of considerable interest because observations show spectrum lines from "anomalously" high ions such as N V and O VI, as well as soft X rays, all of which indicate gas temperatures far in excess of T_{eff} of the star.

A variety of models have been suggested to explain these observations including (1) the *modified cool wind model* in which the gas temperature is about 6×10^4 K and the wind is optically thick in the He II resonance continuum; (2) the *warm wind model* in which the gas temperature is of order 2×10^5 K; and (3) the *hybrid corona plus cool wind model* in which a thin ($\sim 0.1R$) hot corona with $T \sim 5 \times 10^6$ K is surrounded by a cool ($T \approx 0.8T_{\text{eff}}$) envelope. All of these models require a source of nonradiative energy input, such as heating by shocks that grow from instabilities; their relative merits are discussed in (**C4**), (**C5**), (**C6**) and the references cited therein.

All of the models mentioned so far have difficulty in explaining the soft X-ray data. Models developed by Lucy and White (**L9**), (**L11**) to explain the X-ray data invoke the growth of instabilities into the nonlinear regime. In the more recent version of the theory it is argued that small flow perturbations are radiatively amplified into shocks, which survive until "shadowing" by following shocks deprives them of the radiation force that drives them, thus allowing them to dissipate and decay.

Observations show variations in the spectra produced by winds on time-scales from hours to years. They strongly suggest that the winds may in fact be unstable. The stability of line-driven winds has been examined theoretically by several authors (**A2**), (**C2**), (**K2**), (**M1**), (**M5**), (**N1**), (**O5**). The results obtained depend sensitively on the radiation force law adopted.

For example, in an optically thin disturbance, a velocity-induced Doppler shift from the rest position of a saturated line produces a net radiation force $\delta g_{R,l} = Aw_1$, where A is positive. This force is like that for a damped harmonic oscillator, but with a negative "damping coefficient", hence one expects the perturbation to be unstable; this can indeed be the case. Nelson and Hearn (**N1**) and Martens (**M5**) showed that under certain conditions an initial disturbance varying as $e^{i\omega t}$ is *absolutely unstable* (i.e., ω is complex with a negative real part), and grows exponentially. Under similar assumptions MacGregor et al. (**M1**) showed that a driven disturbance (real ω, complex k) is subject to a *drift instability*, and grows in amplitude as it propagates outward in the wind. These results can be understood intuitively by noting that in this case w_1 and $\delta g_{R,l}$ are in phase, hence the work done by the radiation force, which is proportional to $\langle w_1\, \delta g_{R,l}\rangle$ is necessarily positive (**O5**). In contrast, Abbott (**A2**) considered optically thick disturbances and assumed that the line radiation force depends on the velocity gradient, not the velocity perturbation. As discussed earlier, he found stable radiation-modified acoustic waves. His results can also be understood intuitively by noting that in this case w_1 and $\delta g_{R,l}$ are 90° out of phase, hence $\langle w_1\, \delta g_{R,l}\rangle \equiv 0$, so that the radiation force does no net work on the perturbation (**O5**). However Abbott's result applies only to long-wavelength disturbances, assuming the validity of the Sobolev force law, and may not be achieved in real stellar winds. A more complete theory that recovers these two limiting cases and works at intermediate optical thicknesses as well has been constructed by Owocki and Rybicki (**O6**). They conclude that the wind must inevitably be unstable to short-wavelength disturbances.

References

(A1) Abbott, D. C. (1978) *Astrophys. J.*, **225,** 893.
(A2) Abbott, D. C. (1980) *Astrophys. J.*, **242,** 1183.
(A3) Abbott, D. C. (1982) *Astrophys. J.*, **259,** 282.
(A4) Abbott, D. C., Bieging, J. H., and Churchwell, E. (1981) *Astrophys. J.*, **250,** 645.
(A5) Abbott, D. C., Bieging, J. H., Churchwell, E., and Cassinelli, J. P. (1980) *Astrophys. J.*, **238,** 196.
(A6) Anderson, D. (1973) *Astron. Astrophys.*, **29,** 23.
(A7) Ashraf, S. and Ahmad, Z. (1974) *Indian J. Pure Appl. Math.*, **6,** 1090.
(A8) Axford, W. I. (1961) *Phil. Trans. Roy. Soc. (London)*, **A253,** 301.
(B1) Barfield, W. D., von Holdt, R., and Zachariasen, F. (1954) *Los Alamos Scientific Laboratory Report No. LA-1709.* Los Alamos: University of California.
(B2) Barlow, M. J. and Cohen, M. (1977) *Astrophys. J.*, **213,** 737.
(B3) Belokon, V. A. (1959) *Soviet Phys. J.E.T.P.*, **9,** 235.
(B4) Berthomieu, G., Provost, J., and Rocca, A. (1976) *Astron. Astrophys.*, **47,** 413.
(B5) Bond, J. W., Watson, K. M., and Welch, J. A. (1965) *Atomic Theory of Gas Dynamics.* Reading: Addison-Wesley.

(B6) Bray, R. J. and Loughhead, R. E. (1974) *The Solar Chromosphere.* London: Chapman and Hall.

(C1) Campbell, P. M. and Nelson, R. G. (1964) *Lawrence Radiation Laboratory Report No. UCRL-7838.* Livermore: University of California.

(C2) Carlberg, R. G. (1980) *Astrophys. J.*, **241,** 1131.

(C3) Carslaw, H. S. and Jaeger, J. C. (1959) *Conduction of Heat in Solids.* (2nd ed.) Oxford: Oxford University Press.

(C4) Cassinelli, J. P. (1979) *Ann. Rev. Astron. Astrophys.*, **17,** 275.

(C5) Cassinelli, J. P. (1979) in *Mass Loss and Evolution of O-Type Stars*, ed. P. S. Conti and C. W. H. de Loore, p. 201. Dordrecht: Reidel.

(C6) Cassinelli, J. P., Castor, J. I., and Lamers, H. J. G. L. M. (1976) *Pub. Astron. Soc. Pacific*, **90,** 496.

(C7) Cassinelli, J. P., Olson, G. L., and Stalio, R. (1978) *Astrophys. J.*, **220,** 573.

(C8) Castor, J. I. (1970) *Mon. Not. Roy. Astron. Soc.*, **149,** 111.

(C9) Castor, J. I. (1974) *Mon. Not. Roy. Astron. Soc.*, **169,** 279.

(C10) Castor, J. I. (1979) in *Mass Loss and Evolution of O-Type Stars*, ed P. S. Conti and C. W. H. de Loore, p. 175. Dordrecht: Reidel.

(C11) Castor, J. I., Abbott, D. C., and Klein, R. I. (1975) *Astrophys. J.*, **195,** 157.

(C12) Castor, J. I., Abbott, D. C., and Klein, R. I. (1976) in *Physique des Mouvements dans les Atmospheres Stellaires*, ed. R. Cayrel and M. Steinberg, p. 363. Paris: Centre National de la Recherche Scientifique.

(C13) Chevalier, R. A. (1974) *Astrophys. J.*, **188,** 501.

(C14) Chevalier, R. A. (1976) *Astrophys. J.*, **207,** 872.

(C15) Chevalier, R. A. and Klein, R. I. (1978) *Astrophys. J.*, **219,** 994.

(C16) Chevalier, R. A. and Klein, R. I. (1979) *Astrophys. J.*, **234,** 597.

(C17) Clark, P. A. and Clark, A. (1973) *Solar Phys.*, **30,** 319.

(C18) Clarke, J. H. and Ferrari, C. (1965) *Phys. Fluids*, **8,** 2121.

(C19) Colgate, S. A. and White, R. H. (1966) *Astrophys. J.*, **143,** 626.

(C20) Courant, R. and Friedrichs, K. O. (1976) *Supersonic Flow and Shock Waves.* New York: Springer.

(C21) Cox, D. P. (1972) *Astrophys. J.*, **178,** 159.

(C22) Cox, D. P. (1972) *Astrophys. J.*, **178,** 169.

(C23) Cox, J. P. and Giuli, R. T. (1968) *Principles of Stellar Structure.* New York: Gordon and Breach.

(C24) Cram, L. E. (1977) *Astron. Astrophys.*, **59,** 151.

(D1) Delache, P. and Froeschle, C. (1972) *Astron. Astrophys.*, **16,** 348.

(E1) Elliot, L. A. (1960) *Proc. Roy. Soc. (London)*, **A258,** 287.

(E2) Elmegreen, B. G. and Lada, C. J. (1977) *Astrophys. J.*, **214,** 725.

(E3) Epstein, R. I. (1981) *Astrophys. J. Letters*, **244,** L89.

(E4) Erickson, G. G. and Olfe, D. B. (1973) *Phys. Fluids*, **16,** 2121.

(F1) Falk, S. W. (1978) *Astrophys. J. Letters*, **226,** L113.

(F2) Falk, S. W. and Arnett, W. D. (1977) *Astrophys. J. Suppl.*, **33,** 515.

(F3) Friend, D. B. and Castor, J. I. (1983) *Astrophys. J.*, **272,** 259.

(F4) Friend, D. B. and MacGregor, K. B. (1984) *Astrophys. J.*, in press.

(F5) Froeschle, C. (1973) *Astron. Astrophys.*, **26,** 229.

(F6) Froeschle, C. (1977) *Astron. Astrophys.*, **55,** 45.

(G1) Garmany, C. D., Olson, G. L., Conti, P. S., and van Steenberg, M. E. (1981) *Astrophys. J.*, **250,** 660.

(G2) Ghoniem, A. F., Kamel, M. M., Berger, S. A., and Oppenheim, A. K. (1982) *J. Fluid Mech.*, **117,** 473.

(G3) Gingerich, O., Noyes, R. W., and Kalkofen, W. (1971) *Solar Phys.*, **18,** 347.

(G4) Giovanelli, R. G. (1978) *Solar Phys.*, **59,** 293.

(G5) Giovanelli, R. G. (1979) *Solar Phys.*, **62,** 253.

(G6) Goldsworthy, F. A. (1961) *Phil. Trans. Roy. Soc.* (*London*), **A253,** 277.

(G7) Goulard, R. (1966) in *Aerodynamic Phenomena in Stellar Atmospheres*, ed. R. N. Thomas, p. 247. London: Academic Press.

(H1) Hearn, A. G. (1972) *Astron. Astrophys.*, **19,** 417.

(H2) Hearn, A. G. (1973) *Astron. Astrophys.*, **23,** 97.

(H3) Heaslet, M. A. and Baldwin, B. S. (1963) *Phys. Fluids*, **6,** 781.

(H4) Helliwell, J. B. (1969) *J. Fluid Mech.*, **37,** 497.

(H5) Hjellming, R. M. (1966) *Astrophys. J.*, **143,** 420.

(I1) Imshennik, V. S. (1962) *Soviet Physics J.E.T.P.*, **15,** 167.

(I2) Imshennik, V. S. (1975) *Sov. J. Plasma Phys.*, **1,** 108.

(K1) Kahn, F. D. (1954) *Bull. Astron. Inst. Netherlands*, **12,** 187.

(K2) Kahn, F. D. (1981) *Mon. Not. Roy. Astron. Soc.*, **196,** 641.

(K3) Kalkofen, W. and Ulmschneider, P. (1977) *Astron. Astrophys.*, **57,** 193.

(K4) Kass, W. and O'Keeffe, M. (1966) *J. Appl. Phys.*, **37,** 2377.

(K5) Klein, R. I. and Chevalier, R. A. (1978) *Astrophys. J.*, **223,** L109.

(K6) Klein, R. I., Sandford, M. T., and Whitaker, R. W. (1983) *Astrophys. J. Letters*, **271,** L69.

(K7) Klein, R. I., Stein, R. F., and Kalkofen, W. (1976) *Astrophys. J.*, **205,** 499.

(K8) Klein, R. I., Stein, R. F., and Kalkofen, W. (1978) *Astrophys. J.*, **220,** 1024.

(K9) Kneer, F. and Nakagawa, Y. (1976) *Astron. Astrophys.*, **46,** 65.

(L1) Lamers, H. J. G. L. M. and Morton, D. C. (1976) *Astrophys. J. Suppl.*, **32,** 715.

(L2) Landau, L. D. and Lifschitz, E. M. (1959) *Fluid Mechanics*. Reading: Addison-Wesley.

(L3) Lasher, G. (1975) *Astrophys. J.*, **201,** 194.

(L4) Lasher, G. J. and Chan, K. L. (1979) *Astrophys. J.*, **230,** 742.

(L5) Lasker, B. M. (1966) *Astrophys. J.*, **143,** 700.

(L6) Laumbach, D. D. and Probstein, R. F. (1970) *Phys. Fluids*, **13,** 1178.

(L7) Le Guet, F. (1972) *Astron. Astrophys.*, **16,** 356.

(L8) Levy, M. (1974) *Astron. Astrophys.*, **31,** 451.

(L9) Lucy, L. B. (1982) *Astrophys. J.*, **255,** 286.

(L10) Lucy, L. B. and Solomon, P. M. (1970) *Astrophys. J.*, **159,** 879.

(L11) Lucy, L. B. and White, R. L. (1980) *Astrophys. J.*, **241,** 300.

(M1) MacGregor, K. B., Hartmann, L., and Raymond, J. C. (1979) *Astrophys. J.*, **231,** 514.

(M2) Manheimer, W. M., Colombant, D. G., and Gardner, J. H. (1982) *Phys. Fluids*, **25,** 1644.

(M3) Marlborough, J. M. and Roy, J. R. (1970) *Astrophys. J.*, **160,** 221.

(M4) Marshak, R. E. (1958) *Phys. Fluids*, **1,** 24.

(M5) Martens, P. C. H. (1979) *Astron. and Astrophys.*, **75,** L7.

(M6) Mathews, W. G. (1965) *Astrophys. J.*, **142,** 1120.

(M7) Mathews, W. G. and O'Dell, C. R. (1969) *Ann. Rev. Astron. Astrophys.*, **7,** 67.

(M8) Mihalas, B. R. W. (1979) Ph.D. Thesis, University of Colorado.

(M9) Mihalas, B. W. and Toomre, J. (1982) *Astrophys. J.*, **263,** 386.

(M10) Mihalas, D. (1978) *Stellar Atmospheres.* (2nd ed.) San Francisco: Freeman.
(M11) Mihalas, D., Kunasz, P. B., and Hummer, D. G. (1975) *Astrophys. J.*, **202,** 465.
(M12) Mitchner, M. and Vinokur, M. (1963) *Phys. Fluids,* **6,** 1682.
(M13) Morse, P. M. and Feshbach, H. (1953) *Methods of Theoretical Physics.* New York: McGraw-Hill.
(N1) Nelson, G. D. and Hearn, A. G. (1978) *Astron. and Astrophys.*, **65,** 223.
(N2) Nerney, S. (1980) *Astrophys. J.*, **242,** 723.
(N3) NiCastro, J. R. A. J. (1970) *Phys. Fluids,* **13,** 2000.
(O1) Ojha, S. N. (1972) *Acta Phys. Acad. Sci. Hungar.*, **31,** 375.
(O2) Oort, J. H. and Spitzer, L. (1955) *Astrophys. J.*, **121,** 6.
(O3) Osterbrock, D. E. (1961) *Astrophys. J.*, **134,** 347.
(O4) Osterbrock, D. E. (1974) *Astrophysics of Gaseous Nebulae.* San Francisco: Freeman.
(O5) Owocki, S. P. and Rybicki, G. B. (1983) Paper presented at the 161st Meeting of the American Astronomical Society. Cambridge, Massachusetts.
(O6) Owocki, S. P. and Rybicki, G. B. (1984) *Astrophys. J.*, in press.
(P1) Pai, S.-I. (1966) *Radiation Gas Dynamics.* New York: Springer.
(P2) Petschek, A. G., Williamson, R. E., and Wooten, J. K. (1960) *Los Alamos Scientific Laboratory Report No. LAMS-2421.* Los Alamos: University of California.
(P3) Pomraning, G. C. (1967) *J. Appl. Phys.*, **38,** 3845.
(P4) Poveda, A. and Woltjer, L. (1968) *Astron. J.*, **73,** 65.
(P5) Prokof'ev, V. A. (1952) *Uch. Zap. Mos. Gos. Univ. Mekh.*, **172,** 79.
(R1) Raizer, Yu. P. (1957) *Soviet Phys. J.E.T.P.*, **5,** 1242.
(R2) Raizer, Yu. P. (1958) *Soviet Phys. J.E.T.P.*, **6,** 77.
(R3) Ray, G. D. and Bhowmick, J. B. (1975) *Indian J. Pure Appl. Math.*, **7,** 96.
(S1) Sachdev, P. L. and Ashraf, S. (1971) *Phys. Fluids,* **14,** 2107.
(S2) Sachs, R. G. (1946) *Phys. Rev.* **69,** 514.
(S3) Sandford, M., Whitaker, R., and Klein, R. I. (1982) *Astrophys. J.*, **260,** 183.
(S4) Schatzman, E. (1949) *Ann. d'Astrophys.*, **12,** 203.
(S5) Schmieder, B. (1977) *Solar Phys.*, **54,** 269.
(S6) Schmieder, B. (1978) *Solar Phys.*, **57,** 245.
(S7) Schmitz, F. and Ulmschneider, P. (1980) *Astron. Astrophys.*, **84,** 93.
(S8) Schmitz, F. and Ulmschneider, P. (1980) *Astron. Astrophys.*, **84,** 191.
(S9) Schmitz, F. and Ulmschneider, P. (1981) *Astron. Astrophys.*, **93,** 178.
(S10) Schwarzschild, M. (1958) *Structure and Evolution of the Stars.* Princeton: Princeton University Press.
(S11) Shafranov, V. D. (1957) *Soviet Phys. J.E.T.P.*, **5,** 1183.
(S12) Skalafuris, A. J. (1965) *Astrophys. J.*, **142,** 351.
(S13) Skalafuris, A. J. (1969) *Astrophys. Space Sci.*, **2,** 258.
(S14) Sobolev, V. V. (1958) in *Theoretical Astrophysics,* ed. V. A. Ambartsumian, Chap. 29. London: Pergamon.
(S15) Sobolev, V. V. (1960) *Moving Envelopes of Stars.* Cambridge: Harvard University Press.
(S16) Souffrin, P. (1966) *Ann. d'Astrophys.*, **29,** 55.
(S17) Souffrin, P. (1972) *Astron. Astrophys.*, **17,** 458.
(S18) Spiegel, E. A. (1957) *Astrophys. J.*, **126,** 202.
(S19) Spiegel, E. A. (1976) in *Physique des Mouvements dans les Atmospheres*

Stellaires, ed. R. Cayrel and M. Steinberg, p. 19. Paris: Centre National de la Recherche Scientifique.
(S20) Spitzer, L. (1968) *Diffuse Matter in Space.* New York: Interscience.
(S21) Spitzer, L. (1978) *Physical Processes in the Interstellar Medium.* New York: Wiley.
(S22) Spitzer, L. and Savedoff, M. P. (1950) *Astrophys. J.*, **111,** 593.
(S23) Stein, R. F. and Spiegel, E. A. (1967) *J. Acous. Soc. America,* **42,** 866.
(S24) Stix, M. (1970) *Astron. Astrophys.*, **4,** 189.
(S25) Stokes, G. G. (1851) *Phil. Mag.*, **1,** 305.
(S26) Strömgren, B. (1939) *Astrophys. J.*, **89,** 526.
(T1) Traugott, S. C. (1965) *Phys. Fluids,* **8,** 834.
(T2) Tscharnuter, W. M. and Winkler, K.-H. (1979) *Comp. Phys. Comm.*, **18,** 171.
(U1) Ulmschneider, P. (1970) *Solar Phys.*, **12,** 403.
(U2) Ulmschneider, P. (1971) *Astron. Astrophys.*, **12,** 297.
(U3) Ulmschneider, P. (1971) *Astron. Astrophys.*, **14,** 275.
(U4) Ulmschneider, P. and Kalkofen, W. (1977) *Astron. Astrophys.*, **57,** 199.
(U5) Ulmschneider, P., Kalkofen, W., Nowak, T., and Bohn, H. U. (1977) *Astron. Astrophys.*, **54,** 61.
(U6) Ulmschneider, P., Schmitz, F., Kalkofen, W., and Bohn, H. U. (1978) *Astron. Astrophys.*, **70,** 487.
(U7) Ulmschneider, P., Schmitz, F., Renzini, A., Cacciari, C., Kalkofen, W., and Kurucz, R. (1977) *Astron. Astrophys.*, **70,** 487.
(U8) Ulrich, R. K. (1970) *Astrophys. J.*, **162,** 993.
(U9) Unno, W. and Spiegel, E. A. (1966) *Pub. Astron. Soc. Japan,* **18,** 85.
(V1) Vandervoort, P. O. (1963) *Astrophys. J.*, **137,** 381.
(V2) Vandervoort, P. O. (1963) *Astrophys. J.*, **138,** 426.
(V3) Vandervoort, P. O. (1964) *Astrophys. J.*, **139,** 889.
(V4) Vernazza, J. E., Avrett, E. H., and Loeser, R. (1973) *Astrophys. J.*, **184,** 605.
(V5) Vernazza, J. E., Avrett, E. H., and Loeser, R. (1976) *Astrophys. J. Suppl.*, **30,** 1.
(V6) Vincenti, W. G. and Baldwin, B. S. (1962) *J. Fluid Mech.*, **12,** 449.
(V7) Vincenti, W. G. and Kruger, C. H. (1965) *Introduction to Physical Gas Dynamics.* New York: Wiley.
(W1) Wang, K. C. (1964) *J. Fluid Mech.*, **20,** 447.
(W2) Weaver, T. A. (1976) *Astrophys. J. Suppl.*, **32,** 233.
(W3) Weber, S. V. (1981) *Astrophys. J.*, **243,** 954.
(W4) Weymann, R. (1960) *Astrophys. J.*, **132,** 452.
(W5) Whitney, C. A. (1963) *Astrophys. J.*, **138,** 537.
(W6) Whitney, C. A. and Skalafuris, A. J. (1963) *Astrophys. J.*, **138,** 200.
(W7) Winkler, K.-H. A. and Newman, M. J. (1980) *Astrophys. J.*, **236,** 201.
(W8) Winkler, K.-H. A. and Newman, M. J. (1980) *Astrophys. J.*, **238,** 311.
(Z1) Zel'dovich, Ya. B. (1957) *Soviet Phys. J.E.T.P.*, **5,** 919.
(Z2) Zel'dovich, Ya. B. and Raizer, Yu. P. (1957) *Usp. Fiz. Nauk,* **63,** 613.
(Z3) Zel'dovich, Ya. B. and Raizer, Yu. P. (1966) *Physics of Shock Waves and High-Temperature Hydrodynamic Phenomena.* New York: Academic.
(Z4) Zwicky, F. (1965) in *Stellar Structure,* ed. L. H. Aller and D. B. McLaughlin, Chap. 7. Chicago: University of Chicago.

APPENDIX

Elements of Tensor Calculus

The equations of radiation hydrodynamics are most naturally expressed in terms of vectors and tensors. We summarize here the concepts used elsewhere in this book. While reasonably complete derivations are given, no attempt at mathematical rigor is made; the reader should consult the references listed at the end of §A3 for further details.

A1 Notation

The three types of geometrical objects with which we will deal are *scalars*, *vectors*, and *tensors* (of the second rank). Scalars will be written as italic or Greek symbols, usually without an affix. Suffixes may be used in some instances to denote a quantity evaluated at a particular position or time, or in a particular reference frame. Vectors and tensors will be distinguished by the use of a special type font or by indices that denote components. Vectors will be written in boldface type (e.g., **v**); tensors will be written in Gothic type (e.g., R). Individual components of vectors and tensors will be denoted by italic or Greek symbols with one more suffixes (e.g., v^i, $R^{\alpha\beta}$). In the text, Roman indices range from 1 to 3, and denote components in a three-dimensional Euclidian space, while Greek indices range from 0 to 3, and denote components in the four-dimensional spacetime of special relativity, 0 indicating time. To avoid confusion with powers of scalars, specific components of vectors and tensors with definite numerical (or symbolic) values assigned to their indices may be written e.g., $V^{(k)}$ or $R^{(\gamma)(\delta)}$. Finally, *matrices*, two-dimensional rectangular arrays such as appear in a transformation of coordinates (e.g., rotation or Lorentz transformation) will also be written in boldface type. These may be of arbitrarily large dimensionality, depending on the use to which they are put. The distinction we make between a matrix and a tensor (which sometimes is represented by a matrix of its components) is that the latter is a *physical* or *geometrical* entity whose components transform, under a change of coordinate systems, according to particular transformation laws, while the former is merely an array of numbers defined in such a way as to systematize algebraic manipulations involving systems of equations or coordinate transformations.

As we will see below, in curvilinear coordinates vectors and tensors can be described by *abstract components* of two different kinds, called *contravariant* and *covariant*, which have different transformation properties under a change of coordinates. Contravariant components will be denoted with superscripts (e.g., v^i, $T^{\alpha\beta}$) and covariant components with subscripts (e.g., V_α, R_{ij}). In general these abstract components differ from the *physical components*, which give the values of the components in physical units along the directions of the coordinate curves. Physical components will be labeled with subscripts that indicate the relevant coordinate [e.g., v_r, v_θ, v_ϕ for the spherical polar coordinates (r, θ, ϕ)].

In Cartesian coordinates, all three kinds of components (contravariant, covariant, and physical) are identical, and usually no distinction is made among them by changes in the positions of component labels. We will often depart from this practice, however, and write even Cartesian tensors with subscripts and superscripts when it serves our purposes to do so (in particular we always write the coordinates themselves as contravariant quantities x^i). An advantage is gained by this device because one can then see by inspection the invariance and transformation properties of an equation under a change of coordinates. As we will see, the power of tensor notation is that it allows us to write equations in a *covariant form*, which means that the equation has the *same form in all coordinate systems.* This formalism is thus responsive to the demands of relativity, which insists that equations expressing genuine physical laws must remain valid in all coordinate systems.

The Einstein summation convention, by which repeated indices imply sums over the appropriate range, will be used throughout. For example

$$a^i b_i \equiv a^1 b_1 + a^2 b_2 + a^3 b_3, \tag{A1.1}$$

and similarly for Greek indices. Summed indices are *dummy* and may be replaced by any other symbol without changing the meaning of the expression (e.g., $a_i b^i \equiv a_k b^k$, etc.). In cases where repeated indices appear but summation is not implied we will write the indices in parentheses [e.g., $g_{(i)(i)}$ denotes that particular tensor component].

Ordinary *partial derivatives* $\partial/\partial x^i$ will often be abbreviated to the notation $_{,i}$ thus: $(\partial v^j/\partial x^i) = v^j_{,i}$. When convenient to do so we will sometimes abbreviate $\partial/\partial t$ to $_{,t}$. *Covariant derivatives* (cf. §A3.10) will be written $_{;\alpha}$ thus: $T^{\alpha\beta}_{;\beta}$.

A2 Cartesian Tensors

Let us now consider vectors and tensors in a three-dimensional space with orthogonal Cartesian coordinates. It is straightforward to generalize most of the results obtained to n dimensions, but we will not pursue this matter.

A2.1. Vectors and Their Algebra

Choose an origin O and three mutually perpendicular coordinate axes with a right-handed orientation. A vector $\mathbf{a}$ is a directed line segment drawn

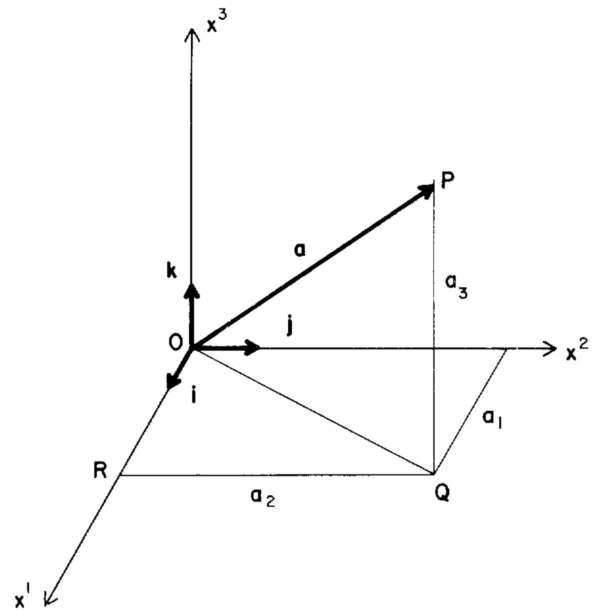

Fig. A1 Right-handed coordinate system.

from O to some point P whose coordinates are (a_1, a_2, a_3). This number triple completely specifies the vector by giving the components along each coordinate axis, that is, the length of the projection of the vector onto that axis (see Figure A1).

By applying the Pythagorean theorem to triangles OPQ and OQR in Figure A1 we see that the *length* (or *magnitude*) of $\mathbf{a}$ is

$$a = |\mathbf{a}| = (a_i a_i)^{1/2}. \tag{A2.1}$$

Unit vectors are vectors of unit length. In particular we may choose *basis vectors*

$$\mathbf{e}_{(1)} = \mathbf{i} = (1, 0, 0); \qquad \mathbf{e}_{(2)} = \mathbf{j} = (0, 1, 0); \qquad \text{and} \qquad \mathbf{e}_{(3)} = \mathbf{k} = (0, 0, 1). \tag{A2.2}$$

Then

$$\mathbf{a} = a_1\mathbf{i} + a_2\mathbf{j} + a_3\mathbf{k}. \tag{A2.3}$$

If we multiply a vector $\mathbf{A}$ by a scalar α we obtain a new vector $\mathbf{B} = \alpha\mathbf{A}$ with components $B_i = \alpha A_i$. $\mathbf{B}$ lies along $\mathbf{A}$, has magnitude $|\mathbf{B}| = \alpha\,|\mathbf{A}|$, and points in the same direction (or opposite to) as $\mathbf{A}$ according to whether α is greater than (or less than) zero. Vectors may be added and subtracted; thus $\mathbf{C} = \mathbf{A} \pm \mathbf{B}$ has components $C_i = A_i \pm B_i$. Furthermore, $\mathbf{A} + \mathbf{B} = \mathbf{B} + \mathbf{A}$; $(\mathbf{A} + \mathbf{B}) + \mathbf{C} = \mathbf{A} + (\mathbf{B} + \mathbf{C})$; $\mathbf{A} - (-\mathbf{B}) = \mathbf{A} + \mathbf{B}$; and $\alpha(\mathbf{A} + \mathbf{B}) = \alpha\mathbf{A} + \alpha\mathbf{B}$.

If some vector quantity, say velocity $\mathbf{v}$, can be assigned a definite value at each point $\mathbf{x}=(x^{(1)}, x^{(2)}, x^{(3)})$ within some region during a definite time interval, then $\mathbf{v}$ is a *vector field*. Similarly we may have *scalar fields* [e.g., pressure $p(x^{(1)}, x^{(2)}, x^{(3)}, t)$] and *tensor fields* (e.g., the radiation stress-energy tensor R).

A2.2. Scalar Product

Consider two vectors $\mathbf{a}$ and $\mathbf{b}$ and their difference $\mathbf{c}=\mathbf{a}-\mathbf{b}$, as shown in Figure A2. Then from the familar law of cosines we know that $c^2=a^2+b^2-2ab\cos\theta$, hence

$$2ab\cos\theta = a_i a_i + b_i b_i - (a_i - b_i)(a_i - b_i) = 2a_i b_i. \tag{A2.4}$$

The quantity

$$\mathbf{a}\cdot\mathbf{b} \equiv a_i b_i \tag{A2.5}$$

is called the *scalar* (or *inner*, or *dot*) *product* of $\mathbf{a}$ and $\mathbf{b}$. If $\mathbf{m}$ and $\mathbf{n}$ are unit vectors along $\mathbf{a}$ and $\mathbf{b}$, we see from (A2.4) that

$$\cos\theta = \mathbf{m}\cdot\mathbf{n} = a_i b_i/(ab). \tag{A2.6}$$

This is a convenient way to determine the angle between any two vectors. Notice that when two vectors $\mathbf{a}$ and $\mathbf{b}$ are *orthogonal*, $\theta=\pi/2$, hence $\mathbf{a}\cdot\mathbf{b}=0$; in particular $\mathbf{i}\cdot\mathbf{j}=\mathbf{i}\cdot\mathbf{k}=\mathbf{j}\cdot\mathbf{k}=0$ as would be expected from (A2.2). If $\mathbf{b}\equiv\mathbf{a}$ then $\theta=0$ and (A2.4) yields (A2.1) for the length of a vector. In general the scalar product gives the length of one vector times the projection of the length of another vector onto the first.

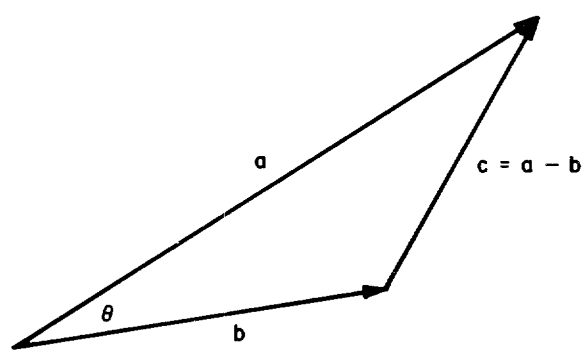

Fig. A2 Vector subtraction.

A2.3. Orthogonal Transformations

Let us now inquire how vectors are affected by changes in the coordinate system. Having fixed the origin O, the only significant change we can make is to perform a rigid rotation of the three axes around O. (We could also reflect, that is, reverse the direction of, axes, but we will not consider that case in this book.) We then obtain new basis vectors $\bar{\mathbf{e}}_j$. Let l_{ij} be the cosine of the angle between $\mathbf{e}_i$ and $\bar{\mathbf{e}}_j$. Then $\bar{\mathbf{e}}_j$ can be resolved along the old basis set and expressed as

$$\bar{\mathbf{e}}_i = l_{ji}\mathbf{e}_j. \tag{A2.7}$$

Similarly, we can resolve $\mathbf{e}_i$ along the new basis set to find

$$\mathbf{e}_i = l_{ij}\bar{\mathbf{e}}_j. \tag{A2.8}$$

Now choose some vector $\mathbf{a}$; we can express $\mathbf{a}$ in terms of its components in either system. Noting that we get the same vector in either case, we see that

$$\mathbf{a} = a_i\mathbf{e}_i \equiv \bar{\mathbf{a}} = \bar{a}_j\bar{\mathbf{e}}_j = \bar{a}_j l_{ij}\mathbf{e}_i, \tag{A2.9}$$

hence

$$a_i = l_{ij}\bar{a}_j. \tag{A2.10}$$

By reversing the argument we find

$$\bar{a}_i = l_{ji}a_j. \tag{A2.11}$$

The matrix $\mathbf{L}$ whose element in the ith row and jth column is l_{ij} is the *transformation matrix* from basis set $\bar{\mathbf{e}}_i$ to set $\mathbf{e}_i$. From (A2.7) and (A2.8) or (A2.10) and (A2.11) we see that the *inverse transformation* $\mathbf{L}^{-1}$ has a matrix $\mathbf{L}^t$ that is the *transpose* of $\mathbf{L}$. This implies that $\mathbf{L}$ must be an *orthogonal* matrix. It is easy to prove that this is so. Let the *Kronecker* δ *symbol* be defined such that $\delta_{ij} = 0$ if $i \neq j$, and $\delta_{(i)(i)} = 1$. Then $\mathbf{e}_i \cdot \mathbf{e}_j = \delta_{ij} = \bar{\mathbf{e}}_i \cdot \bar{\mathbf{e}}_j$. Hence

$$\delta_{ij} = \mathbf{e}_i \cdot \mathbf{e}_j = (l_{ik}\bar{\mathbf{e}}_k) \cdot (l_{jm}\bar{\mathbf{e}}_m) = l_{ik}l_{jm}(\bar{\mathbf{e}}_k \cdot \bar{\mathbf{e}}_m) = l_{ik}l_{jm}\,\delta_{km} = l_{ik}l_{jk}. \tag{A2.12}$$

Thus the row vectors of $\mathbf{L}$ are *orthonormal* (i.e., of unit length and mutually orthogonal). Starting from $\bar{\mathbf{e}}_i \cdot \bar{\mathbf{e}}_j$ one can show that the column vectors of $\mathbf{L}$ are also orthonormal. Therefore $\mathbf{L}$ is in fact orthogonal, and $(\mathbf{L}\mathbf{L}^t) = (\mathbf{L})_{ik}(\mathbf{L}^t)_{kj} = l_{ik}l_{jk} = \delta_{ij} = (\mathbf{I})_{ij}$ where $\mathbf{I}$ is the *identity matrix*.

Although here we started with the geometrical notion of a vector and then deduced its transformation properties, a perfectly consistent set of results is obtained if one proceeds in the opposite direction and *defines* a vector $\mathbf{a}$ to be an object whose components (a_1, a_2, a_3) become $(\bar{a}_1, \bar{a}_2, \bar{a}_3)$, where $\bar{a}_i = l_{ji}a_j$, under a rotation of axes having a transformation matrix $(\mathbf{L})_{ij} = l_{ij}$. The naturalness of this approach becomes evident when one considers general vectors and tensors in curvilinear coordinates.

A2.4. Transformation Properties and Algebra of Tensors

We define a Cartesian tensor of *rank n* to be a geometrical object with n indices, which transforms according to the rule

$$\bar{A}_{ab\ldots n} = l_{pa}l_{qb}\ldots l_{tn}A_{pq\ldots t}. \tag{A2.13}$$

Vectors as defined above are obviously tensors of rank one. Scalars do not change their value under coordinate transformation ($\bar{\alpha} = \alpha$) and thus can be considered to be tensors of rank zero. Aside from scalars and vectors, the tensors we shall most frequently encounter in this book are of rank two (e.g., A_{ij} or $T_{\alpha\beta}$, having 9 or 16 components in three- and four-dimensional spaces, respectively). For example, the Kronecker δ symbol δ_{ij} is a tensor of the second rank, which has the property of being invariant under coordinate transformation:

$$\bar{\delta}_{ij} = l_{ki} l_{mj}\, \delta_{km} = l_{ki} l_{kj} = \delta_{ij}. \tag{A2.14}$$

For this reason it is sometimes called the *isotropic tensor.*

Tensors obey simple algebraic rules. Thus if $\mathsf{B} = \alpha\mathsf{A}$ then $B_{ij} = \alpha A_{ij}$. Tensors of identical rank may be added and subtracted; thus if $\mathsf{C} = \mathsf{A} \pm \mathsf{B}$, $C_{ij} = A_{ij} \pm B_{ij}$. Similarly, $\mathsf{A} + \mathsf{B} = \mathsf{B} + \mathsf{A}$; $\mathsf{A} + (\mathsf{B} + \mathsf{C}) = (\mathsf{A} + \mathsf{B}) + \mathsf{C}$; and $\alpha(\mathsf{A} + \mathsf{B}) = \alpha\mathsf{A} + \alpha\mathsf{B}$. Tensors may also be multiplied. Thus if $A_{ab\ldots m}$ and $B_{pq\ldots n}$ are tensors of rank m and n, respectively, then the set of products $A_{ab\ldots m} B_{pq\ldots n}$ are the components of a tensor of rank $m + n$. In particular if we form the *outer* (or *tensor*) *product* of two vectors a_i and b_i we obtain a second-rank tensor $T_{ij} = a_i b_j$.

A2.5. Symmetry

A tensor is *symmetric* with respect to two indices, say i and j, if interchange of the indices does not change the value of the tensor component (e.g., if $A_{ab\ldots i\ldots j\ldots n} = A_{ab\ldots j\ldots i\ldots n}$). A tensor is *antisymmetric* (or *skew symmetric*) with respect to two indices if their interchange produces a component of the same magnitude but opposite sign.

Any tensor T_{ij} of rank two can be uniquely decomposed into a symmetric part S_{ij} and an antisymmetric part A_{ij}. Thus defining

$$S_{ij} \equiv \tfrac{1}{2}(T_{ij} + T_{ji}) \tag{A2.15}$$

and

$$A_{ij} \equiv \tfrac{1}{2}(T_{ij} - T_{ji}) \tag{A2.16}$$

we have

$$T_{ij} = S_{ij} + A_{ij}. \tag{A2.17}$$

In three dimensions a second-rank symmetric tensor has only six distinct components and a second-rank antisymmetric tensor has only three distinct nonzero components.

A2.6 Contraction

Given a tensor of order n, we may form a new tensor of order $n - 2$ by *contraction* in which we set two indices to the same value and sum over their range. The rank of a tensor is thus equal to the number of *free* indices. For example, if we contract the second-rank tensor $T_{ij} = a_i b_j$ we get the scalar (tensor of rank zero) $T_{ii} = a_i b_i$, the usual inner product of **a** and **b**. We can verify directly that the inner product is in fact a scalar invariant under coordinate transformation:

$$\bar{a}_i \bar{b}_i = l_{ji} a_j l_{ki} b_k = (l_{ji} l_{ki}) a_j b_k = \delta_{jk} a_j b_k = a_j b_j. \tag{A2.18}$$

By contracting a tensor A_{ij} of rank two we can form a unique scalar A_{ii}, called the *trace*, the sum of the diagonal elements. From an argument similar to (A2.18) we can show that A_{ii} is invariant, a fact we exploit in our discussion of fluid kinematics in §21. Notice that for the Kronecker δ tensor, $\delta_{ii} = n$ where n is the dimensionality of the space.

Contraction of the fourth-order tensor formed by the multiplication of two second-order tensors, e.g., $A_{ijkl} = B_{ij} C_{kl}$, yields four distinct "inner products," each of which is a second-order tensor, namely $B_{ij} C_{il}$, $B_{ij} C_{kj}$, $B_{ij} C_{ki}$, and $B_{ij} C_{jl}$. Thus while $\mathbf{a} \cdot \mathbf{b}$ has a unique meaning for vectors, a similar notation for tensors is ambiguous, and we will avoid it, preferring instead to use component notation, which is explicit.

A2.7. The Permutation Symbol

In a space of three dimensions we define the *permutation symbol* e_{ijk} such that

$$e_{ijk} = \begin{cases} +1 \text{ if } ijk \text{ is an even permutation of } 123, \\ -1 \text{ if } ijk \text{ is an odd permutation of } 123, \\ \ \ 0 \text{ if any two indices are the same.} \end{cases} \tag{A2.19}$$

The generalization to n dimensions is obvious. This symbol proves to be extraordinarily useful in a variety of contexts. A result of particular importance is the statement

$$e_{ijk} e_{ilm} \equiv \delta_{jl} \delta_{km} - \delta_{jm} \delta_{kl}, \tag{A2.20}$$

which follows immediately from a direct enumeration of cases. From (A2.20) we easily have $e_{ijk} e_{ijl} = 2\delta_{kl}$. We show below that e_{ijk} is a tensor of rank three whose value is invariant under coordinate rotation.

A2.8. Determinants

The *determinant* of the $(n \times n)$ matrix **a** with components a_{ij} is defined to be the sum of the $n!$ distinct products composed of one element from each row (in order) and column, each given a positive or negative sign according to whether an even or odd number of permutations is required to restore the column indices to ascending numerical order. The same definition with the words "row" and "column" interchanged also holds. Thus

$$|\mathbf{a}| = |a_{ij}| = \begin{vmatrix} a_{11} a_{12} \ldots a_{1n} \\ a_{21} a_{22} \ldots a_{2n} \\ \vdots \quad \vdots \qquad \vdots \\ a_{n1} a_{n2} \ldots a_{nn} \end{vmatrix} \equiv a \tag{A2.21}$$

can be written compactly as

$$a = e_{j_1 j_2 \ldots j_n} a_{1j_1} a_{2j_2} \ldots a_{nj_n} = e_{i_1} e_{i_2} \ldots e_{i_n} a_{i_1 1} a_{i_2 2} \ldots a_{i_n n}. \tag{A2.22}$$

For simplicity in constructing proofs, let us temporarily set $n = 3$, so that

$$a = e_{ijk} a_{1i} a_{2j} a_{3k} = e_{ijk} a_{i1} a_{j2} a_{k3}. \tag{A2.23}$$

From (A2.23) one sees immediately that the determinant of the transpose of a matrix equals the determinant of the matrix itself. Let us now show that the sum $e_{ijk} a_{pi} a_{qj} a_{rk}$ is skew symmetric under interchange of two rows, say p and q:

$$e_{ijk} a_{pi} a_{qj} a_{rk} = e_{jik} a_{pj} a_{qi} a_{rk} = e_{jik} a_{qi} a_{pj} a_{rk} = -e_{ijk} a_{qi} a_{pj} a_{rk}. \tag{A2.24}$$

A similar result is obtained for interchanges of the other indices. It follows that

$$e_{ijk} a_{ip} a_{jq} a_{kr} = e_{pqr} a. \tag{A2.25}$$

By a similar analysis we find

$$e_{ijk} a_{pi} a_{qj} a_{rk} = e_{pqr} a. \tag{A2.26}$$

Equations (A2.25) and (A2.26) show that if any two rows or columns are identical (or even scalar multiples of one another) the determinant is zero.

Determinants can also be expanded in *cofactors*. For example, expanding along the first row we have

$$a = |a_{ij}| = a_{1j_1} e_{j_1 j_2 \ldots j_n} a_{2j_2} \ldots a_{nj_n} = a_{(1)k} A^k_{(1)}, \tag{A2.27}$$

where the cofactor

$$A^k_{(1)} \equiv e_{kj_2 \ldots j_n} a_{2j_2} \ldots a_{nj_n}. \tag{A2.28}$$

From (A2.28) we immediately see that $a_{(i)k} A^k_{(j)} = \delta_{ij} a$.

Consider now the determinant of the matrix $\mathbf{c}$, which is the product of two matrices $\mathbf{a}$ and $\mathbf{b}$, so that $c_{ij} = a_{ik} b_{kj}$. Then

$$\begin{aligned} c = |c_{ij}| &= e_{pq \ldots t} c_{p1} c_{q2} \ldots c_{tn} = e_{pq \ldots t} (a_{pi} b_{i1})(a_{qj} b_{j2}) \ldots (a_{tl} b_{ln}) \\ &= (e_{pq \ldots t} a_{pi} a_{qj} \ldots a_{tl}) b_{i1} b_{j2} \ldots b_{ln} = |a_{ij}|\, e_{ij \ldots l} b_{i1} b_{j2} \ldots b_{ln} \\ &= |a_{ij}|\, |b_{ij}|, \end{aligned} \tag{A2.29}$$

where we have used (A2.25). We thus recover the familiar rule that the determinant of the product of two matrices equals the product of the determinants of those matrices.

Applying this result to the transformation matrix $\mathbf{L}$ introduced in §A2.3 we find

$$L^2 = |\mathbf{L}^t|\, |\mathbf{L}| = |\mathbf{L}^t \mathbf{L}| = |\mathbf{L}^{-1} \mathbf{L}| = |\mathbf{I}| = 1, \tag{A2.30}$$

so that $L = \pm 1$. The case $L = +1$ applies to *rotations* of coordinates, and $L = -1$ applies if an odd number of the coordinate axes undergoes *reflection*, thereby changing the system from right handed to left handed; we consider only rotations. We can now see that the permutation symbol is invariant under rotations:

$$\bar{e}_{ijk} = l_{pi}l_{qj}l_{rk}e_{pqr} = e_{ijk}\,|l_{ij}| = Le_{ijk} = e_{ijk}. \tag{A2.31}$$

A2.9. Cross Products; Triple Products

We define the *cross* (or *vector*) *product* of **a** and **b** to be the vector $\mathbf{c} = \mathbf{a} \times \mathbf{b}$, whose components are

$$c_i = e_{ijk}a_jb_k. \tag{A2.32}$$

Note then that $\mathbf{b} \times \mathbf{a} = -(\mathbf{a} \times \mathbf{b})$ and that $\mathbf{a} \times \mathbf{a} = 0$ for any **a**. Using (A2.2) in (A2.32) one finds $\mathbf{i} \times \mathbf{j} = \mathbf{k}$; $\mathbf{j} \times \mathbf{k} = \mathbf{i}$; $\mathbf{k} \times \mathbf{i} = \mathbf{j}$; $\mathbf{i} \times \mathbf{i} = \mathbf{j} \times \mathbf{j} = \mathbf{k} \times \mathbf{k} = 0$. From (A2.32) we see that **c** can be written symbolically as the determinant

$$\mathbf{c} = \begin{vmatrix} \mathbf{i} & \mathbf{j} & \mathbf{k} \\ a_1 & a_2 & a_3 \\ b_1 & b_2 & b_3 \end{vmatrix}. \tag{A2.33}$$

Consider now the geometrical interpretation of $\mathbf{a} \times \mathbf{b}$. Without changing **a**, **b**, or **c** we can rotate the coordinate axes so that $\mathbf{i}'$ lies along **a**, and $\mathbf{i}'$ and $\mathbf{j}'$ lie in the plane defined by **a** and **b**. We can then write $\mathbf{a} = a\mathbf{i}'$ and $\mathbf{b} = b \cos\theta\mathbf{i}' + b \sin\theta\mathbf{j}'$ where θ is the angle between **a** and **b**. Therefore

$$\mathbf{c} = a\mathbf{i}' \times b(\cos\theta\mathbf{i}' + \sin\theta\mathbf{j}') = ab \sin\theta\mathbf{k}'. \tag{A2.34}$$

Thus **c** is a vector perpendicular to the plane of **a** and **b**, whose magnitude is $ab \sin\theta$; this is the area of the parallelogram generated by **a** and **b** (i.e., **a** and **b** along two of its sides).

We can define two kinds of triple products of vectors. The *scalar triple product* is

$$\mathbf{a} \cdot (\mathbf{b} \times \mathbf{c}) = e_{ijk}a_ib_jc_k. \tag{A2.35}$$

This product has a simple geometrical interpretation: it is the length of **a** projected onto a vector perpendicular to the plane of **b** and **c**, times the area of the parallelogram generated by **b** and **c**, and hence is the volume of the parallelepiped whose sides are **a**, **b**, and **c**. Notice that (A2.35) is unaltered by *cyclic permutation* (i.e., $i \to j \to k \to i$), hence

$$\mathbf{a} \cdot (\mathbf{b} \times \mathbf{c}) = \mathbf{b} \cdot (\mathbf{c} \times \mathbf{a}) = \mathbf{c} \cdot (\mathbf{a} \times \mathbf{b}), \tag{A2.36}$$

which is also self-evident from the geometrical meaning of the scalar triple product.

The *vector triple product* is $\mathbf{d} = \mathbf{a} \times (\mathbf{b} \times \mathbf{c})$. Because $(\mathbf{b} \times \mathbf{c})$ is perpendicular to **b** and **c**, while **d** is perpendicular to $(\mathbf{b} \times \mathbf{c})$, it follows that **d** lies in the plane of **b** and **c**. We see this explicitly by using (A2.20) to show that

$$d_i = e_{ijk}a_j(e_{klm}b_lc_m) = (\delta_{il}\,\delta_{jm} - \delta_{im}\,\delta_{jl})a_jb_lc_m = b_i(a_jc_j) - c_i(a_jb_j), \tag{A2.37}$$

and hence

$$\mathbf{a}\times(\mathbf{b}\times\mathbf{c})=(\mathbf{a}\cdot\mathbf{c})\mathbf{b}-(\mathbf{a}\cdot\mathbf{b})\mathbf{c}. \tag{A2.38}$$

By similar use of (A2.20) it is easy to prove the useful relations

$$(\mathbf{a}\times\mathbf{b})\cdot(\mathbf{c}\times\mathbf{d})=(\mathbf{a}\cdot\mathbf{c})(\mathbf{b}\cdot\mathbf{d})-(\mathbf{a}\cdot\mathbf{d})(\mathbf{b}\cdot\mathbf{c}) \tag{A2.39}$$

and

$$\begin{aligned}(\mathbf{a}\times\mathbf{b})\times(\mathbf{c}\times\mathbf{d})&=\mathbf{c}\cdot(\mathbf{d}\times\mathbf{a})\mathbf{b}-\mathbf{c}\cdot(\mathbf{d}\times\mathbf{b})\mathbf{a}\\&=\mathbf{a}\cdot(\mathbf{b}\times\mathbf{d})\mathbf{c}-\mathbf{a}\cdot(\mathbf{b}\times\mathbf{c})\mathbf{d}.\end{aligned} \tag{A2.40}$$

A2.10. Gradient, Divergence, Laplacian, and Curl

Thus far we have dealt with the algebra of individual vectors. We now turn to the calculus of (continuous and differentiable) vector fields. First, notice that (A2.10) and (A2.11) can be applied to the position vector of a point, from which it follows that

$$\frac{\partial x^i}{\partial \bar{x}^j}=l_{ij} \tag{A2.41a}$$

and

$$\frac{\partial \bar{x}^i}{\partial x^j}=l_{ji}. \tag{A2.41b}$$

Starting with the scalar field $f=f(x, y, z)$, form the vector

$$\nabla f=\frac{\partial f}{\partial x}\mathbf{i}+\frac{\partial f}{\partial y}\mathbf{j}+\frac{\partial f}{\partial z}\mathbf{k}, \tag{A2.42}$$

which is called the *gradient* of f. We can verify that ∇f is, in fact, a vector in the sense of §A2.3 by noting that in a new coordinate system the component $(\nabla f)_i=(\partial f/\partial x^i)=f_{,i}$ becomes

$$\overline{(\nabla f)}_i=(\partial f/\partial \bar{x}^i)=(\partial f/\partial x^j)(\partial x^j/\partial \bar{x}^i)=l_{ji}(\partial f/\partial x_j)=l_{ji}(\nabla f)_j \tag{A2.43}$$

which is consistent with (A2.10). Now choose a *level surface* on which $f(x, y, z)\equiv$ a constant; then for any $d\mathbf{r}=(dx, dy, dz)$ lying in this surface

$$df=\frac{\partial f}{\partial x}dx+\frac{\partial f}{\partial y}dy+\frac{\partial f}{\partial z}dz=(\nabla f)\cdot d\mathbf{r}\equiv 0. \tag{A2.44}$$

Thus geometrically ∇f is a vector field perpendicular to level surfaces of f, and $(\nabla f)\cdot d\mathbf{r}$, for arbitrary $d\mathbf{r}$, measures the change in the value of f along the increment $d\mathbf{r}$.

In Cartesian coordinates, n successive differentiations of a tensor of rank n yield a new tensor of rank $m+n$. For example, consider $A_{ij,pq}$, which we see is in fact a tensor of rank four because

$$\bar{A}_{ab,cd} = \frac{\partial^2 \bar{A}_{ab}}{\partial \bar{x}^c \, \partial \bar{x}^d} = \frac{\partial^2}{\partial \bar{x}^c \, \partial \bar{x}^d}(l_{ia} l_{jb} A_{ij}) = \frac{\partial x^k}{\partial \bar{x}^c} \frac{\partial}{\partial x^k} \left[\frac{\partial x^l}{\partial \bar{x}^d} \frac{\partial}{\partial x^l}(l_{ia} l_{jb} A_{ij}) \right]$$
$$= l_{ia} l_{jb} l_{kc} l_{ld} A_{ij,kl} \tag{A2.45}$$

Here we have used (A2.41a) and the constancy of the l_{ij}'s under a given rotation of coordinates.

We may regard

$$\nabla = \frac{\partial}{\partial x}\mathbf{i} + \frac{\partial}{\partial y}\mathbf{j} + \frac{\partial}{\partial z}\mathbf{k}, \tag{A2.46}$$

called *del*, as a symbolic vector. The dot product of del with a vector field $\mathbf{a}$ yields the *divergence* of $\mathbf{a}$:

$$\nabla \cdot \mathbf{a} = (\partial a_1/\partial x) + (\partial a_2/\partial y) + (\partial a_3/\partial z) = a_{i,i} \tag{A2.47}$$

The divergence of a vector is obviously a scalar, a fact also indicated by the notation $a_{i,i}$ which shows that it is the contraction of the second-order tensor $a_{i,j}$. By direct calculation it is easy to see that

$$\nabla \cdot (\alpha \mathbf{a}) = (\alpha a_i)_{,i} = \alpha_{,i} a_i + \alpha a_{i,i} = \mathbf{a} \cdot (\nabla \alpha) + \alpha \nabla \cdot \mathbf{a}. \tag{A2.48}$$

If we calculate the divergence of the gradient of a scalar field f we obtain the *Laplacian* of f:

$$\nabla^2 f = \nabla \cdot (\nabla f) = (f_{,i})_{,i} = f_{,ii} = (\partial^2 f/\partial x^2) + (\partial^2 f/\partial y^2) + (\partial^2 f/\partial z^2) \tag{A2.49}$$

where the summation convention holds. The Laplacian of a vector $\mathbf{a}$ is a new vector $\mathbf{b} = \nabla^2 \mathbf{a}$ whose components are $b_i = a_{i,jj}$ (sum on j).

The symbolic cross product of ∇ with a vector field $\mathbf{a}$ yields a new vector field called the *curl* of $\mathbf{a}$. It has components

$$b_i = (\nabla \times \boldsymbol{a})_i = e_{ijk}(\partial/\partial x^j) a_k = e_{ijk} a_{k,j}. \tag{A2.50}$$

Thus $b_1 = (a_{3,2} - a_{2,3})$, etc. The curl is sometimes written as the symbolic determinant

$$\nabla \times \mathbf{a} = \begin{vmatrix} \mathbf{i} & \mathbf{j} & \mathbf{k} \\ \partial/\partial x & \partial/\partial y & \partial/\partial z \\ a_1 & a_2 & a_3 \end{vmatrix}, \tag{A2.51}$$

but in practice (A2.50) is more useful in establishing vector identities. For example, to calculate the curl of the curl of a vector we write

$$[\nabla \times (\nabla \times \mathbf{a})]_i = e_{ijk}(e_{klm} a_{m,l})_{,j} = e_{kij} e_{klm} a_{m,jl} = (\delta_{il}\, \delta_{jm} - \delta_{im}\, \delta_{jl}) a_{m,jl}$$
$$= a_{j,ji} - a_{i,jj} = [\nabla(\nabla \cdot \mathbf{a})]_i - (\nabla^2 \mathbf{a})_i, \tag{A2.52}$$

hence

$$\nabla \times (\nabla \times \mathbf{a}) = \nabla(\nabla \cdot \mathbf{a}) - \nabla^2 \mathbf{a}. \tag{A2.53}$$

By similar reasoning it is easy to prove the useful relations

$$\boldsymbol{\nabla}\cdot(\boldsymbol{\nabla}\times\mathbf{a})=0, \tag{A2.54}$$

$$\boldsymbol{\nabla}\cdot(\mathbf{a}\times\mathbf{b})=\mathbf{b}\cdot(\boldsymbol{\nabla}\times\mathbf{a})-\mathbf{a}\cdot(\boldsymbol{\nabla}\times\mathbf{b}), \tag{A2.55}$$

$$\boldsymbol{\nabla}\times(\boldsymbol{\nabla}f)=0, \tag{A2.56}$$

$$\boldsymbol{\nabla}\times(\alpha\mathbf{a})=(\boldsymbol{\nabla}\alpha)\times\mathbf{a}+\alpha(\boldsymbol{\nabla}\times\mathbf{a}), \tag{A2.57}$$

$$\boldsymbol{\nabla}\times(\mathbf{a}\times\mathbf{b})=(\boldsymbol{\nabla}\cdot\mathbf{b})\mathbf{a}-(\boldsymbol{\nabla}\cdot\mathbf{a})\mathbf{b}+(\mathbf{b}\cdot\boldsymbol{\nabla})\mathbf{a}-(\mathbf{a}\cdot\boldsymbol{\nabla})\mathbf{b}, \tag{A2.58}$$

and

$$\boldsymbol{\nabla}(\mathbf{a}\cdot\mathbf{b})=(\mathbf{a}\cdot\boldsymbol{\nabla})\mathbf{b}+(\mathbf{b}\cdot\boldsymbol{\nabla})\mathbf{a}+\mathbf{a}\times(\boldsymbol{\nabla}\times\mathbf{b})+\mathbf{b}\times(\boldsymbol{\nabla}\times\mathbf{a}). \tag{A2.59}$$

A2.11. Duals

Consider an antisymmetric second-rank tensor Ω_{ij} in three-space. With any such tensor we may associate a vector by the definition

$$\omega_i=\tfrac{1}{2}e_{ijk}\Omega_{jk}. \tag{A2.60}$$

The vector ω_i is called the *dual* of Ω_{jk} because of the reciprocal relation that

$$\Omega_{ij}=e_{ijk}\omega_k, \tag{A2.61}$$

which can easily be verified by substitution from (A2.60) and use of (A2.20). Thus

$$\boldsymbol{\Omega}=\begin{pmatrix} 0 & \omega_3 & -\omega_2 \\ -\omega_3 & 0 & \omega_1 \\ \omega_2 & -\omega_1 & 0 \end{pmatrix}. \tag{A2.62}$$

The dual concept can be generalized to spaces of higher dimension and tensors of higher rank, see (**S2,** 134–135) and (**S2,** 245–247).

A result of considerable importance is that

$$\Omega_{jk}a_j=e_{ijk}\omega_i a_j=(\boldsymbol{\omega}\times\mathbf{a})_k, \tag{A2.63}$$

which shows that this particular sum of a vector against an antisymmetric tensor is identical to the cross product of the vector with the vector dual of the tensor. We exploit this result in our discussion of fluid kinematics in §21.

Vectors of the type described above are called *axial vectors* (or *pseudovectors* because they are "really" tensors of rank two). Important examples of axial vectors are the cross product, $\mathbf{c}=\mathbf{a}\times\mathbf{b}$, for which the associated tensor has components $C_{ij}=a_ib_j-a_jb_i$, and the curl, $\mathbf{b}=\boldsymbol{\nabla}\times\mathbf{a}$, for which the associated tensor has components $B_{ij}=a_{j,i}-a_{i,j}$. An interesting distinction between axial vectors and vectors of the type defined in §A2.1, called *polar vectors*, is that under reversal of the directions of the coordinate axes, the components of polar vectors change sign whereas the components of axial vectors are unaltered. This statement is obviously true for the two examples given above. As discussed in §21, the angular velocity $\boldsymbol{\omega}$ of a rigid body or an infinitesimal element of fluid may be considered to be an axial vector.

A2.12. The Divergence Theorem

The *divergence theorem* (also known as *Gauss's theorem* or *Green's theorem*) is one of the most useful tools of tensor calculus, and is employed frequently in almost all branches of theoretical physics. Let V be a simple convex volume with surface S. Let $\mathbf{n}$ be the outward-pointing normal at any point on S. Then at each position on S we can write an *oriented surface element* as $d\mathbf{S} = \mathbf{n}\, dS$. It is easy to see that the projection of $d\mathbf{S}$ onto a plane perpendicular to any particular direction $\mathbf{l}$ is $\mathbf{l} \cdot d\mathbf{S} = \mathbf{l} \cdot \mathbf{n}\, dS$.

The divergence theorem states that for any differentiable function f,

$$\int_V f_{,i}\, dV = \int_S f n_i\, dS. \tag{A2.64}$$

To prove this theorem, choose $i = 3$ and partition S into upper and lower surfaces S^+ and S^- with respect to the $(x^{(1)}, x^{(2)})$ plane (see Figure A3). Consider an elementary vertical rectangular tube within V, having a volume δV and a projection Σ on the $(x^{(1)}, x^{(2)})$ plane. Let S^+ be given by $x^{(3)} = g^+(x^{(1)}, x^{(2)})$ and S^- by $x^{(3)} = g^-(x^{(1)}, x^{(2)})$. Then carrying out the integration over δV we have

$$\int_{\delta V} f_{,3}\, dx^{(1)}\, dx^{(2)}\, dx^{(3)} = \int_\Sigma \{f[x^{(1)}, x^{(2)}, g^+(x^{(1)}, x^{(2)})] - f[x^{(1)}, x^{(2)}, g^-(x^{(1)}, x^{(2)})]\}\, dx^{(1)}\, dx^{(2)}. \tag{A2.65}$$

But from the definition of the oriented surface element we see that on S^+

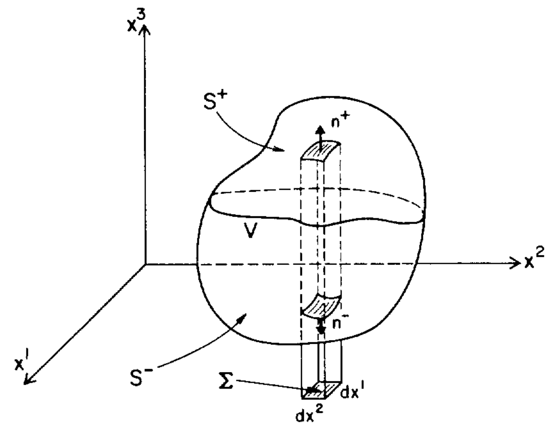

Fig. A3 Geometry of surface and volume integrals.

we have $dx^{(1)}\,dx^{(2)} = n_3^+\,dS^+$, and on S^-, $dx^{(1)}\,dx^{(2)} = -n_3^-\,dS^-$. Hence

$$\begin{aligned}\int_{\delta V} f_{,3}\,dV &= \int_{\delta S^+} f[x^{(1)}, x^{(2)}, g^+(x^{(1)}, x^{(2)})]n_3^+\,dS^+ \\ &\quad + \int_{\delta S^-} f[x^{(1)}, x^{(2)}, g^-(x^{(1)}, x^{(2)})]n_3^-\,dS^- \qquad \text{(A2.66)} \\ &= \int_{\delta S^+} f^+ n_3^+\,dS^+ + \int_{\delta S^-} f^- n_3^-\,dS^-,\end{aligned}$$

where now f^+ and f^- denote the value of f on S^+ and S^-, respectively. Finally, by summing over all elementary tubes, and recognizing that S is the union of S^+ and S^-, we recover (A2.64) for $i = 3$; the choice of i is arbitrary, hence the theorem holds for all i.

Perhaps the most familiar form of the divergence theorem is that for a vector, say $\mathbf{F}$. Writing $f = F^i$ in (A2.64) and summing we have

$$\int_V F^i_{,i}\,dV = \int_S F^i n_i\,dS, \qquad \text{(A2.67)}$$

or

$$\int_V \nabla\cdot\mathbf{F}\,dV = \int_S \mathbf{F}\cdot\mathbf{n}\,dS. \qquad \text{(A2.68)}$$

As another example, if we choose $f = e_{ijk}a_j$, then $f_{,i} = e_{kij}a_{j,i} = (\nabla\times\mathbf{a})_k$, while $fn_i = e_{ijk}n_i a_j = (\mathbf{n}\times\mathbf{a})_k$, so that

$$\int_V (\nabla\times\mathbf{a})\,dV = \int_S (\mathbf{n}\times\mathbf{a})\,dS. \qquad \text{(A2.69)}$$

It is very important to note that (A2.64) is quite general, and holds for *any* differentiable f, whether scalar, vector, or tensor (the latter usually being considered one component at a time, or as the contraction of a set of components against the derivative). In fact the theorem is actually a result from analysis, and has no roots in vector or tensor analysis per se.

A2.13. Stokes's Theorem

If S is a caplike surface bounded by a closed curve C, *Stokes's theorem* states that for a differentiable vector field $\mathbf{a}$,

$$\int_S (\nabla\times\mathbf{a})\cdot\mathbf{n}\,dS = \oint_C \mathbf{a}\cdot\mathbf{t}\,ds, \qquad \text{(A2.70)}$$

where $\mathbf{t}$ is the unit tangent to C. To prove (A2.70), cover S with a rectilinear coordinate mesh (u, v) so that S is a collection of points $\mathbf{r}(u, v)$. Consider the integrals in (A2.70) for an element $\alpha\beta\gamma\delta$ bounded by the curve Γ, where $\alpha=(u, v)$, $\beta=(u+du, v)$, $\gamma=(u+du, v+dv)$, $\delta=(u, v+dv)$. Then to first order

$$\mathbf{a}(u+du, v)=\mathbf{a}(u, v)+\left[\left(\frac{\partial \mathbf{r}}{\partial u}\,du\right)\cdot \boldsymbol{\nabla}\right]\mathbf{a}, \tag{A2.71}$$

and similarly for $\mathbf{a}(u, v+dv)$. Then, calculating the line integral to first order we have

$$\oint_{\Gamma} \mathbf{a}\cdot \mathbf{t}\,ds=\left\{\left[\left(\frac{\partial \mathbf{r}}{\partial u}\cdot \boldsymbol{\nabla}\right)\mathbf{a}\right]\cdot \frac{\partial \mathbf{r}}{\partial v}-\left[\left(\frac{\partial \mathbf{r}}{\partial v}\cdot \boldsymbol{\nabla}\right)\mathbf{a}\right]\cdot \frac{\partial \mathbf{r}}{\partial u}\right\}du\,dv. \tag{A2.72}$$

But by using component notation and (A2.20), (A2.32), and (A2.50) we see that

$$\begin{aligned}\frac{\partial r_j}{\partial u}\,a_{k,j}\frac{\partial r_k}{\partial v}-\frac{\partial r_j}{\partial v}\,a_{k,j}\frac{\partial r_k}{\partial u}&=(\delta_{jl}\,\delta_{km}-\delta_{jm}\,\delta_{kl})a_{k,j}\frac{\partial r_l}{\partial u}\frac{\partial r_m}{\partial v}\\ &=e_{ijk}a_{k,j}e_{ilm}\frac{\partial r_l}{\partial u}\frac{\partial r_m}{\partial v}\\ &=(\boldsymbol{\nabla}\times\mathbf{a})\cdot\left(\frac{\partial \mathbf{r}}{\partial u}\times\frac{\partial \mathbf{r}}{\partial v}\right).\end{aligned} \tag{A2.73}$$

From the geometrical meaning of the cross product we know that $[(\partial\mathbf{r}/\partial u)\times(\partial\mathbf{r}/\partial v)]\,du\,dv$ is just the oriented area $\delta\mathbf{S}$ of $\alpha\beta\gamma\delta$. We therefore find that (A2.70) holds for the element $\alpha\beta\gamma\delta$. Now sum over all elements. The line integrals on the interior mesh lines cancel in pairs, leaving only the line integral around the bounding curve C; the surface integrals sum to the integral over the whole surface. Thus (A2.70) is valid as stated.

As was true for the divergence theorem, Stokes's theorem is quite general, and can be written

$$\int_S e_{ijk}a_{k,j}n_i\,dS=\oint_C a_it_i\,ds \tag{A2.74}$$

where a_k may be the components of any differentiable tensor (e.g., T_{klm} with lm fixed).

A3 General Tensors

We now consider general tensors in curvilinear coordinates. We will not usually specify the dimensionality of the space, and most of the results are valid in n dimensions. In this section, unless specified otherwise, both roman and Greek indices are assumed to run from 1 to n.

A3.1. Transformation Properties

In order to deal with vectors and tensors in curvilinear coordinates, we must now consider transformations of a quite general, but not arbitrary, kind. We restrict attention to what we shall call *admissible transformations*, which have the following properties.

1. They are real, single-valued transformations of the form

$$\bar{x}^i = f^i(x^{(1)}, \ldots, x^{(n)}), \qquad (i = 1, \ldots, n). \tag{A3.1}$$

2. They are *reversible* so that

$$x^i = g^i(\bar{x}^{(1)}, \ldots, \bar{x}^{(n)}), \qquad (i = 1, \ldots, n). \tag{A3.2}$$

3. The g^i are single valued so that the direct and inverse transformations are one to one.

To guarantee these properties it is sufficient to demand that the f^i and g^i be continuous and have continuous derivatives, and that the Jacobian determinant

$$J \equiv \left|\frac{\partial x^i}{\partial \bar{x}^\gamma}\right| \tag{A3.3}$$

be nonzero everywhere in the domain of the transformation.

Under general transformations, vectors and tensors are represented by two different kinds of abstract components, called *contravariant* and *covariant*, each of which will in general differ from the *physical* components of the tensor. We emphasize that all three sets of components represent the *same physical quantity*, and all are related by definite rules (cf §§A3.5 and A3.7); the three representations can be used interchangeably as convenient.

A *contravariant tensor* of rank m has components $A^{ab\ldots m}$ that transform according to the rule

$$\bar{A}^{\alpha\beta\ldots\mu} = \frac{\partial \bar{x}^\alpha}{\partial x^a}\frac{\partial \bar{x}^\beta}{\partial x^b}\cdots\frac{\partial \bar{x}^\mu}{\partial x^m} A^{ab\ldots m}. \tag{A3.4}$$

In particular a contravariant vector transforms as

$$\bar{A}^\alpha = (\partial \bar{x}^\alpha/\partial x^a) A^a. \tag{A3.5}$$

The archetype for a contravariant vector is the set of coordinate differentials dx^i for which we obviously have $d\bar{x}^\alpha = (\partial \bar{x}^\alpha/\partial x^a)\, dx^a$.

A *covariant tensor* of rank m has components $A_{ab\ldots m}$ that transform according to the rule

$$A_{\alpha\beta\ldots\mu} = \frac{\partial x^a}{\partial \bar{x}^\alpha}\frac{\partial x^b}{\partial \bar{x}^\beta}\cdots\frac{\partial x^m}{\partial \bar{x}^\mu} A_{ab\ldots m}. \tag{A3.6}$$

In particular a covariant vector transforms as

$$\bar{A}_\alpha = (\partial x^a/\partial \bar{x}^\alpha) A_a. \tag{A3.7}$$

The archetype for a covariant vector is the gradient $\phi_{,a}$ for which we obviously have $\bar{\phi}_{,\alpha} = (\partial x^a/\partial \bar{x}^\alpha)\phi_{,a}$.

A *mixed tensor* of contravariant rank m and covariant rank n has components $A^{ab\ldots m}_{kl\ldots n}$ that transform according to the rule

$$\bar{A}^{\alpha\beta\ldots\mu}_{\kappa\lambda\ldots\nu}=\frac{\partial\bar{x}^\alpha}{\partial x^a}\frac{\partial\bar{x}^\beta}{\partial x^b}\cdots\frac{\partial\bar{x}^\mu}{\partial x^m}\frac{\partial x^k}{\partial\bar{x}^\kappa}\frac{\partial x^l}{\partial\bar{x}^\lambda}\cdots\frac{\partial x^n}{\partial\bar{x}^\nu}A^{ab\ldots m}_{kl\ldots n}. \tag{A3.8}$$

In general we suppose that tensors of the kinds defined above can exist throughout a finite region of space, and thereby constitute a tensor field.

A3.2. Tensor Algebra

General tensors obey simple rules of algebra. We may multiply a tensor whose components are $A^{ab\ldots c}_{ij\ldots k}$ by a scalar α to obtain a tensor whose components are $\alpha A^{ab\ldots c}_{ij\ldots k}$. We can add and subtract tensors of identical contravariant and covariant ranks (which are shown by the number of *free*, that is, unsummed, indices of the appropriate kinds); these operations are associative. For a tensor $A^{ab\ldots c}_{ij\ldots k}$ of contravariant rank c and covariant rank k, and a tensor $B^{lm\ldots n}_{pq\ldots r}$ of contravariant rank n and covariant rank r, the outer product

$$C^{ab\ldots clm\ldots n}_{ij\ldots kpq\ldots r}=A^{ab\ldots c}_{ij\ldots k}B^{lm\ldots n}_{pq\ldots r} \tag{A3.9}$$

is a tensor of contravariant rank $(c+n)$ and covariant rank $(k+r)$, as can be verified immediately by application of (A3.8). The outer product is distributive.

From a tensor $A^{ab\ldots k}_{mn\ldots t}$ of contravariant rank k and covariant rank t one may construct a new tensor of contravariant rank $(k-1)$ and covariant rank $(t-1)$ by the operation of contraction, in which one covariant and one contravariant index are set to the same value and summed. For example, contract A^{ab}_{lm} to form A^{ab}_{lb}. Then

$$\bar{A}^{\alpha\beta}_{\lambda\mu}=\frac{\partial\bar{x}^\alpha}{\partial x^a}\frac{\partial\bar{x}^\beta}{\partial x^b}\frac{\partial x^l}{\partial\bar{x}^\lambda}\frac{\partial x^m}{\partial\bar{x}^\mu}A^{ab}_{lm}. \tag{A3.10}$$

implies that

$$\bar{A}^{\alpha\beta}_{\lambda\beta}=\frac{\partial\bar{x}^\alpha}{\partial x^a}\frac{\partial x^l}{\partial\bar{x}^\lambda}\left(\frac{\partial\bar{x}^\beta}{\partial x^b}\frac{\partial x^m}{\partial\bar{x}^\beta}\right)A^{ab}_{lm}. \tag{A3.11}$$

But

$$\frac{\partial\bar{x}^\beta}{\partial x^b}\frac{\partial x^m}{\partial\bar{x}^\beta}\equiv\frac{\partial x^m}{\partial x^b}=\delta^m_b \tag{A3.12}$$

where δ^m_b is the mixed tensor that represents the Kronecker δ symbol. Note in passing that δ^i_j is the isotropic tensor whose value is the same in all coordinate systems (which is trivial to prove). Using (A3.12) in (A3.11) we have

$$\bar{A}^{\alpha\beta}_{\lambda\beta}=\frac{\partial\bar{x}^\alpha}{\partial x^a}\frac{\partial x^l}{\partial\bar{x}^\lambda}A^{ab}_{lb}, \tag{A3.13}$$

which is the correct transformation for tensor whose contravariant and covariant ranks are unity (and hence reduced by one from those of the original tensor, as claimed above).

The *null tensor* is that tensor whose components are all zero in some coordinate system. It follows from (A3.4), (A3.6), and (A3.8) that its components must remain zero in all other admissible coordinate systems. This result is of great importance in physics, for it implies that if we can express a physical law as a tensor equation in some frame, say $A^{ab\ldots k}_{lm\ldots p} = B^{ab\ldots k}_{lm\ldots p}$, then this equation remains true in *all* coordinate systems (hence the physical law is covariant) because $(A^{ab\ldots k}_{lm\ldots p} - B^{ab\ldots k}_{lm\ldots p}) \equiv 0$ in the first frame, and hence in every frame.

If the interchange of two contravariant (or covariant) indices of a tensor does not alter the value of any of its components, the tensor is symmetric with respect to those indices. A tensor is antisymmetric with respect to a pair of indices if their interchange changes the sign but not the magnitude of the tensor's components. The symmetry properties of pure contravariant or pure covariant tensors are intrinsic (i.e., they remain the same in all coordinate frames). Symmetry (or antisymmetry) is *not* intrinsic to mixed tensors, however, because the relationship $A_j^{\,i} = A^i_{\,j}$, for example, in one coordinate system will not in general carry over to another. These statements may be proved directly by application of (A3.8).

A3.3. Relative Tensors

The tensors described above are *absolute* tensors. *Relative* tensors transform according to a more general law: a relative tensor of contravariant rank m, covariant rank n, and *weight* W transforms as

$$\bar{A}^{\alpha\beta\ldots\mu}_{\kappa\lambda\ldots\nu} = J^W \frac{\partial \bar{x}^\alpha}{\partial x^a} \cdots \frac{\partial \bar{x}^\mu}{\partial x^m} \frac{\partial x^k}{\partial \bar{x}^\kappa} \cdots \frac{\partial x^n}{\partial \bar{x}^\nu} A^{ab\ldots m}_{kl\ldots n}, \tag{A3.14}$$

where J is the Jacobian of the transformation, $J = |\partial x^i / \partial \bar{x}^\gamma|$. Absolute tensors are obviously relative tensors of weight zero; similarly a relative scalar of weight zero is an absolute scalar. Scalars and tensors of weight one are often given the special names scalar and tensor *density* for reasons indicated in §A3.4.

A3.4. The Line Element and the Metric Tensor

In a Euclidian three-space E_3 the length ds of the line element corresponding to an infinitesimal displacement vector dy^k in orthogonal Cartesian coordinates is given by

$$ds^2 = dy^k \, dy^k \tag{A3.15}$$

where k is summed. Generalizing, we adopt (A3.15) as the definition of ds^2 in E_n, where k now runs from 1 to n. Suppose now we transform to a curvilinear coordinate system x^i, and that we can express $y^k = y^k(x^{(1)}, x^{(2)}, \ldots, x^{(n)})$ and hence $dy^k = (\partial y^k/\partial x^i)\, dx^i$. Then in terms of the new coordinates the line element is

$$ds^2 = \left(\frac{\partial y^k}{\partial x^i}\right)\left(\frac{\partial y^k}{\partial x^j}\right) dx^i\, dx^j \equiv g_{ij}\, dx^i\, dx^j, \tag{A3.16}$$

where k is summed from 1 to n.

The tensor g_{ij} is the *metric tensor*; any space characterized by a metric tensor is called a *Riemannian space*. The metric tensor is obviously symmetric in its indices, and is an absolute covariant tensor of rank two, which implies that the line element is a scalar. We verify these statements directly by transforming to a new coordinate system $\bar{x}^i$; then

$$\bar{g}_{ab} \equiv \frac{\partial y^k}{\partial \bar{x}^a}\frac{\partial y^k}{\partial \bar{x}^b} = \frac{\partial x^i}{\partial \bar{x}^a}\frac{\partial y^k}{\partial x^i}\frac{\partial x^j}{\partial \bar{x}^b}\frac{\partial y^k}{\partial x^j} = \frac{\partial x^i}{\partial \bar{x}^a}\frac{\partial x^j}{\partial \bar{x}^b}\, g_{ij}, \tag{A3.17}$$

which is the correct transformation law for a second-rank covariant tensor. The fact that ds is a scalar is then obvious. In Cartesian coordinates the elements of the metric tensor are $g_{ij} = \delta_{ij}$ (the Kronecker δ), and hence are everywhere constant. Any coordinate system in which the elements of g_{ij} are constant, but not necessarily δ_{ij}, may also be considered to be Cartesian because in this case one can reduce g_{ij} to δ_{ij} by a suitable linear transformation.

As an example of a metric in curvilinear coordinates, consider spherical polar coordinates $(x^{(1)}, x^{(2)}, x^{(3)}) = (r, \theta, \phi)$, for which $y^{(1)} = r \sin\theta \cos\phi$, $y^{(2)} = r\sin\theta\sin\phi$, and $y^{(3)} = r\cos\theta$. Then from (A3.16) we find

$$ds^2 = dr^2 + r^2\, d\theta^2 + r^2 \sin^2\theta\, d\phi^2, \tag{A3.18}$$

so that $g_{11} = 1$, $g_{22} = r^2$, $g_{33} = r^2\sin^2\theta$, and $g_{ij} = 0$ for $i \neq j$.

Given the covariant tensor g_{ij}, we can construct a second-order contravariant tensor g^{ij}, which is called the *reciprocal* (or *conjugate*) *tensor*, defined such that

$$g_{ij}g^{jk} \equiv \delta_i^k. \tag{A3.19}$$

Equation (A3.19) states that the components of g^{ij} are the elements of the inverse of the matrix whose components are g_{ij}. As long as $\mathbf{g}$ is nonsingular (i.e., $g = |g_{ij}| \neq 0$), its inverse is unique; therefore (A3.19) uniquely determines g^{ij}, and specifically implies that $g^{ij} = G^{ij}/g$ where G^{ij} is the cofactor of element g_{ij} in $|g_{ij}|$.

The determinant g appears in many tensor formulae. We can show that g is a relative scalar by taking determinants in (A3.17) and using (A2.29) to find

$$\bar{g} = |\bar{g}_{ij}| = \left|\frac{\partial x^a}{\partial \bar{x}^i}\frac{\partial x^b}{\partial \bar{x}^j}\, g_{ab}\right| = \left|\frac{\partial x^a}{\partial \bar{x}^i}\right| \left|\frac{\partial x^b}{\partial \bar{x}^j}\right| |g_{ab}| = J^2 g \tag{A3.20}$$

where J is the Jacobian of the transformation; this is the transformation law for a relative scalar of weight two. It follows that $g^{1/2}$ is a relative scalar of weight one.

The factor g also appears in definitions of volume elements via the formula

$$dV = dy^{(1)}\,dy^{(2)}\ldots dy^{(n)} = \begin{vmatrix} \dfrac{\partial y^{(1)}}{\partial x^{(1)}} & \dfrac{\partial y^{(1)}}{\partial x^{(2)}} \cdots & \dfrac{\partial y^{(1)}}{\partial x^{(n)}} \\ \vdots & & \vdots \\ \dfrac{\partial y^{(n)}}{\partial x^{(1)}} & \dfrac{\partial y^{(n)}}{\partial x^{(2)}} \cdots & \dfrac{\partial y^{(n)}}{\partial x^{(n)}} \end{vmatrix} dx^{(1)}\,dx^{(2)}\ldots dx^{(n)}$$

$$= g^{1/2}\,dx^{(1)}\,dx^{(2)}\ldots dx^{(n)} \qquad \text{(A3.21)}$$

where the y^i again denote orthogonal Cartesian coordinates. We can justify (A3.21) in two different ways. First, we can regard it as a result from analysis obtained by a direct evaluation of an n-dimensional iterated integral (**J1**, 183 *et seq.*). By direct transformation $y^i \to x^i$ one finds

$$I = \int dy^{(n)} \int dy^{(n-1)} \ldots \int dy^{(1)} f[y^{(1)}, y^{(2)}, \ldots, y^{(n)}]$$

$$\equiv \int dx^{(n)} \int dx^{(n-1)} \ldots \int dx^{(1)} f[y^{(1)}, y^{(2)}, \ldots, y^{(n)}] J(y^{(1)}, \ldots, y^{(n)}/x^{(1)}, \ldots, x^{(n)}) \qquad \text{(A3.22)}$$

where in the second integral y^i is regarded as $y^i(x^{(1)}, \ldots, x^{(n)})$, and J denotes the Jacobian of the transformation. Alternatively we can recognize that (A3.21) is the natural generalization of (A2.35) to an n-dimensional space, and view it as giving the volume of an n-dimensional parallelepiped whose sides are spanned by the elementary vectors $(dx^{(1)}, 0, \ldots, 0)$, $\ldots, (0, 0, \ldots, dx^{(n)})$. Under the transformation $x^i \to y^i$ these vectors become $\left(\dfrac{\partial y^{(1)}}{\partial x^{(1)}}, \dfrac{\partial y^{(2)}}{\partial x^{(1)}}, \ldots, \dfrac{\partial y^{(n)}}{\partial x^{(1)}}\right) dx^1, \ldots, \left(\dfrac{\partial y^{(1)}}{\partial x^{(n)}}, \dfrac{\partial y^{(2)}}{\partial x^{(n)}}, \ldots, \dfrac{\partial y^{(n)}}{\partial x^{(n)}}\right) dx^{(n)}$, which again leads to (A3.21). We thus identify the rightmost member of (A3.21) as the *invariant volume element*; the *volume* of any finite region is then

$$V = \iint \ldots \int g^{1/2}\,dx^{(1)}\,dx^{(2)}\ldots dx^{(n)}. \qquad \text{(A3.23)}$$

Finally, suppose we calculate the mass within some volume containing fluid of density ρ; then

$$M = \iint \ldots \int \rho\,dy^{(1)}\ldots dy^{(n)} = \iint \ldots \int \rho g^{1/2}\,dx^{(1)}\ldots dx^{(n)}$$

$$\equiv \iint \ldots \int \bar{\rho}\,dx^{(1)}\ldots dx^{(n)}. \qquad \text{(A3.24)}$$

Thus in terms of $\bar{\rho} \equiv g^{1/2}\rho$, a relative scalar of weight one, the integral giving the mass assumes an invariant form. It is this result that motivates the name scalar "density" for relative scalars of weight one.

A3.5. Associated Tensors

Having at our disposal the metric tensor and its reciprocal we can carry out the operation of *raising* and *lowering indices* to construct new tensors *associated* with any given tensor. To lower a contravariant index (say j) we multiply the tensor by g_{ij} and sum against j; for example

$$g_{ij}T^{kj}_{\cdot\cdot ab} = T^{k}_{\cdot iab}. \tag{A3.25a}$$

Notice that it may be necessary to use a notation that shows explicitly which index is affected, as was done here by filling vacant positions with dots, because in general the tensors $g_{ij}T^{jk} = T_i^{\cdot k}$ and $g_{ij}T^{kj} = T^{k}_{\cdot i}$ will be different. The operation of raising covariant indices proceeds similarly; for example

$$g^{ij}T^{k}_{\cdot iab} = T^{kj}_{\cdot\cdot ab}, \tag{A3.25b}$$

which shows explicitly that the operation of raising is the direct inverse of lowering. These operations can also be performed on relative tensors.

In the case of vectors the notation is unambiguous, and we can write

$$A_i = g_{ij}A^j \tag{A3.26a}$$

and

$$A^i = g^{ij}A_j. \tag{A3.26b}$$

Moreover we have

$$A_i = g_{ij}A^j = g_{ij}g^{jk}A_k = \delta_i^k A_k \equiv A_i \tag{A3.27}$$

which shows the complete reciprocity of contravariant and covariant components.

The fact that we can raise and lower indices at will shows convincingly that, as mentioned before, the contravariant, covariant, and physical components of a tensor are all merely different representations of the same physical entity. A direct geometrical interpretation of this relationship can be most easily provided for vectors. Choose a set of basis vectors along coordinate curves:

$$\mathbf{a}_i \equiv \mathbf{r}_{,i}. \tag{A3.28}$$

Then

$$ds^2 = d\mathbf{r}\cdot d\mathbf{r} = (\mathbf{r}_{,i}\,dx^i)\cdot(\mathbf{r}_{,j}\,dx^j) = (\mathbf{a}_i\cdot\mathbf{a}_j)\,dx^i\,dx^j = g_{ij}\,dx^i\,dx^j \tag{A3.29}$$

shows that $\mathbf{a}_i\cdot\mathbf{a}_j = g_{ij}$. Furthermore we see that these vectors are not in general unit vectors because $\mathbf{a}_{(i)}\cdot\mathbf{a}_{(i)} = g_{(i)(i)}$ is not necessarily unity. Now resolve $\mathbf{A}$ along this basis: $\mathbf{A} = A^i\mathbf{a}_i$. Then we can see that the geometrical interpretation of the contravariant components of $\mathbf{A}$ is that $(g_{(i)(i)})^{1/2}A^i$ is the length, along the unit vector $\mathbf{e}_i \equiv \mathbf{a}_i/(g_{(i)(i)})^{1/2}$, of the ith edge of the parallelepiped whose diagonal is $\mathbf{A}$.

Alternatively, define the reciprocal basis set

$$\mathbf{a}^i \equiv (\mathbf{a}_j \times \mathbf{a}_k)/g^{1/2} \tag{A3.30}$$

where (ijk) is a cyclic permutation of (123). Then clearly $\mathbf{a}_i \cdot \mathbf{a}^j = \delta_i^j$, and by using (A3.30) in (A2.40) it is easy to show that

$$\mathbf{a}_i = g^{1/2}(\mathbf{a}^j \times \mathbf{a}^k), \tag{A3.31}$$

where again (ijk) is a cyclic permutation of (123). Moreover, because

$$ds^2 = d\mathbf{r} \cdot d\mathbf{r} = (\mathbf{a}^i\, dx_i) \cdot (\mathbf{a}^j\, dx_j) = (\mathbf{a}^i \cdot \mathbf{a}^j)g_{il}g_{jm}\, dx^l\, dx^m \equiv g_{lm}\, dx^l\, dx^m, \tag{A3.32}$$

we see that $g_{lm} = g_{il}g_{jm}(\mathbf{a}^i \cdot \mathbf{a}^j)$. Contracting both sides of this equality against $g^{l\beta}g^{m\alpha}$ we find

$$g^{l\beta}g^{m\alpha}g_{lm} = g^{l\beta}\,\delta_l^\alpha = g^{\alpha\beta} = g^{l\beta}g^{m\alpha}g_{il}g_{jm}(\mathbf{a}^i \cdot \mathbf{a}^j) = \delta_i^\beta\,\delta_j^\alpha(\mathbf{a}^i \cdot \mathbf{a}^j) = \mathbf{a}^\alpha \cdot \mathbf{a}^\beta, \tag{A3.33}$$

so that we must have $\mathbf{a}^i \cdot \mathbf{a}^j = g^{ij}$.

Now resolve $\mathbf{A}$ along the $\mathbf{a}^i$ as $\mathbf{A} = A_i\mathbf{a}^i$. Then

$$\mathbf{A} \cdot \mathbf{a}_i = (A_k\mathbf{a}^k) \cdot \mathbf{a}_i = A_k\,\delta_i^k = A_i \equiv (A^k\mathbf{a}_k) \cdot \mathbf{a}_i = (\mathbf{a}_i \cdot \mathbf{a}_k)A^k = g_{ik}A^k \tag{A3.34}$$

which shows that the A_i are in fact the covariant components associated with the contravariant components A^i. In addition we can now see that $A_i/(g_{(i)(i)})^{1/2} = \mathbf{A} \cdot \mathbf{e}_i$ so that the geometrical interpretation of the covariant components A_i is that $A_i/(g_{(i)(i)})^{1/2}$ is the length of the orthogonal projection of $\mathbf{A}$ onto the unit vector that is tangent to the x^i coordinate curve. [See (**A2,** §§7.22 and 7.35) and (**S1,** §45) for further details.]

The geometrical interpretations given above show that in orthogonal Cartesian coordinates, for which the $g_{(i)(i)} = 1$, the contravariant and covariant coordinates of a vector are identical. But in curvilinear coordinates one sees [e.g., from (A3.18) and (A3.26)] that the two types of abstract components can be quite different, and moreover, from the discussion above, that individual components of a given type do not necessarily even have the same physical units (cf. §A3.7).

A3.6. Scalar Product

The natural covariant generalization of (A2.5) is

$$\mathbf{a} \cdot \mathbf{b} = a_j b^j = g_{ij}a^ib^j = g^{ij}a_ib_j. \tag{A3.35}$$

This expression is manifestly invariant under coordinate transformation:

$$\bar{a}_i\bar{b}^i = (\partial x^p/\partial \bar{x}^i)a_p(\partial \bar{x}^i/\partial x^q)b^q = \delta_q^p a_p b^q = a_q b^q. \tag{A3.36}$$

The natural covariant generalization of (A2.1) for the magnitude of a vector is

$$|\mathbf{a}| = (a_i a^i)^{1/2} = (g_{ij} a^i a^j)^{1/2} = (g^{ij} a_i a_j)^{1/2}. \tag{A3.37}$$

Furthermore, this suggests that we take as the covariant generalization of (A2.6) the expression

$$\cos\theta = (a_i b^i)/[(a_i a^i)^{1/2}(b_i b^i)^{1/2}] = (g_{ij} a^i b^j)/[(g_{ij} a^i a^j)^{1/2}(g_{ij} b^i b^j)^{1/2}]. \tag{A3.38}$$

As before, two vectors are considered to be orthogonal if $\cos\theta = 0$.

Choosing displacement vectors $(dx^{(1)}, 0, 0)$, $(0, dx^{(2)}, 0)$, and $(0, 0, dx^{(3)})$ along the coordinate curves of a three space we find from (A3.38) that the angles θ_{12}, θ_{13}, and θ_{23} between these curves are

$$\cos\theta_{12} = g_{12}/(g_{11} g_{22})^{1/2} \tag{A3.39a}$$

$$\cos\theta_{13} = g_{13}/(g_{11} g_{33})^{1/2} \tag{A3.39b}$$

and

$$\cos\theta_{23} = g_{23}/(g_{22} g_{33})^{2}. \tag{A3.39c}$$

From (A3.39) it immediately follows that the necessary and sufficient condition for a curvilinear coordinate system to be orthogonal is that $g_{ij} \equiv 0$ for $i \neq j$. In this important case, which is the only one we consider in our work, the metric tensor is diagonal and its reciprocal is simply $g^{(i)(i)} = 1/g_{(i)(i)}$. For example, in spherical polar coordinates $g^{11} = 1$, $g^{22} = 1/r^2$, $g^{33} = 1/r^2 \sin^2\theta$.

A3.7. *Physical Components*

Consider an orthogonal coordinate system in three-space. The metric is diagonal and the line element can be written

$$ds^2 = (h_1\, dx^{(1)})^2 + (h_2\, dx^{(2)})^2 + (h_3\, dx^{(3)})^2, \tag{A3.40}$$

where $h_i \equiv (g_{(i)(i)})^{1/2}$. It is clear that the increment of path length associated with a coordinate increment dx^i is not dx^i itself, but $ds^{(i)} = h_{(i)}\, dx^{(i)}$. More generally, using (A3.37) to calculate the length of a vector we have $a^2 = (h_1 a^{(1)})^2 + (h_2 a^{(2)})^2 + (h_3 a^{(3)})^2$. To obtain consistency with the Pythagorean theorem, we find that with the abstract contravariant component $a^{(i)}$ we must associate the *physical component*

$$a(i) = h_{(i)} a^{(i)}. \tag{A3.41}$$

Using (A3.37) again, now for covariant components, and noting that $g^{(i)(i)} = (1/h_i)^2$, we have $a^2 = (a_{(1)}/h_1)^2 + (a_{(2)}/h_2)^2 + (a_{(3)}/h_3)^2$ which shows that the physical components are related to covariant components by the expression

$$a(i) = a_{(i)}/h_{(i)}. \tag{A3.42}$$

To compute the physical components of a tensor T we notice that in Cartesian coordinates if λ^i and μ^i are unit vectors along some coordinate axes, then the expression

$$c = T_{ij}\lambda^i\mu^j \tag{A3.43}$$

gives the physical component of the tensor along those axes. But this expression is an invariant, and can be applied in curvilinear coordinates as well. If $\boldsymbol{\lambda}$ is to be a unit vector, we must have $h_i^2(\lambda^i)^2 = 1$. Thus if we choose three unit vectors along the $x^{(1)}$, $x^{(2)}$, and $x^{(3)}$ coordinate curves, we must have $\boldsymbol{\lambda}_{(1)} = (1/h_1, 0, 0)$, $\boldsymbol{\lambda}_{(2)} = (0, 1/h_2, 0)$, and $\boldsymbol{\lambda}_{(3)} = (0, 0, 1/h_3)$, respectively. Using these vectors in (A3.43) we find that the physical components of T in terms of its covariant components are

$$T(i, j) = T_{(i)(j)}/(h_{(i)}h_{(j)}). \tag{A3.44}$$

Carrying out the same analysis for contravariant components we have

$$T(i, j) = h_{(i)}h_{(j)}T^{(i)(j)}. \tag{A3.45}$$

Generalization of these expressions to nonothogonal systems is discussed in (**A2,** §§7.42 and 7.43).

As a specific example, the relations between the abstract and physical components of a vector in spherical coordinates are:

$$v^{(1)} = v_r,\ v^{(2)} = v_\theta/r,\ v^{(3)} = v_\phi/(r \sin\theta); \tag{A3.46a}$$

and

$$v_1 = v_r, \qquad v_2 = rv_\theta, \qquad v_3 = (r\sin\theta)v_\phi; \tag{A3.46b}$$

For a symmetric tensor in spherical coordinates we have

$$\begin{aligned} &T^{11} = T_{rr},\ T^{12} = T_{r\theta}/r,\ T^{13} = T_{r\phi}/(r\sin\theta),\ T^{22} = T_{\theta\theta}/r^2, \\ &T^{23} = T_{\theta\phi}/(r^2\sin\theta), \qquad \text{and} \qquad T^{33} = T_{\phi\phi}/(r\sin\theta)^2, \end{aligned} \tag{A3.47}$$

with analogous formulae for covariant components.

A3.8. The Levi-Civita Tensor

In curvilinear coordinates where index position is significant, the appropriate generalizations of (A2.25) and (A2.26) are

$$e_{pq\ldots t}\,|a^b_c| = e_{ij\ldots n}a^i_p a^j_q \ldots a^n_t, \tag{A3.48}$$

and

$$e^{pq\ldots t}\,|a^b_c| = e^{ij\ldots n}a^p_i a^q_j \ldots a^t_n, \tag{A3.49}$$

where a^b_c is the element in the bth row and cth column. In particular, if we set $a^b_c = (\partial x^b/\partial \bar{x}^c)$, (A3.48) becomes

$$\bar{e}_{pq\ldots t}J = \left(\frac{\partial x^i}{\partial \bar{x}^p}\right)\left(\frac{\partial x^j}{\partial \bar{x}^q}\right)\ldots\left(\frac{\partial x^n}{\partial \bar{x}^t}\right)e_{ij\ldots n}, \tag{A3.50}$$

which shows that the covariant permutation symbol is a relative tensor of weight -1. By a similar analysis one finds that $e^{pq\ldots t}$ is a relative tensor of weight $+1$. Recalling from (A3.20) that $J=(\bar{g}/g)^{1/2}$ and that g is a relative scalar of weight two, we then see that

$$\varepsilon_{ij\ldots k} \equiv g^{1/2} e_{ij\ldots k} \tag{A3.51}$$

and

$$\varepsilon^{ij\ldots k} \equiv g^{-1/2} e^{ij\ldots k} \tag{A3.52}$$

are of weight zero, and hence are absolute tensors. These are the covariant and contravariant components of the *Levi-Civita tensor*, which is skew symmetric in all indices.

Using the Levi-Civita tensor we can write a covariant generalization of the cross product (A2.32) as

$$c_i = \varepsilon_{ijk} a^j b^k \tag{A3.53a}$$

or

$$c^i = \varepsilon^{ijk} a_j b_k. \tag{A3.53b}$$

Similarly the covariant generalization of (A2.60) for the vector dual associated with an antisymmetric tensor in three-space is

$$\omega_i = \tfrac{1}{2}\varepsilon_{ijk}\Omega^{jk}, \tag{A3.54}$$

and

$$\Omega^{jk} = \varepsilon^{ijk}\omega_i. \tag{A3.55}$$

A3.9. Christoffel Symbols

As will be seen in §A3.10, certain combinations of partial derivatives of the metric tensor appear when we attempt to construct a covariant generalization of the operation of differentiation. Thus we define the *Christoffel symbol of the first kind* to be

$$[ij, k] \equiv \tfrac{1}{2}(g_{ik,j} + g_{jk,i} - g_{ij,k}), \tag{A3.56}$$

and the *Christoffel symbol of the second kind* as

$$\begin{Bmatrix} i \\ j\ k \end{Bmatrix} \equiv g^{il}[jk, l]. \tag{A3.57}$$

The rather cumbersome (and customary) notation employed here emphasizes that the *Christoffel symbols are not tensors* (see below). By inspection of (A3.56) it is obvious that $[ij, k] \equiv [ji, k]$, and hence that $\{{}_{j}{}^{i}{}_{k}\} \equiv \{{}_{k}{}^{i}{}_{j}\}$. Notice that *in Cartesian coordinates all Christoffel symbols* (*of both kinds*) *are identically zero.*

From (A3.56) we easily find the useful result

$$g_{ij,k} = [ik, j] + [jk, i] \tag{A3.58}$$

and hence

$$g_{ij,k} = g_{jl}\begin{Bmatrix} l \\ i\ k \end{Bmatrix} + g_{il}\begin{Bmatrix} l \\ j\ k \end{Bmatrix}. \tag{A3.59}$$

We can also write an extremely important formula for the derivative of the determinant g in terms of Christoffel symbols of the second kind. From the fact that $g = g_{(i)j}G^{(i)j}$, where G^{ij} is the cofactor of g_{ij}, and recalling that $G^{ij} = gg^{ij}$, we see from (A3.59) that

$$\begin{aligned} g_{,k} &= (\partial g/\partial g_{ij})g_{ij,k} = G^{ij}g_{ij,k} = gg^{ij}\left(g_{jl}\begin{Bmatrix} l \\ i\ k \end{Bmatrix} + g_{il}\begin{Bmatrix} l \\ j\ k \end{Bmatrix}\right) \\ &= g\left(\begin{Bmatrix} i \\ i\ k \end{Bmatrix} + \begin{Bmatrix} j \\ j\ k \end{Bmatrix}\right) = 2g\begin{Bmatrix} i \\ i\ k \end{Bmatrix}. \end{aligned} \tag{A3.60}$$

Therefore

$$\begin{Bmatrix} i \\ i\ k \end{Bmatrix} = (\ln g^{1/2})_{,k}. \tag{A3.61}$$

For orthogonal coordinate systems, the Christoffel symbols can be written in a very compact form that is useful for computation. If $g_{ij} = 0$ when $j \neq i$ one easily finds from (A3.56) and (A3.57) that

$$\begin{Bmatrix} i \\ i\ i \end{Bmatrix} = \tfrac{1}{2}(\ln g_{ii})_{,i}, \tag{A3.62a}$$

$$\begin{Bmatrix} i \\ i\ j \end{Bmatrix} = \tfrac{1}{2}(\ln g_{ii})_{,j}, \tag{A3.62b}$$

$$\begin{Bmatrix} i \\ j\ j \end{Bmatrix} = -\tfrac{1}{2}(g_{jj})_{,i}/g_{ii}, \tag{A3.62c}$$

and

$$\begin{Bmatrix} i \\ j\ k \end{Bmatrix} = 0. \tag{A3.62d}$$

In (A3.62), i, j, and k are distinct, and there is no sum on repeated indices. In particular, for spherical coordinates we find, using (A3.18) and (A3.62) that the nonzero Christoffel symbols are

$$\begin{aligned} &\begin{Bmatrix} 1 \\ 2\ 2 \end{Bmatrix} = -r, && \begin{Bmatrix} 1 \\ 3\ 3 \end{Bmatrix} = -r\sin^2\theta, \\ &\begin{Bmatrix} 2 \\ 3\ 3 \end{Bmatrix} = -\sin\theta\cos\theta, \quad \text{and} && \begin{Bmatrix} 2 \\ 1\ 2 \end{Bmatrix} = 1/r, \\ &\begin{Bmatrix} 3 \\ 2\ 3 \end{Bmatrix} = \cot\theta, && \begin{Bmatrix} 3 \\ 1\ 3 \end{Bmatrix} = 1/r. \end{aligned} \tag{A3.63}$$

Last, we must develop the transformation law for Christoffel symbols. Consider two curvilinear coordinate systems y^i and x^α with metric tensors

h_{ij} and $g_{\alpha\beta}$, respectively. Then

$$h_{ij} = (\partial x^\alpha/\partial y^i)(\partial x^\beta/\partial y^j) g_{\alpha\beta} \equiv x^\alpha_{,i} x^\beta_{,j} g_{\alpha\beta} \tag{A3.64}$$

and

$$h^{ij} = (\partial y^i/\partial x^\alpha)(\partial y^j/\partial x^\beta) g^{\alpha\beta} \equiv y^i_{,\alpha} y^j_{,\beta} g^{\alpha\beta}. \tag{A3.65}$$

Differentiating h_{ij} we have

$$\begin{aligned} h_{ij,k} &= g_{\alpha\beta}(x^\alpha_{,ik} x^\beta_{,j} + x^\alpha_{,i} x^\beta_{,kj}) + x^\alpha_{,i} x^\beta_{,j} x^\gamma_{,k} g_{\alpha\beta,\gamma} \\ &= g_{\alpha\beta}(x^\alpha_{,ik} x^\beta_{,j} + x^\alpha_{,kj} x^\beta_{,i}) + x^\alpha_{,i} x^\beta_{,j} x^\gamma_{,k} g_{\alpha\beta,\gamma}. \end{aligned} \tag{A3.66}$$

The second step follows because α and β are dummy and $g_{\alpha\beta}$ is symmetric. Now permuting $i \to j \to k \to i$ in (A3.66) and adding, we find that

$$[ij, k] = \tfrac{1}{2}(h_{jk,i} + h_{ki,j} - h_{ij,k}) = x^\alpha_{,i} x^\beta_{,j} x^\gamma_{,k} [\alpha\beta, \gamma] + x^\alpha_{,ij} x^\beta_{,k} g_{\alpha\beta}, \tag{A3.67}$$

which shows that $[\alpha\beta, \gamma]$ is, in general, *not* a tensor. It would be a tensor only if the second term on the right-hand side were to vanish identically, which happens to be true if the coordinate transformation is linear (i.e., $x^\alpha = c^\alpha_i y^i$ where the c's are constants), but not in general. Using (A3.57) and (A3.65) in (A3.67) we find

$$\begin{aligned} \begin{Bmatrix} l \\ i\ j \end{Bmatrix} &= y^l_{,\varepsilon} y^k_{,\zeta} g^{\varepsilon\zeta} (x^\alpha_{,i} x^\beta_{,j} x^\gamma_{,k} [\alpha\beta, \gamma] + x^\alpha_{,ij} x^\beta_{,k} g_{\alpha\beta}) \\ &= y^l_{,\varepsilon} x^\alpha_{,i} x^\beta_{,j} g^{\varepsilon\gamma} [\alpha\beta, \gamma] + y^l_{,\varepsilon} x^\alpha_{,ij} g^{\varepsilon\beta} g_{\alpha\beta}, \end{aligned} \tag{A3.68}$$

which simplifies to

$$\begin{Bmatrix} k \\ i\ j \end{Bmatrix} = y^k_{,\gamma} x^\alpha_{,i} x^\beta_{,j} \begin{Bmatrix} \gamma \\ \alpha\ \beta \end{Bmatrix} + y^k_{,\alpha} x^\alpha_{,ij}. \tag{A3.69}$$

Equation (A3.69) shows that $\{^{\,k}_{i\,j}\}$ is also not in general a tensor, although it would be if the coordinate transformation were linear. Finally, by contracting (A3.69) against $x^\lambda_{,k}$ we obtain the useful result

$$x^\lambda_{,ij} = x^\lambda_{,k} \begin{Bmatrix} k \\ i\ j \end{Bmatrix} - x^\alpha_{,i} x^\beta_{,j} \begin{Bmatrix} \lambda \\ \alpha\ \beta \end{Bmatrix}. \tag{A3.70}$$

A3.10. Covariant Differentiation

We are now in a position to generalize the notion of differentiation into a covariant form. Suppose we differentiate the covariant vector

$$B_i \equiv (\partial x^\alpha/\partial y^i) A_\alpha \equiv x^\alpha_{,i} A_\alpha. \tag{A3.71}$$

We obtain

$$B_{i,j} = x^\alpha_{,i} x^\beta_{,j} A_{\alpha,\beta} + x^\alpha_{,ij} A_\alpha. \tag{A3.72}$$

It is obvious from (A3.72) that $B_{i,j}$ is not a tensor. But if we use (A3.70) in

(A3.72) we can rewrite the equation as

$$B_{i,j} = x^{\alpha}_{,i} x^{\beta}_{,j}\left(A_{\alpha,\beta} - \begin{Bmatrix} \lambda \\ \alpha\ \beta \end{Bmatrix} A_{\lambda}\right) + \begin{Bmatrix} k \\ i\ j \end{Bmatrix} x^{\lambda}_{,k} A_{\lambda}, \tag{A3.73}$$

or

$$B_{i,j} - \begin{Bmatrix} k \\ i\ j \end{Bmatrix} B_k = x^{\alpha}_{,i} x^{\beta}_{,j}\left(A_{\alpha,\beta} - \begin{Bmatrix} \lambda \\ \alpha\ \beta \end{Bmatrix} A_{\lambda}\right). \tag{A3.74}$$

Thus the combination

$$B_{i;j} \equiv B_{i,j} - \begin{Bmatrix} k \\ i\ j \end{Bmatrix} B_k \tag{A3.75}$$

is a covariant second-rank tensor, and reduces to the ordinary partial derivative of B_i in Cartesian coordinates. We therefore take (A3.75) as the definition of the *covariant derivative* of the vector B_i.

By a similar analysis, one can show that the covariant derivative of a contravariant vector is a mixed tensor of the second rank:

$$B^{i}_{;j} \equiv B^{i}_{,j} + \begin{Bmatrix} i \\ j\ k \end{Bmatrix} B^k. \tag{A3.76}$$

The extra terms containing Christoffel symbols that appear in equations (A3.75) and (A3.76) account for the effects of curvature of the coordinate system [see (**S1**, §46) for a detailed discussion].

These formulae are easily extended to mixed tensors of arbitrary rank. We find that the covariant derivative of the mixed tensor $A^{ab\ldots c}_{ij\ldots k}$ is

$$\begin{aligned} A^{ab\ldots c}_{ij\ldots k;q} = A^{ab\ldots c}_{ij\ldots k,q} &+ \begin{Bmatrix} a \\ \alpha\ q \end{Bmatrix} A^{\alpha b\ldots c}_{ij\ldots k} + \begin{Bmatrix} b \\ \alpha\ q \end{Bmatrix} A^{a\alpha\ldots c}_{ij\ldots k} + \ldots + \begin{Bmatrix} c \\ \alpha\ q \end{Bmatrix} A^{ab\ldots \alpha}_{ij\ldots k} \\ &- \begin{Bmatrix} \alpha \\ i\ q \end{Bmatrix} A^{ab\ldots c}_{\alpha j\ldots k} - \begin{Bmatrix} \alpha \\ j\ q \end{Bmatrix} A^{ab\ldots c}_{i\alpha\ldots k} - \ldots - \begin{Bmatrix} \alpha \\ k\ q \end{Bmatrix} A^{ab\ldots c}_{ij\ldots \alpha}. \end{aligned} \tag{A3.77}$$

In particular, for a contravariant tensor of the second rank,

$$T^{ij}_{;k} = T^{ij}_{,k} + \begin{Bmatrix} i \\ l\ k \end{Bmatrix} T^{lj} + \begin{Bmatrix} j \\ l\ k \end{Bmatrix} T^{il}. \tag{A3.78}$$

Note in passing that the covariant derivative of a scalar is identical to its ordinary partial derivative, and that the operation of covariant differentiation increases the rank of the resulting tensor by one relative to the original tensor. Furthermore, it is straightforward to generalize (A3.77) to relative tensors [see, e.g., (**L1,** §36) or (**S2,** §7.2)], but we will not require this result in our work.

The derivation of formulae for covariant differentiation given above proceeds by direct analysis. While this approach has the merit of brevity, it fails to communicate the deeper geometrical significance of the process, which raises questions concerning parallel transport and transplantation of vectors in a curved space. Discussions of these important and interesting matters, and generalizations of covariant differentiation to nonmetrical spaces, can be found in (**A1,** §§2.1, 2.2, and 3.1), (**L2,** §§33–36 and 39–41), and (**S2,** Chap. 8).

Let us now calculate the covariant derivative of the metric tensor; from (A3.77) we have

$$g_{ij;k} = g_{ij,k} - \left\{ \begin{matrix} l \\ i\ k \end{matrix} \right\} g_{lj} - \left\{ \begin{matrix} l \\ j\ k \end{matrix} \right\} g_{il}. \tag{A3.79}$$

But from (A3.59) the right-hand side is identically zero. Thus we have *Ricci's theorem*: the covariant derivative of the metric tensor (or its reciprocal) is identically zero in any coordinate system. This implies that in tensor equations we may freely interchange the operations of raising and lowering indices and of covariant differentiation. By a similar calculation we find that the Kronecker delta also behaves like a constant under covariant differentiation:

$$\delta^i_{j;k} = \delta^i_{j,k} + \left\{ \begin{matrix} i \\ k\ l \end{matrix} \right\} \delta^l_j - \left\{ \begin{matrix} l \\ j\ k \end{matrix} \right\} \delta^i_l = 0 + \left\{ \begin{matrix} i \\ k\ j \end{matrix} \right\} - \left\{ \begin{matrix} i \\ j\ k \end{matrix} \right\} \equiv 0. \tag{A3.80}$$

Suppose now that through some region in which a tensor field $A^{ab\ldots c}_{ij\ldots k}$ is defined, we choose a specific path, parameterized in terms of a path-length variable s as $x^i(s)$. Then we define the *intrinsic* (or *absolute*) *derivative* of the tensor field along this path to be

$$\begin{aligned} \frac{\delta A^{ab\ldots c}_{ij\ldots k}}{\delta s} &\equiv A^{ab\ldots c}_{ij\ldots k;q} \frac{dx^q}{ds} \\ &= \frac{dA^{ab\ldots c}_{ij\ldots k}}{ds} + \left(\left\{ \begin{matrix} a \\ m\ q \end{matrix} \right\} A^{mb\ldots c}_{ij\ldots k} + \ldots - \left\{ \begin{matrix} m \\ i\ q \end{matrix} \right\} A^{ab\ldots c}_{mj\ldots k} - \ldots \right) \frac{dx^q}{ds}. \end{aligned} \tag{A3.81}$$

Here we have written $(dA^{ab\ldots c}_{ij\ldots k}/ds) \equiv (\partial A^{ab\ldots c}_{ij\ldots k}/\partial x^q)(dx^q/ds)$. In particular, for a contravariant vector A^i,

$$\frac{\delta A^i}{\delta s} = \frac{dA^i}{ds} + \left\{ \begin{matrix} i \\ j\ k \end{matrix} \right\} A^j \frac{dx^k}{ds}. \tag{A3.82}$$

In (A3.81) and (A3.82), s is an arbitrary path-length parameter. But in problems of fluid flow, it is natural to describe the path followed by a fluid element in terms of the time t, so that $x^i = x^i(t)$, and $(dx^i/dt) \equiv x^i_{,t} = v^i$, the velocity of the fluid element. In addition we must then allow for the possibility that any vector or tensor field may be an explicit function of time as well as of position, say $A^i = A^i(\mathbf{r}, t)$. Suppose now we choose time as the independent variable; then the intrinsic derivative with respect to time is the derivative with respect to time along the path followed by the fluid, that is, as measured in a frame moving with the fluid. In physical terms it is therefore identical to the *Lagrangean derivative* employed in descriptions of fluid kinematics and dynamics (cf. §15). For example

$$(\delta A^i/\delta t) \equiv (DA^i/Dt) = A^i_{,t} + A^i_{,j}v^j + \begin{Bmatrix} i \\ j\ k \end{Bmatrix} A^j v^k. \tag{A3.83}$$

Equation (A3.83) is the covariant generalization of the customary Lagrangean derivative for the vector field A^i; similar formulae can be written for tensors.

A3.11. Gradient, Divergence, Laplacian, and Curl

Covariant generalizations of the various operations with the symbolic operator ∇ discussed in §A2.10 can in most instances be obtained simply by replacing the partial derivatives with covariant derivatives. In the case of the gradient of a scalar field, the two derivatives are identical $f_{,i} \equiv f_{;i}$, and we obtain a covariant vector, say $\mathbf{F}$. For instance, in spherical coordinates the covariant components of $\mathbf{F}$ are $(\partial f/\partial r, \partial f/\partial \theta, \partial f/\partial \phi)$. Then from (A3.42) we find physical components

$$\nabla f = \left(\frac{\partial f}{\partial r}, \frac{1}{r}\frac{\partial f}{\partial \theta}, \frac{1}{r \sin\theta}\frac{\partial f}{\partial \phi}\right). \tag{A3.84}$$

One can of course also form the gradient of vector and tensor fields, for example, $(\nabla v^i)_j = v^i_{;j}$, etc.

The covariant generalization of the divergence of a vector is

$$\nabla \cdot \mathbf{v} = v^i_{;i} = v^i_{,i} + \begin{Bmatrix} i \\ i\ j \end{Bmatrix} v^j. \tag{A3.85}$$

In view of (A3.61) we can rewrite (A3.85) as

$$v^i_{;i} = g^{-1/2}(g^{1/2}v^i)_{,i} \tag{A3.86}$$

which is a convenient form for calculating $\nabla \cdot \mathbf{v}$ in curvilinear coordinates. For example, in spherical coordinates $g^{1/2} = r^2 \sin\theta$, and we find

$$v^i_{;i} = \frac{\partial v^{(1)}}{\partial r} + \frac{\partial v^{(2)}}{\partial \theta} + \frac{\partial v^{(3)}}{\partial \phi} + \frac{2v^{(1)}}{r} + \cot\theta\, v^{(2)}. \tag{A3.87}$$

Converting to physical components via (A3.46a) we recover the familiar result

$$v^i_{;i} = \frac{1}{r^2}\frac{\partial(r^2 v_r)}{\partial r} + \frac{1}{r\sin\theta}\frac{\partial(\sin\theta\, v_\theta)}{\partial \theta} + \frac{1}{r\sin\theta}\frac{\partial v_\phi}{\partial \phi}. \tag{A3.88}$$

For an arbitrary tensor we can form a divergence by contracting the covariant derivative index against any contravariant index, for example, $A^{i_1 \ldots i_k \ldots i_n}_{j_1 \ldots j_m ; i_k}$. In our work we have occasion to deal only with second-rank tensors, which, in view of (A2.17), we can assume to have a definite symmetry. Applying (A3.78) to a symmetric tensor we find, using (A3.61),

$$S^{ij}_{;j} = S^{ij}_{,j} + \left\{ {i \atop k\ j} \right\} S^{kj} + \left\{ {j \atop k\ j} \right\} S^{ik} = g^{-1/2}(g^{1/2} S^{ij})_{,j} + \left\{ {i \atop j\ k} \right\} S^{jk}. \tag{A3.89}$$

For an antisymmetric tensor, individual terms in the last sum in (A3.89) cancel in pairs because the Christoffel symbols are symmetric in j and k, and we obtain the simpler result

$$A^{ij}_{;j} = g^{-1/2}(g^{1/2} A^{ij})_{,j}. \tag{A3.90}$$

Using (A3.89) and (A3.63) for a symmetric tensor T^{ij} in spherical coordinates and converting to physical components via (A3.47) we obtain the useful results:

$$T^{1j}_{;j} = \frac{1}{r^2}\frac{\partial(r^2 T_{rr})}{\partial r} + \frac{1}{r \sin\theta}\frac{\partial(\sin\theta T_{r\theta})}{\partial\theta} + \frac{1}{r\sin\theta}\frac{\partial T_{r\phi}}{\partial\phi} - \frac{1}{r}(T_{\theta\theta} + T_{\phi\phi}), \tag{A3.91a}$$

$$T^{2j}_{;j} = \frac{1}{r}\left[\frac{1}{r^2}\frac{\partial(r^2 T_{r\theta})}{\partial r} + \frac{1}{r \sin\theta}\frac{\partial(\sin\theta T_{\theta\theta})}{\partial\theta} + \frac{1}{r\sin\theta}\frac{\partial T_{\theta\phi}}{\partial\phi} + \frac{1}{r}(T_{r\theta} - \cot\theta T_{\phi\phi})\right] \tag{A3.91b}$$

and

$$T^{3j}_{;j} = \frac{1}{r\sin\theta}\left[\frac{1}{r^2}\frac{\partial(r^2 T_{r\phi})}{\partial r} + \frac{1}{r \sin\theta}\frac{\partial(\sin\theta T_{\theta\phi})}{\partial\theta} + \frac{1}{r\sin\theta}\frac{\partial T_{\phi\phi}}{\partial\phi} + \frac{1}{r}(T_{r\phi} + \cot\theta T_{\theta\phi})\right]. \tag{A3.91c}$$

The additional factors outside the square brackets account for the fact that the quantities on the left-hand side of (A3.91) are contravariant components, not physical components.

The easiest way to find a covariant expression for the Laplacian of a scalar is to follow (A2.49) and take the divergence of the vector obtained by forming the gradient of f. Thus $g^{ij}f_{,i}$ is a contravariant representation of ∇f, hence

$$\nabla^2 f = (g^{ij} f_{,i})_{;j} = g^{-1/2}(g^{1/2} g^{ij} f_{,i})_{,j} \tag{A3.92}$$

where we have used (A3.86). Similarly, for a vector we could write $\nabla^2 a^k = (g^{ij} a^k_{;i})_{;j}$.

As an example, the Laplacian of a scalar in spherical coordinates is, from

(A3.92),

$$\nabla^2 f = \frac{1}{r^2 \sin\theta}\left[\frac{\partial}{\partial r}\left(r^2 \sin\theta \frac{\partial f}{\partial r}\right) + \frac{\partial}{\partial\theta}\left(\sin\theta \frac{\partial f}{\partial\theta}\right) + \frac{\partial}{\partial\phi}\left(\frac{1}{\sin\theta}\frac{\partial f}{\partial\phi}\right)\right]$$
$$= \frac{1}{r^2}\frac{\partial}{\partial r}\left(r^2 \frac{\partial f}{\partial r}\right) + \frac{1}{r^2 \sin\theta}\frac{\partial}{\partial\theta}\left(\sin\theta \frac{\partial f}{\partial\theta}\right) + \frac{1}{r^2 \sin^2\theta}\frac{\partial^2 f}{\partial\phi^2}. \qquad \text{(A3.93)}$$

For the curl of a vector we can obtain a covariant generalization of (A2.50) by replacing the permutation symbol with the Levi-Civita tensor and partial derivatives with covariant derivatives. Then

$$(\nabla \times \mathbf{a})^i = \varepsilon^{ijk} a_{k;j} = g^{-1/2} e^{ijk} a_{k;j} = g^{-1/2}(a_{k;j} - a_{j;k})$$
$$= g^{-1/2}\left(a_{k,j} - \left\{ {l \atop k\ j} \right\} a_l - a_{j,k} + \left\{ {l \atop j\ k} \right\} a_l\right) \qquad \text{(A3.94)}$$

where (i, j, k) are distinct and are a cyclic permutation of (1, 2, 3). But the Christoffel symbols are symmetric in their lower indices, so that (A3.94) reduces to

$$(\nabla \times \mathbf{a})^i = g^{-1/2}(a_{k,j} - a_{j,k}), \qquad \text{(A3.95)}$$

which is easy to evaluate. For example, in spherical coordinates $g^{1/2} = r^2 \sin\theta$, and converting to physical components via (A3.46) one easily finds

$$(\nabla \times \mathbf{a})_r = \frac{1}{r\sin\theta}\left[\frac{\partial(\sin\theta\, a_\phi)}{\partial\theta} - \frac{\partial a_\theta}{\partial\phi}\right], \qquad \text{(A3.96a)}$$

$$(\nabla \times \mathbf{a})_\theta = \frac{1}{r}\left[\frac{1}{\sin\theta}\frac{\partial a_r}{\partial\phi} - \frac{\partial(r a_\phi)}{\partial r}\right], \qquad \text{(A3.96b)}$$

and

$$(\nabla \times \mathbf{a})_\phi = \frac{1}{r}\left[\frac{\partial(r a_\theta)}{\partial r} - \frac{\partial a_r}{\partial\theta}\right]. \qquad \text{(A3.96c)}$$

Finally, note in passing that (A3.94) shows that $(\nabla \times \mathbf{a})$ is the dual of the antisymmetric tensor $A_{ij} = a_{j,i} - a_{i,j}$.

A3.12. Geodesics

Suppose that a constant vector $\mathbf{A}$ in Cartesian coordinates is moved parallel to itself through a displacement dy^i; we know that all components A^i remain unchanged, so that $dA^i \equiv 0$. Now consider the same operation transformed to curvilinear coordinates in which $B^\alpha = (\partial x^\alpha/\partial y^i)A^i = x^\alpha_{,i} A^i$. Then

$$dB^\alpha = x^\alpha_{,ij} A^i\, dy^j + x^\alpha_{,i}\, dA^i = x^\alpha_{,ij} A^i y^j_{,\beta}\, dx^\beta \qquad \text{(A3.97)}$$

because $dA^i = 0$. Thus for *parallel displacement*,

$$dB^\alpha = x^\alpha_{,ij} y^j_{,\beta} y^i_{,\gamma} B^\gamma \, dx^\beta. \tag{A3.98}$$

Now using (A3.70) with $\left\{ {k \atop i\ j} \right\} = 0$ for Cartesian coordinates, (A3.98) becomes

$$dB^\alpha = -B^\gamma x^\rho_{,i} x^\sigma_{,j} \left\{ {\alpha \atop \rho\ \sigma} \right\} y^i_{,\gamma} y^j_{,\beta} \, dx^\beta = -\delta^\rho_\gamma \delta^\sigma_\beta \left\{ {\alpha \atop \rho\ \sigma} \right\} B^\gamma \, dx^\beta = -\left\{ {\alpha \atop \beta\ \gamma} \right\} B^\beta \, dx^\gamma. \tag{A3.99}$$

If we parameterize a path as $x^i(s)$, then (A3.99) shows that for parallel displacement of **B** along that path the intrinsic derivative will be identically zero:

$$\frac{\delta B^\alpha}{\delta s} = \frac{dB^\alpha}{ds} + \left\{ {\alpha \atop \beta\ \gamma} \right\} B^\beta \frac{dx^\gamma}{ds} = B^\alpha_{;\beta} \frac{dx^\beta}{ds} \equiv 0. \tag{A3.100}$$

In a Euclidian space we can construct a *straight line* by choosing the curve that has the property that an arbitrary vector displaced along it always remains parallel to itself. We generalize the notion of a straight line in a Riemannian space to that of a *geodesic*, which is the curve generated by parallel displacement of its unit tangent vector; that is, along a geodesic the tangents at all points are parallel, so that the curve's direction remains "constant" in the curved space. The equations describing a geodesic follow immediately by substituting $B^i = \lambda^i = (dx^i/ds)$ into (A3.100), which yields

$$\frac{d^2 x^i}{ds^2} + \left\{ {i \atop j\ k} \right\} \frac{dx^j}{ds} \frac{dx^k}{ds} = 0. \tag{A3.101}$$

Other forms are discussed in (**S2,** §2.4).

Another property of straight lines in Euclidian space is that they are the shortest distance between two points. If one requires that a geodesic have the property of minimizing the path length between two points and therefore that

$$\delta \int_{P_1}^{P_2} ds = \delta \int_{P_1}^{P_2} \left(g_{ij} \frac{dx^i}{ds} \frac{dx^j}{ds} \right)^{1/2} ds = 0, \tag{A3.102}$$

then a variational analysis leads again to (A3.101) [see e.g. (**A1,** 55–57), (**L1,** §128), or (**S1,** §58)].

A3.13. Integral Theorems

It is possible to generalize the divergence theorem and Stokes's theorem to curvilinear coordinates in n dimensions, and also to nonmetrical spaces. We will not develop these generalizations here because we do not require them in our work; the reader may pursue these matters in (**S2,** Chap. 7).

References

(A1) Adler, R., Bazin, M., and Schiffer, M. (1975) *Introduction to General Relativity*. New York: McGraw-Hill.

(A2) Aris, R. (1962) *Vectors, Tensors, and the Basic Equations of Fluid Mechanics*. Englewood Cliffs: Prentice-Hall.

(J1) Jeffreys, H. and Jeffreys, B. D. (1950) *Methods of Mathematical Physics*. Cambridge: Cambridge University Press.

(L1) Lass, H. (1950) *Vector and Tensor Analysis*. New York: McGraw-Hill.

(L2) Lawden, D. F. (1975) *An Introduction to Tensor Calculus and Relativity*. London: Chapman and Hall.

(S1) Sokolnikoff, I. S. (1964) *Tensor Analysis*. New York: Wiley.

(S2) Synge, J. L. and Schild, A. (1949) *Tensor Calculus*. Toronto: University of Toronto Press.

Glossary of Physical Symbols

a	Sound speed
a_n	Frequency quadrature weight
a_R	Radiation density constant
a_T	Isothermal sound speed
a_x, a_y, a_z	Components of acceleration in (x, y, z) directions
a_0	Bohr radius
$\mathbf{a}$	Acceleration
$\mathscr{a}$	Invariant opacity
A	Atomic weight
A	Surface area
A_i	Vector part of Chapman–Enskog solution of Boltzmann equation
A_{ji}	Einstein spontaneous emission probability
A_k	Amplitude of kth Fourier component
A^{α}	Four acceleration
$\mathscr{A}_0$	Avogadro's number
b	Impact parameter in collision
b_i	Non-LTE departure coefficient, n_i/n_i^*
b_m	Angle quadrature weight
$\mathscr{b}$	Dimensionless impact parameter
B_{ij}	Tensor part of Chapman–Enskog solution of Boltzmann equation
B_{ij}	Einstein absorption probability
B_{ji}	Einstein stimulated emission probability
$B(T), B$	Integrated Planck function
$B_\nu(T), B(\nu, T), B_\nu$	Planck function
Bo	Boltzmann number
c	Speed of light
c_p	Specific heat at constant pressure
$\tilde{c}_p$	Specific heat at constant pressure per heavy particle
c_v	Specific heat at constant volume
$\tilde{c}_v$	Specific heat at constant volume per heavy particle
C	Heat capacity
C_{AB}	Bimolecular collision frequency
C_I	Numerical constant in Saha ionization formula
C_{ij}	Collision rate from level i to level j
$C_{i\kappa}$	Collisional ionization rate from level i

C_v	Heat capacity at constant volume
C_α	Coefficient in power-law potential
d	Diameter of rigid elastic sphere
d_0	Average distance between particles
D	Debye length
D_{ij}	Traceless rate of strain tensor
$D_{\alpha\beta}$	Covariant traceless shear tensor
(D/Dt)	Lagrangean time derivative (fluid element fixed)
$(Df/Dt)_{\text{coll}}$	Collisional source term in Boltzmann equation
$\mathscr{D}f$	Differential operator in Boltzmann equation
D	Traceless shear tensor
e	Electron charge
e	Specific internal energy (per gram)
e_{dissoc}	Internal energy of molecular dissociation
e_{exc}	Internal energy of atomic excitation
e_{ion}	Internal energy of atomic ionization
e_{rot}	Internal energy of molecular rotation
e_{trans}	Translational internal energy
e_{vib}	Internal energy of molecular vibration
e_{ijk}, e^{ijk}	Permutation symbol
$\hat{e}$	Internal energy per unit volume
$\tilde{e}$	Internal energy per particle
$\bar{e}$	Total specific internal energy of radiating fluid, $e_{\text{gas}}+(E/\rho)$
$\mathscr{e}$	Invariant emissivity
$\hat{\mathscr{e}}$	Total internal energy per unit volume, including rest energy, $\rho_0(c^2+e)$
$\tilde{\mathscr{e}}$	Total energy of particle including rest energy
$e(\nu)$	Radiation energy spectral profile
$\mathscr{e}(\infty)$	Energy flux per particle at infinity in stellar wind
$\mathscr{e}_c(\infty)$	Heat-conduction flux per particle at infinity in stellar wind
E_{ij}	Rate of strain tensor
E_w	Energy transported in wave per period
$E_{\alpha\beta}$	Covariant shear tensor
$E^*(T)$, E^*	Radiation energy density in thermal equilibrium at temperature T, $4\pi B/c$
$E^*(\nu, T)$, E_ν^*	Monochromatic radiation energy density in thermal equilibrium at temperature T, $4\pi B_\nu/c$
$E(\mathbf{x}, t)$, E	Radiation energy density
$E(\mathbf{x}, t; \nu)$, E_ν	Monochromatic radiation energy density
$E(z)$	Wave-amplitude scale factor
$\mathscr{E}$	Energy flux in spherical flow
$\mathscr{E}$	Explosion energy
$\mathscr{E}$	Internal energy in a volume V
$\mathscr{E}$	Scalar part of Eckart decomposition of radiation stress-energy tensor
$\mathscr{E}^{n+1}$	Total energy in flow at time t^{n+1}
$\mathscr{E}_c(\infty)$	Heat-conduction flux at infinity in stellar wind
E	Rate of strain tensor
f	Oscillator strength of spectral line

f_l	Line radiation force
$f_\nu, f(\mathbf{x}, t; \nu)$	Monochromatic variable Eddington factor
f_0	Maxwellian velocity distribution
f_1	First-order term in Chapman–Enskog solution of Boltzmann equation
$\hat{f}$	Dimensionless distribution function
$f(\mathbf{x}, \mathbf{u}, t)$	Particle distribution function
$f_R(\mathbf{x}, t; \mathbf{n}, p), f_R$	Photon distribution function
$\mathbf{f}$	Newtonian force density
$\mathbf{f}_R$	Radiation force
$\mathscr{f}_\nu$	Radiation flux spectral profile
F_{BB}	Radiation flux from black body
F^α	Four-force density
$F(v)$	Spontaneous recombination probability for electrons of speed v
$\mathbf{F}$	Force
$\mathbf{F}(\mathbf{x}, t), \mathbf{F}$	Radiation flux
$\mathbf{F}(\mathbf{x}, t; \nu), \mathbf{F}_\nu$	Monochromatic radiation flux
$\mathscr{F}$	Particle flux in spherical flow
$\mathscr{F}^\alpha$	Vector part of Eckart decomposition of radiation stress-energy tensor
g	Acceleration of gravity (planar geometry)
g	Determinant of metric tensor
g	Relative speed of collision partners
g_{electron}	Statistical weight of free electron
g_i	Statistical weight of state i
$g_{ij}, g_{\alpha\beta}$	Metric tensor
g_R	Radiative acceleration
$g_{R,l}$	Radiative acceleration from spectral lines
g_R^0	Invariant photon distribution function for blackbody radiation at rest relative to observer
$\mathbf{g}$	Gravitational acceleration
$\mathbf{g}$	Relative velocity of collision partners
G	Newtonian gravitation constant
G^α	Radiation four-force density
$G(v)$	Induced recombination probability for electrons of speed v
$\mathbf{G}$	Center of mass velocity
$\mathbf{G}$	Space components of radiation four-force density
$\mathbf{G}(\Delta t, k)$	Amplification matrix of system of difference equations
$\mathscr{G}$	Radiative gain rate per unit mass
$\boldsymbol{\mathscr{G}}$	Total radiation momentum density, $\mathbf{F}/c^2$
$\boldsymbol{\mathscr{G}}_\nu$	Monochromatic radiation momentum density, $\mathbf{F}_\nu/c^2$
h	Planck constant
$\hbar$	$h/2\pi$
h	Specific enthalpy
h_1	Normalized flux perturbation, H_1/B_0
$\bar{h}$	Enthalpy per particle
$h(\mu, \nu), h_{\mu\nu}, h$	Antisymmetric part of specific intensity, $\frac{1}{2}[I(+\mu, \nu) - I(-\mu, \nu)]$
$\tilde{h}$	Total enthalpy per particle, including rest energy, $m_0(c^2 + e) + (p/N)$

H	Scale height, density scale height
H_p	Pressure scale height
$\mathbf{H}(\mathbf{x}, t), \mathbf{H}$	Integrated Eddington flux, $\mathbf{F}/4\pi$
$\mathbf{H}(\mathbf{x}, t; \nu), \mathbf{H}_\nu$	Monochromatic Eddington flux, $F_\nu/4\pi$
$\mathbf{i}$	Unit vector along x axis
I	Boltzmann collision integral
$I(\mathbf{x}, t; \mathbf{n}, \nu)$, $I(\mu, \nu), I_\nu, I$	Specific intensity
$I(\mathbf{x}, t; +\mathbf{n}, \nu)$, $I(+\mu, \nu), I^+$	Outward directed intensity
$I(\mathbf{x}, t; -\mathbf{n}, \nu)$, $I(-\mu, \nu), I^-$	Inward directed intensity
$\mathcal{I}$	Boltzmann collision integral
$\mathcal{I}(\mu, \nu), \mathcal{I}$	Invariant intensity
I	Unit tensor
j_1	Normalized mean intensity perturbation, J_1/B_0
$j(\mu, \nu), j_{\mu\nu}, j$	Symmetric part of specific intensity, $\frac{1}{2}[I(+\mu, \nu)+I(-\mu, \nu)]$
$\mathbf{j}$	Unit vector along y axis
J	Jacobian determinant of transformation
$\bar{J}$	Mean intensity averaged over line profile, $\int \phi_\nu J_\nu \, d\nu$
$J(f_i, f_j)$	Boltzmann collision integral for functions f_i and f_j
$J(\mathbf{x}, t; \nu), J_\nu$	Monochromatic mean intensity
k	Boltzmann constant
k	Wavenumber
k_H	χ_H/χ_R
k_J	κ_J/κ_P
k_Q	Dimensionless coefficient in pseudoviscosity
k_x, k_y, k_z	Components of wave vector in (x, y, z) directions
$\mathbf{k}$	Unit vector along z axis
$\mathbf{k}$	Wave vector
K	Coefficient of thermal conductivity
K_e	Electron thermal conduction coefficient
K_L	Conduction coefficient of a Lorentz gas
K_p	Proton thermal conduction coefficient
K_R	Radiative conductivity
K^α	Photon propagation four-vector
K_ν	$(c/4\pi)P_\nu$
$\bar{K}$	Total conductivity of radiating fluid
Kn	Knudsen number
l	Characteristic length
ℓ	Affine path-length variable
L	Wave damping length
L_E	Eddington luminosity
$L(r, t), L(r), L_r, L$	Luminosity passing through sphere of radius r
$\mathbf{L}$	Linear difference operator
$\mathbf{L}, L_\beta^{\alpha'}$	Lorentz transformation matrix
$\mathcal{L}$	Radiative loss rate per unit mass
$\mathcal{L}$	Thermalization length
m	Mass
m	Column mass

m	Electron mass
m	Relativistic mass
m_e	Electron mass
m_H	Mass of hydrogen atom
m_p	Proton mass
m_0	Rest mass
$\dot{m}$	Mass flux (planar geometry)
$\tilde{m}$	Reduced mass of collision partners
$\mathscr{m}$	M_1^2-1, where M_1 is upstream Mach number in shock
M	Total mass of collision partners
M_{cr}	Critical Mach number
M_r	Mass contained within sphere of radius r
M^α	Photon four-momentum
$M^{\alpha\beta}$	Material stress-energy tensor
$M(t)$	Radiation force multiplier
M	Mach number
$\mathcal{M}$	Mass of star
$\dot{\mathcal{M}}$	Radial mass flux (spherical geometry)
M	Material stress-energy tensor
n	Number of moles of gas
n_e	Number density of free electrons
n_H	Number density of neutral hydrogen atoms
n_i^*	Number density in level i in thermal equilibrium
n_p	Number density of protons
n_s	Number density of particles of species s
n_x, n_y, n_z	Components of photon propagation vector in (x, y, z) directions
n_κ	Number density of ions
$n(k)$	Inverse radiative relaxation time for disturbance of wavenumber k
$n_E(k)$	Inverse radiative relaxation time in Eddington approximation for disturbance of wavenumber k
$\mathbf{n}$	Direction of photon propagation
$\mathbf{n}$	Unit normal to surface
N	Total number density of particles
N_H	Number density of all (neutral plus ionized) hydrogen atoms
N_j	Number density of ion state j in all excitation states
Nu	Nusselt number
$\mathcal{N}$	Total number of particles in volume V
p	Impact parameter
p	Pressure
p_g, p_{gas}	Gas pressure
p_ν	Photoionization probability
p_1	Pressure perturbation in wave
$\bar{p}$	Total pressure in radiating fluid, $p_{gas}+p_{rad}$
$\mathbf{p}$	Momentum
$\mathscr{p}$	Fractional pressure jump across shock front, $(p_2-p_1)/p_1$
P	Complex amplitude of pressure perturbation in a wave
P	zz or rr component of radiation pressure tensor

P^*	Thermal radiation pressure
P_c	Average collision probability per unit length
P_d	Photon destruction probability
P_{ij}	Probability of transition from level i to level j
P_{rr}, $P_{\theta\theta}$, $P_{\phi\phi}$	Diagonal components of radiation pressure tensor in spherical geometry
P_{xx}, P_{yy}, P_{zz}	Diagonal components of radiation pressure tensor in planar geometry
P^α	Four-momentum
$P^{\alpha\beta}$	Projection tensor
$P^{\alpha\beta}$, P^{ij}	Radiation pressure tensor
P_ν	zz or rr components of monochromatic radiation pressure tensor
P_ν^*	Monochromatic thermal radiation pressure
$P_e(\tau)$	Photon escape probability
$\bar{P}(\mathbf{x}, t; \nu)$, $\bar{P}_\nu$	Mean monochromatic radiation pressure
Pe	Peclet number
Pr	Prandtl number
$\mathcal{P}^{\alpha\beta}$	Tensor part of Eckart decomposition of radiation stress-energy tensor
P	Projection tensor
P	Radiation pressure tensor
$\mathsf{P}(\mathbf{x}, t; \nu)$, P_ν	Monochromatic radiation pressure tensor
q	Heat transferred to unit mass of gas
$\dot{q}$	Rate of heat input to gas
q_ν	Sphericality factor
$q(\tau)$	Hopf function
$\mathbf{q}$	Thermal conduction flux
$\mathcal{q}^{n+1}$	Integrated heat input to flow at time t^{n+1}
Q	Heat gained or lost by gas
Q	Viscous pressure, pseudoviscous pressure
Q	$-(\partial \ln \rho/\partial \ln T)_p$
Q^α	Heat-flux four-vector
Q	Pseudoviscosity tensor
r	Radial coordinate in spherical coordinate system
r	Ratio of continuum to line opacity, κ_c/χ_l
r	a/cBo
r_c	Core radius
r_c	Critical radius in stellar wind
r_s	Radial position of shock
r_s	Sonic radius in stellar wind
r_0	Maximum compression ratio in shock $(\gamma+1)/(\gamma-1)$
$\hat{\mathbf{r}}$	Radial unit vector in spherical coordinate system
$\mathcal{r}$	Generalized Lagrangean radial coordinate
R	Complex amplitude of density perturbation in a wave
R	Gas constant for particular gas
R	Spectral radius of matrix
R	Stellar radius
R_{ij}	Radiative rate from level i to level j

$R_{i\kappa}$	Photoionization rate from level i
$R^{\alpha\beta}$	Radiation stress-energy tensor
$R(\mathbf{n}', \nu'; \mathbf{n}, \nu)$	Redistribution function
Re	Reynolds number
Re_R	Radiative Reynolds number
$\mathscr{R}$	Universal gas constant
R	Radiation stress-energy tensor
s	Path length
s	Spacetime interval
s	Specific entropy
s_e	Electron scattering coefficients per gram, $n_e\sigma_e/\rho$
s_{elec}	Entropy of electronic excitation
s_{trans}	Translational entropy
S	Entropy in volume V
S	Surface, surface area
S_l	Line source function
S_{rad}	Entropy of thermal radiation
S^{α}	Entropy-flux density four-vector
S^{α}_{β}	Projection tensor
$S^{\alpha\beta}$	Total radiating-fluid stress-energy tensor, $M^{\alpha\beta}+R^{\alpha\beta}$
S_{ν}	Source function
t	Time
t_c	Self-collision time
t_d	Radiation diffusion time, $l^2/c\lambda_p$
t_D	Deflection time
t_E	Energy-exchange time
t_{ee}	Electron self-collision time
t_{ep}	Electron-proton energy-exchange time
t_f	Fluid flow time, l/v
t_{ic}	Inelastic collision time
t_L	Radiation pressure disruption time
t_N	Nuclear time scale
t_{pp}	Proton self-collision time
t_R	Radiation flow time, l/c
t_{rc}	Radiative cooling time
t_{relax}	Relaxation time
t_{rr}	Radiative recombination time
$t_{RR}(k)$, t_{RR}	Radiative relaxation time
t_s	Strong-collision time
t_{λ}	Photon flight time, λ_p/c
$\mathbf{t}$	Surface force on fluid element
$\mathbf{t}_{\mathrm{visc}}$	Viscous drag force
ℓ	Equivalent electron optical depth
T	Temperature
T_e	Electron temperature
T_{eff}	Effective temperature
T_{ij}	Stress tensor
T_{ion}	Ion temperature
T_k	Kinetic temperature

T_p	Proton temperature
T_R	Radiation temperature
T_1	Temperature perturbation in wave
T_-	Temperature immediately in front of shock
T_+	Temperature immediately behind shock
T	Stress tensor
u	Fluid speed relative to shock front
u	Speed
u	Velocity component along x axis
u_D	Critical speed of D-type ionization front
u_g	Horizontal component of group velocity
u_R	Critical speed of R-type ionization front
$\mathbf{u}$	Particle velocity
U	Complex amplitude of horizontal component of wave velocity
U	Random particle speed
U_x, U_y, U_z	Components of particle random velocity in (x, y, z) directions
$\mathbf{U}$	Random velocity of particle
$\mathcal{U}$	Dimensionless random particle speed
$\mathcal{U}_i$	ith component of dimensionless random particle velocity
$\mathcal{U}_i^\circ \mathcal{U}_m$	Traceless outer product of dimensionless random velocity components
$\boldsymbol{\mathcal{U}}$	Dimensionless random particle velocity
v	Specific volume $(1/\rho)$
v	Speed
v	Velocity component along y axis
v_c	Critical velocity in stellar wind
v_{esc}	Escape velocity
v_g	Group speed
$v_{i,j}$	Velocity gradient tensor
v_p	Phase speed
v_r	Radial velocity in spherical coordinate system
v_s	Shock speed
v_t	Phase trace speed
v_x, v_y, v_z	Components of velocity in (x, y, z) directions
v_θ	Tangential velocity in spherical coordinate system
v_ϕ	Azimuthal velocity in spherical coordinate system
v_∞	Terminal flow speed in stellar wind
$\mathbf{v}$	Fluid velocity
$\mathbf{v}_g$	Group velocity
$\mathbf{v}_1$	Velocity perturbation in wave
V	Specific volume in shock theory $(1/\rho)$
V	Volume
V^α	Four-velocity
$\mathcal{V}$	Material volume (fixed in fluid)
w	Velocity component along z axis
w_g	Vertical component of group velocity
w_k	Quadrature weight
w_1	Vertical component of wave velocity
W	Complex amplitude of vertical component of wave velocity

W	Rate of energy input from nonmechanical sources
W	Thermodynamic probability
W	Work done by gas
$\mathcal{W}^{n+1}$	Boundary work term in flow at time t^{n+1}
x	Cartesian coordinate
x	Degree of ionization [e.g., $n_p/(n_H+n_p)$]
x	Dimensionless frequency displacement from line center, $(\nu-\nu_0)/\Delta\nu_D$
x_f	Position of a front
$\mathbf{x}$	Position vector
$\mathbf{x}_1$	Fluid displacement in wave
X	Complex amplitude of horizontal component of wave displacement
$X_\tau[f(x)]$	X operator
y	Cartesian coordinate
z	Cartesian coordinate
z	Dimensionless radiative relaxation rate, nt_λ
z	Dimensionless wavenumber, ak/ω
Z	Charge number
Z	Complex amplitude of vertical component of wave displacement
Z	Partition function
Z_{elec}	Partition function for electronic excitation
Z_{rot}	Partition function for molecular rotation
Z_{trans}	Partition function for translational motions
Z_{vib}	Partition function for molecular vibration
α	Angle of wave phase propagation relative to horizontal plane
α	Exponent in power-law potential
α	Exponent in radiation force law
α	Ratio of radiation pressure to gas pressure in thermal equilibrium, P^*/p_g
$\bar{\alpha}$	Mean photoionization cross section
$\alpha_{ij}(\nu)$	Bound–bound absorption cross section
$\alpha_{i\kappa}(\nu)$	Bound–free absorption cross section
$\alpha_{\kappa\kappa}(\nu, T)$	Free–free absorption cross section
α_ν	Photoionization cross section
β	Coefficient of thermal expansion
β	Effective line optical depth in stellar wind
β	$1/kT$
β	v/c
β_l	$(n_e\sigma_e/\chi_l)=\ell/\tau_l$
γ	Ratio of specific heats
γ	$(1-v^2/c^2)^{-1/2}$
$\boldsymbol{\gamma}$	Dimensionless relative velocity of collision partners
Γ	Circulation
Γ	Force ratio g_R/g
$\Gamma, \Gamma_1, \Gamma_2, \Gamma_3$	Generalized adiabatic exponents
Γ^b_{ac}	Ricci rotation coefficient
$\boldsymbol{\Gamma}$	Dimensionless center of mass velocity

δ	Continuum destruction probability
δ	Width of shock front
δ_{AB}	Phase shift between quantities A and B in a wave
δ_{ij}, δ^{ij}	Kronecker delta symbol
$\delta(x)$	Dirac delta function
$(\delta/\delta t)$	Intrinsic derivative with respect to time
Δ	Thickness of temperature relaxation layer
$\Delta\nu_D$	Line Doppler width
ε	Momentum flux in stellar wind normalized to momentum in radiation field
ε	Rate of thermonuclear energy release (per gram)
ε	Thermalization parameter
ε_a^{α}, ε_{α}^{a}	Transformation between coordinate and tetrad frames
ε_H	Ionization potential (from ground state) of hydrogen
ε_i	Energy above ground of state i
ε_{iH}	Excitation energy of state i of hydrogen
ε_{Ii}	Ionization potential above state i
ε_{ion}	Ionization energy
ε_w	Wave energy density
ε_{∞}	Residual energy at infinity per particle in stellar wind
$\bar{\varepsilon}$	Mean energy per ionizing photon
$\boldsymbol{\varepsilon}_a$	Basis vectors in orthonormal tetrad frame
$\boldsymbol{\varepsilon}_{\alpha}$	Basis vectors of coordinate system
ζ	Coefficient of bulk viscosity
ζ_R	Bulk viscosity coefficient for radiation
ζ_1	Vertical displacement of fluid element in a wave
η	Photoionization sink term in line source function
η	Volume ratio in shock, $V/V_1 = \rho_1/\rho$
η_l	Line emission coefficient
$\eta_{\alpha\beta}$	Lorentz metric
η_*	Maximum compression ratio in radiation-dominated shock
$\eta(\mathbf{x}, t; \mathbf{n}, \nu)$, η_{ν}	Emission coefficient
$\eta^s(\mathbf{x}, t; \mathbf{n}, \nu)$, η_{ν}^s	Scattering emission coefficient
$\boldsymbol{\eta}$	Lorentz metric tensor
θ	Fluid expansion
θ	Polar angle in spherical coordinate system
θ	Recombination source term in line source function
θ	Time-centering coefficient in implicit difference equation, $0 \le \theta \le 1$
θ_1	Normalized temperature perturbation, T_1/T_0
$\hat{\boldsymbol{\theta}}$	Unit vector in direction of increasing polar angle in spherical coordinate system
Θ	Complex amplitude of temperature perturbation in a wave
Θ	Polar angle of radiation propagation vector relative to local outward normal in planar or spherical geometry
κ_c	Continuum opacity
κ_E	Absorption mean opacity
κ_J	Absorption mean opacity
κ_P	Planck mean opacity

$\kappa_{P,g}$	Group Planck mean
κ_s	Coefficient of adiabatic compressibility
κ_T	Coefficient of isothermal compressibility
$\kappa(\mathbf{x}, t; \mathbf{n}, \nu)$, κ_ν, κ	True absorption coefficient
λ	Coefficient of dilatational viscosity (second coefficient of viscosity)
λ	Dimensionless potential energy in stellar wind
λ	Eigenvalue
λ	Particle mean free path
λ_p	Photon mean free path
λ_t	Free-flight distance of photon in time Δt, $c\,\Delta t$
λ_R	Rosseland mean free path, χ_R^{-1}
λ_ν	Photon mean free path at frequency ν, χ_ν^{-1}
Λ	Ratio of maximum to minimum impact parameter
Λ	Wavelength
$\Lambda_\tau[f(x)]$, Λ_τ	Lambda operator
$\mathbf{\Lambda}$	Lorentz transformation in Minkowski metric
μ	Angle cosine of photon propagation vector relative to outward normal, $\mu \equiv \mathbf{n} \cdot \mathbf{k}$ or $\mathbf{n} \cdot \hat{\mathbf{r}}$
μ	Coefficient of dynamical viscosity
μ	Mean molecular weight
μ_e	Electron viscosity coefficient
μ_m	Angle-quadrature point
μ_p	Proton viscosity coefficient
μ_Q	Artificial viscosity coefficient
μ_R	Coefficient of radiative viscosity
$\mu_{\alpha\beta}$	Minkowski metric
μ'	Effective viscosity coefficient for one-dimensional flows, $\mu' = \mu + \frac{3}{4}\zeta$
$\boldsymbol{\mu}$	Momentum density
$\boldsymbol{\mu}_w$	Wave momentum density
ν	Frequency
ν	Kinematic viscosity coefficient (μ/ρ)
ν	Inverse radiative relaxation time for optically thin disturbance
ν_i	Occupation number of state i (number of particles in state i in volume V)
ν_0	Line-center frequency
ξ	Similarity variable
$\bar{\xi}$	Average thermal coupling parameter
ξ_k	Amplification factor of kth Fourier component
ξ_ν	Monochromatic thermalization parameter, $(r+\varepsilon\phi_\nu)/(r+\phi_\nu)$
ξ_1	Horizontal displacement of fluid element in a wave
Π	Gas pressure ratio in radiating shock
Π_{ij}	Momentum flux-density tensor
$\mathbf{\Pi}$	Momentum flux-density tensor
ρ	Newtonian density
ρ	Lab density of proper mass, $\gamma\rho_0$
ρ'	Lab density of relative mass, $\gamma^2\rho_0$
ρ_0	Proper density of proper mass

ρ_{00}	Mass density of fluid including internal energy, $\rho_0(1+e/c^2)$
ρ_{000}	Mass density of fluid including enthalpy, $\rho_0(1+e/c^2)+p/c^2$
ρ_1	$\gamma^2\rho_{000}$
ρ_1	Density perturbation in wave
ρ_*	$\gamma\rho_{000}$
σ_e	Thomson electron scattering cross section
σ_{ij}	Viscous stress tensor
σ_l	Line scattering coefficient
σ_R	Stefan–Boltzmann constant
σ_T, $\sigma_{(0)}$	Total collision cross section
$\sigma_{(2)}$	Collision cross section in transport coefficient
$\sigma(g, \chi)$; $\sigma(\mathbf{u}_1, \mathbf{u}_2; \mathbf{u}_1', \mathbf{u}_2')$	Collision cross section
$\sigma(\mathbf{x}, t; \mathbf{n}, \nu)$, σ_ν	Scattering coefficient
$\boldsymbol{\sigma}$	Viscous stress tensor
Σ	Strength of vortex tube
τ	Average collision time
τ	Dimensionless temperature in stellar wind
τ	Optical depth
τ	Proper time
τ	Scaled temperature in thermal front
τ	Wave period
τ_a	Optical thickness of disturbance of frequency ω traveling with speed of sound, $a\kappa/\omega$
τ_{ac}	Acoustic-cutoff period
τ_c	Optical thickness of disturbance of frequency ω traveling with speed of light, $c\kappa/\omega$
τ_e	Electron optical depth of stellar wind
τ_l	Effective line optical depth
τ_R	Rosseland optical depth
τ_Λ	Optical thickness of disturbance of wavelength Λ
$\tau_\nu(\mathbf{x}, \mathbf{x}')$, τ_ν	Monochromatic optical depth
ϕ	Azimuthal angle in spherical coordinate system
ϕ	Photon number flux
ϕ	Velocity potential
ϕ	Wave phase
ϕ_ν, $\phi(\nu)$	Line profile function
$\phi(r)$, ϕ	Potential
$\boldsymbol{\phi}$	Newtonian three-force
$\boldsymbol{\phi}_w$	Wave energy flux
$\hat{\boldsymbol{\phi}}$	Unit vector in direction of increasing azimuthal angle in spherical coordinate system
Φ	Azimuthal angle of radiation propagation vector around local outward normal in planar or spherical geometry
Φ	Potential
Φ	Viscous dissipation function
Φ_1	Scaled first-order term in Chapman–Enskog solution of Boltzmann equation, f_1/f_0
Φ^α	Four-force

$\Phi_{ij}(T)$	Saha–Boltzmann factor of bound state i of ion state j relative to ground state of ion $j+1$. $[n_{ij}^* = n_e n_{0,j+1} \Phi_{ij}(T)]$
$\Phi_\tau[f(x)]$	Phi operator
χ	Angle of deflection in collision
χ	Thermal diffusivity, $K/\rho c_p$
χ_H	Flux mean opacity
χ_l, $\chi_l(\nu)$	Line absorption coefficient
χ_R	Rosseland mean opacity
$\chi_{R,g}$	Group Rosseland mean
$\chi(\mathbf{x}, t; \mathbf{n}, \nu)$, χ_ν	Opacity coefficient (per unit volume)
ψ	Dimensionless kinetic energy in stellar wind
ψ	Wave phase
$\psi(\mathbf{x}, t; \mathbf{n}, \nu)$, ψ_ν, ψ	Photon number density
$\boldsymbol{\psi}$	Solution vector in complete linearization method
ω	Angular frequency
ω	Solid angle
ω_a	Acoustic cutoff frequency
ω_{BV}	Brunt–Väisälä frequency
ω_g	Brunt–Väisälä frequency in isothermal medium
ω_r, ω_θ, ω_ϕ	Radial, tangential, and azimuthal components of vorticity
ω_x, ω_y, ω_z	Components of vorticity in (x, y, z) directions
$\omega(\nu)$, ω_ν	Opacity per gram, χ_ν/ρ
$\omega_{aN}(t_{RR})$	Effective acoustic-cutoff frequency in Newtonian cooling approximation
$\omega_{gN}(t_{RR})$	Effective maximum gravity-wave frequency in Newtonian cooling approximation
$\boldsymbol{\omega}$	Vorticity
Ω	Solid angle
Ω_{ij}	Vorticity tensor
$\Omega_{\alpha\beta}$	Covariant rotation tensor
$,i$	Partial derivative with respect to coordinate x^i
$,t$	Partial derivative with respect to time
$;\alpha$	Covariant derivative with respect to coordinate x^α
$(\partial/\partial t)$	Eulerian time derivative (space coordinates fixed)
∂_a	Pfaffian derivative
$\boldsymbol{\nabla}_k$	Gradient with respect to wave-vector components
$\oplus$	Earth symbol
$\odot$	Sun symbol

Index